

Toward a quantification of magnitudes of past upper crustal stresses : insights from calcite twinning and stylolite roughness paleopiezometry

Olivier LACOMBE



Why to characterize stresses in the crust ?

The motivation arises :

from applied geological purposes, such as geological hazards, engineering activities and resource exploration;

and

from fundamental geological purposes, such as understanding the mechanical behaviour of geological materials and deciphering various tectonic mechanisms, from those related to plate motions at a large scale to those causing jointing and faulting or even microstructures at a smaller scale.

Despite an increasing number of in situ stress measurements, magnitudes of crustal stresses remain poorly constrained...

Calcite twinning paleopiezometry

Twinning of minerals depends on the magnitude of the shear stress which has been applied to them.

One can make use of this property to evaluate the magnitudes of stresses which have been supported by a rock during its history.

An access to paleostress magnitudes in the upper crust : Calcite twinning paleopiezometry

In the upper crust, brittle deformation of carbonate rocks is accompanied by pressure-solution, porosity reduction and crystalline deformation.

At low T (0-300°) calcite plasticity corresponds to the prevalence of e-twinning

Geometry and significance of calcite twins

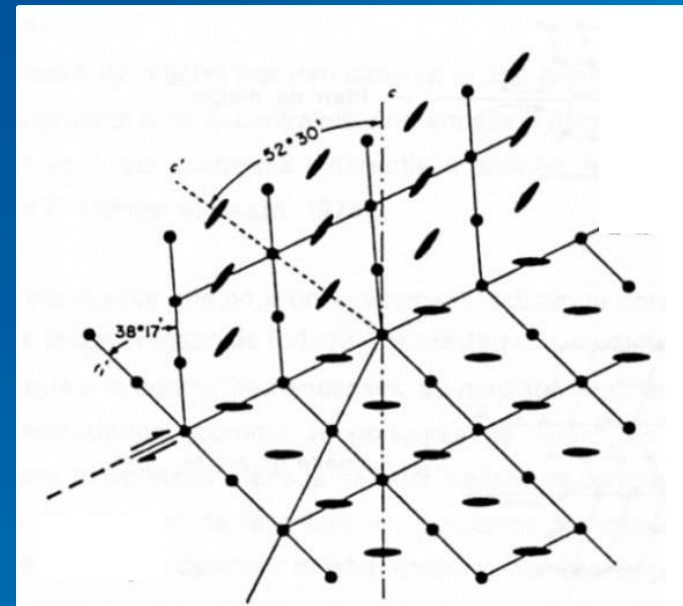
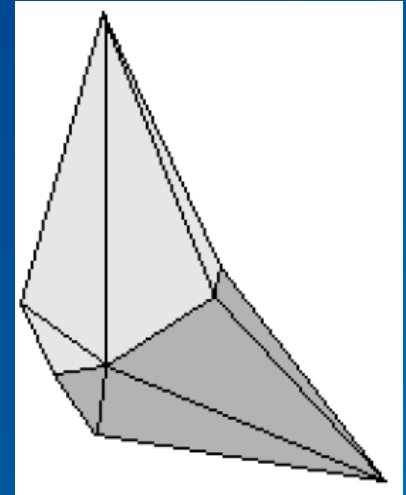
A twin is a polycrystalline association formed by the juxtaposition of two homogeneous parts, or more, of a single crystalline species, oriented one with respect each other following well-specified laws.

The composition plane along which twinning occurs is a plane of high atomic density that separates the twinned portion of the crystal from the host (untwinned) part. The twin plane is the plane that belongs to both portions : it is the equivalent of the shear plane if one considers that a twin lamella results from simple shearing of the crystal.

The twinning direction is the « gliding » direction : this is the line that connects an atom before twinning to the same atom after twinning; it belongs to the twin plane.

The orientation of the twinned portion of the crystal can be deduced from the orientation of the host crystal by a rotation that accounts for the geometry of the lattice. However, this rotation is virtual and by no means corresponds to the physical mechanism of twinning.

What's a twin ?



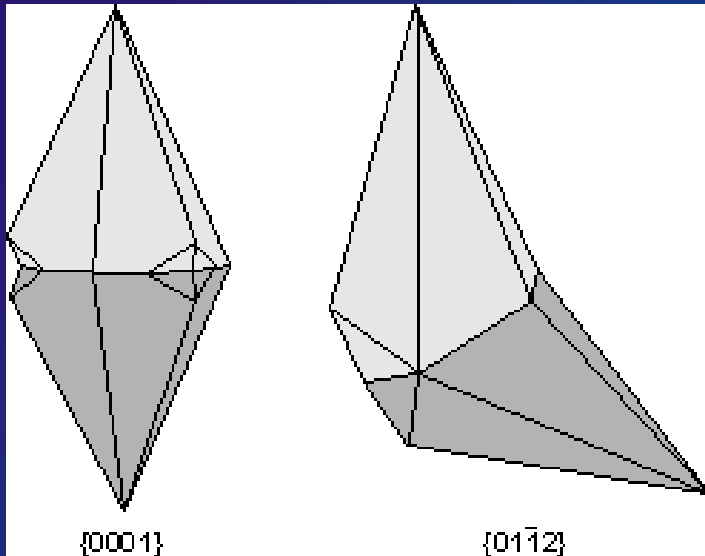
Types of twinning

- Twins may be classified on the basis of their physical properties
- There are two basic types of twin
 - Contact twins
 - Penetration twins

Origin of twinning

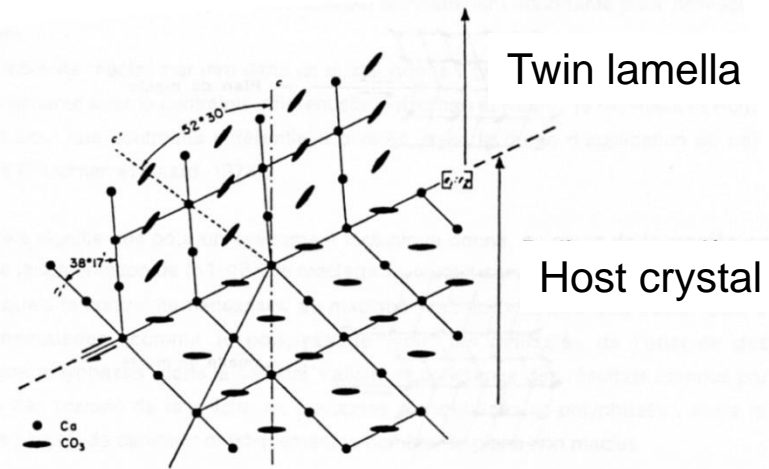
- Twinning can originate in 3 different ways
 - Growth twins
 - Transformation twins
 - Deformation twins

Calcite twinning

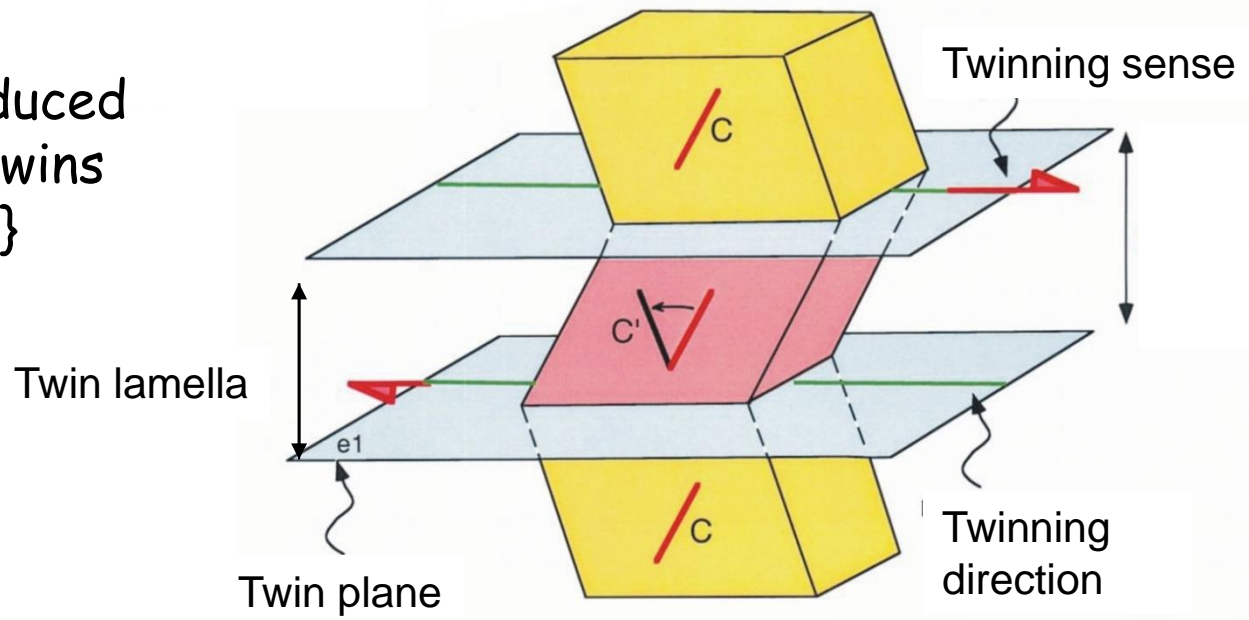


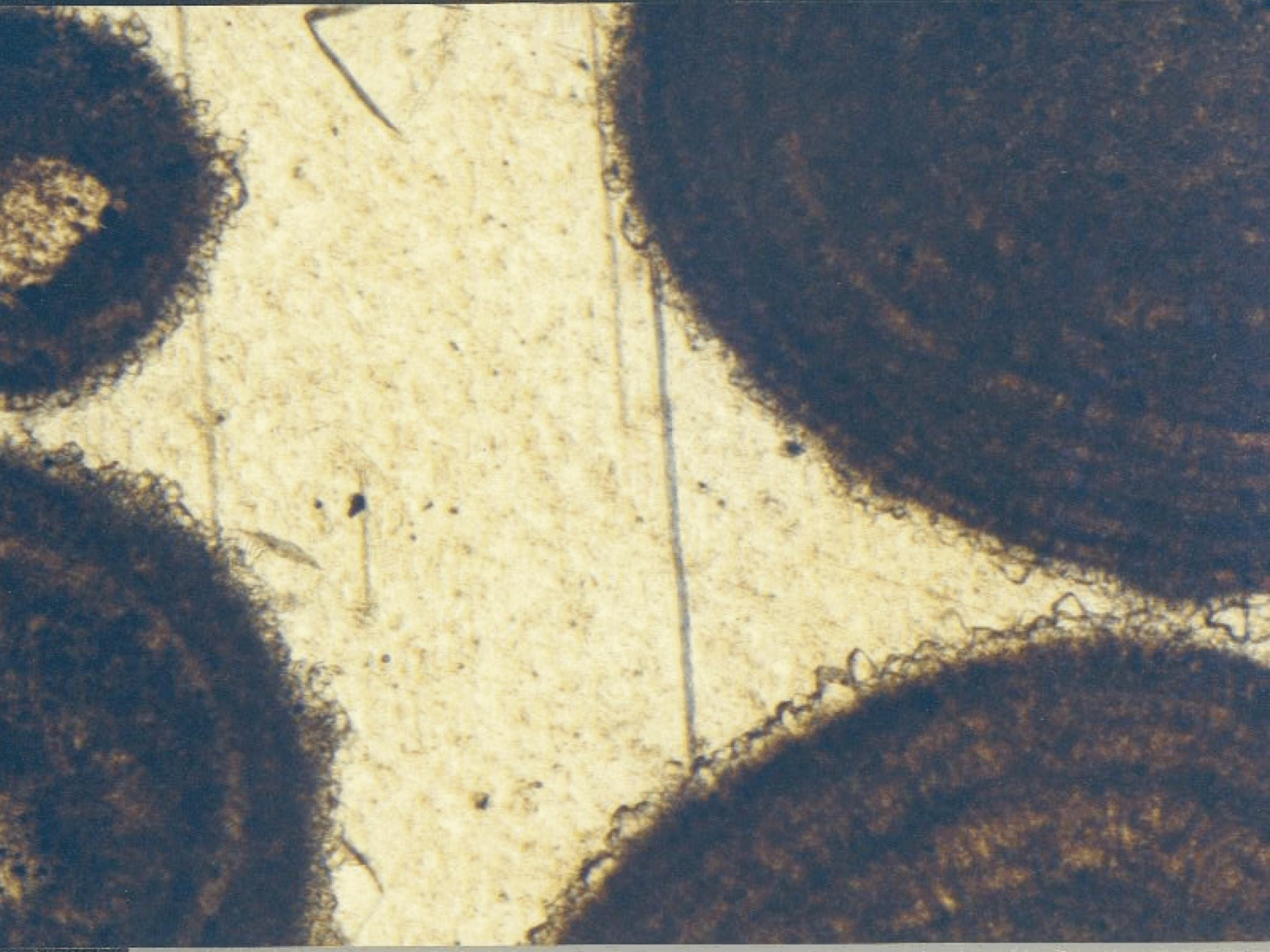
- Most common twin laws that are observed in calcite crystals are $\{0001\}$ and the rhombohedron $\{01\bar{1}2\}$
- Both are contact twins, but the $\{01\bar{1}2\}$ twins can also occur as polysynthetic twins that result from deformation

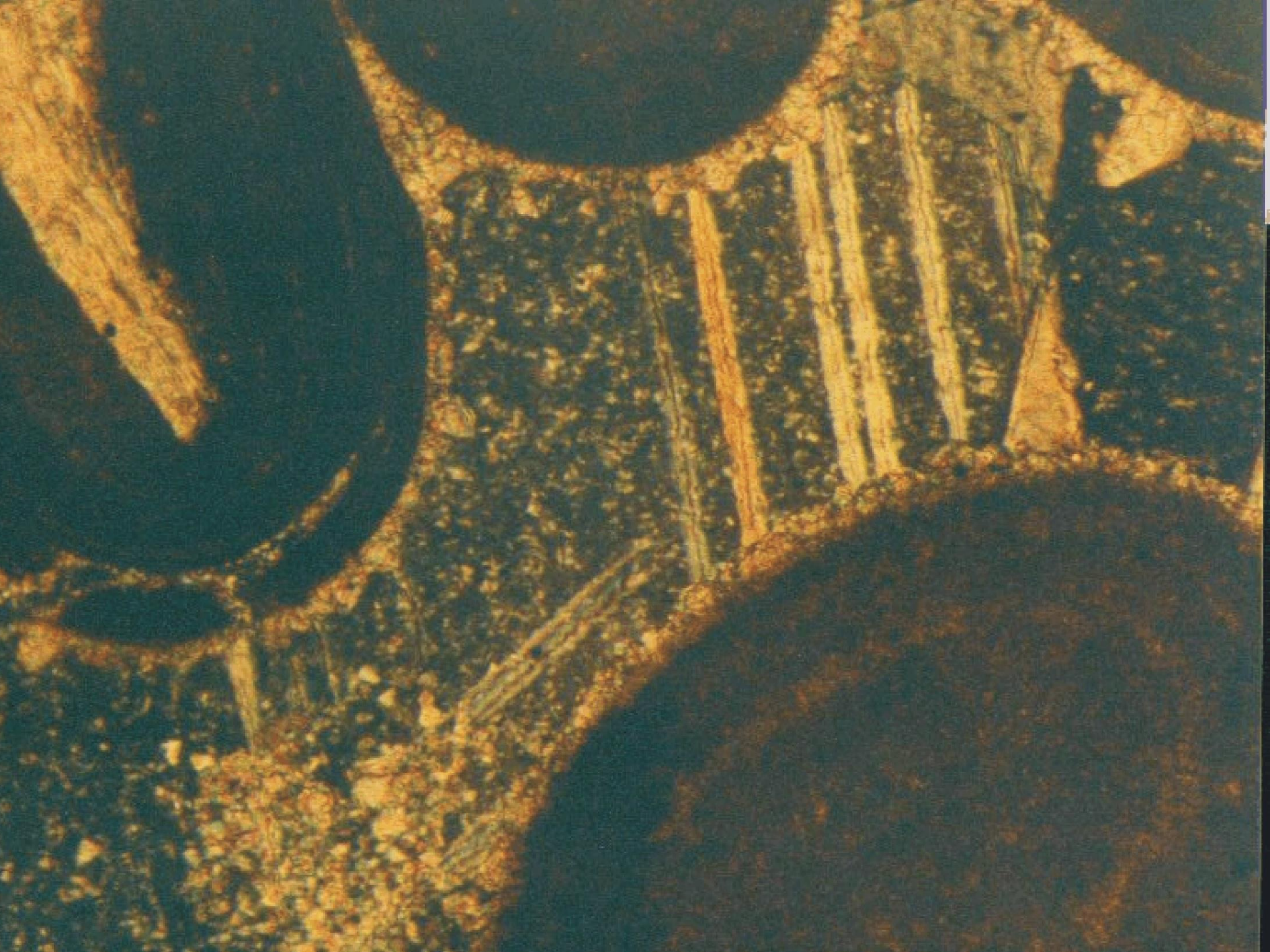
Twinning ~ simple shearing in a particular sense and direction along e-planes {01-12}

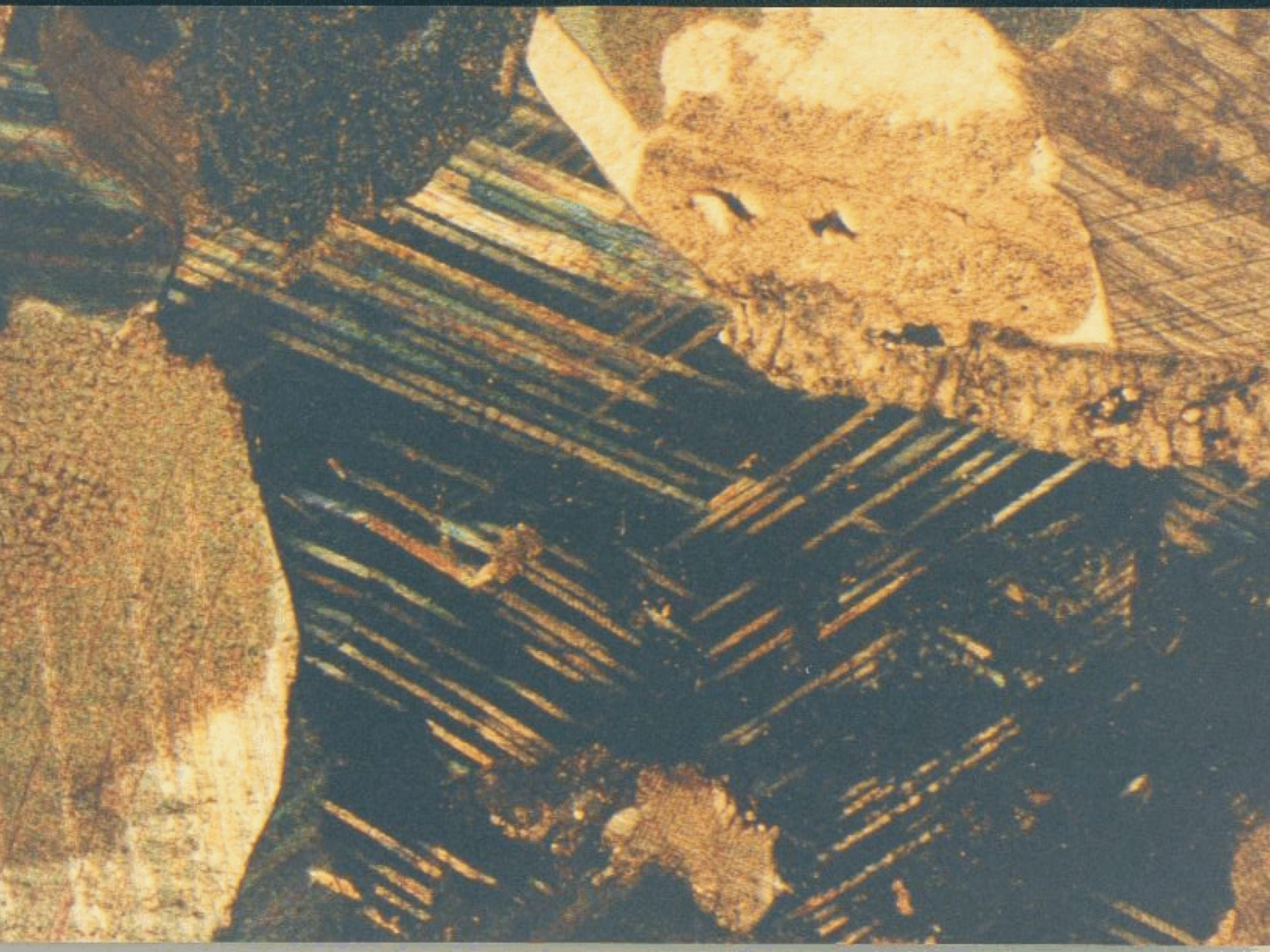


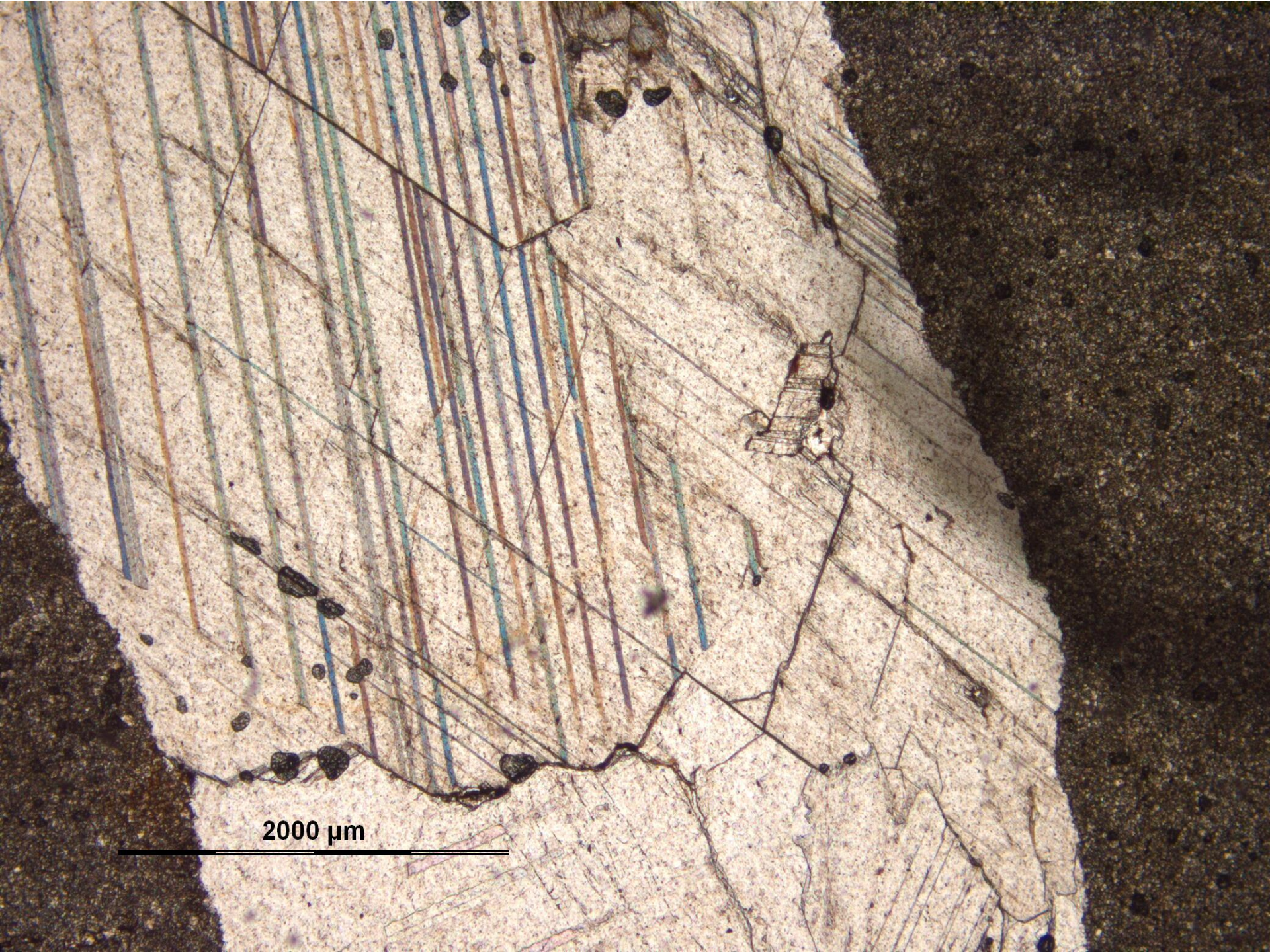
Deformation-induced polysynthetic twins on e {01-12}



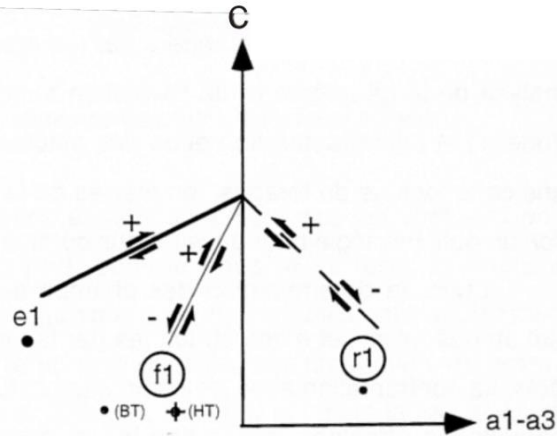
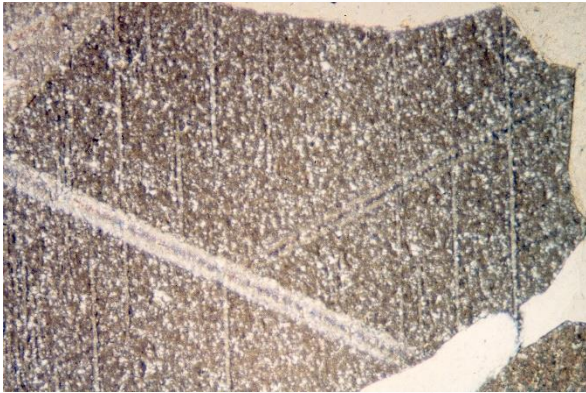




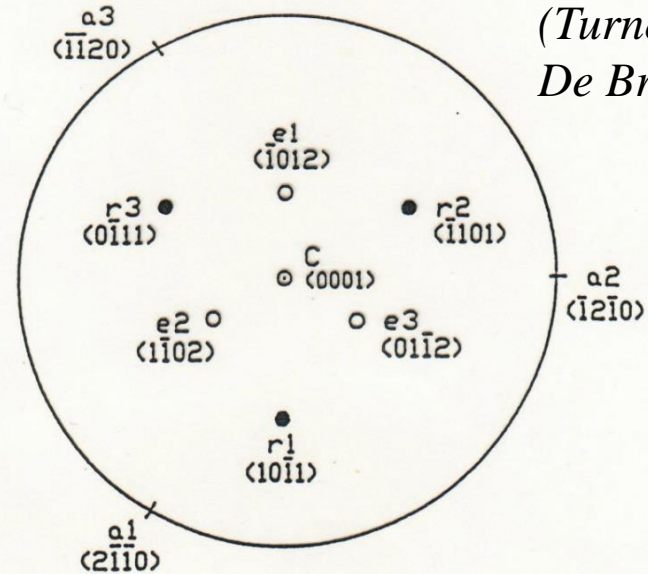
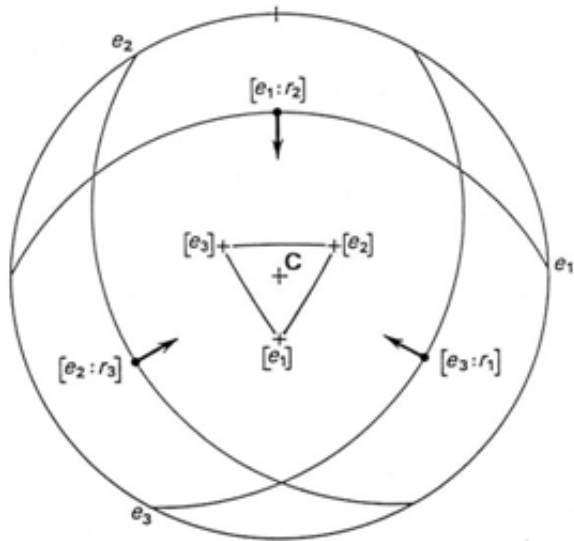




2000 μm

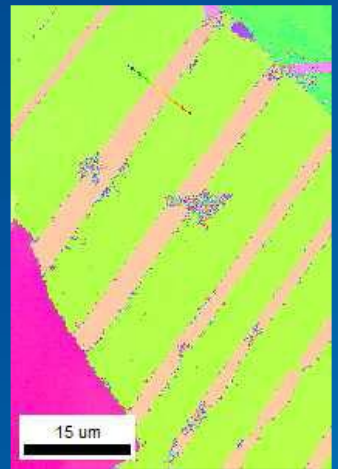
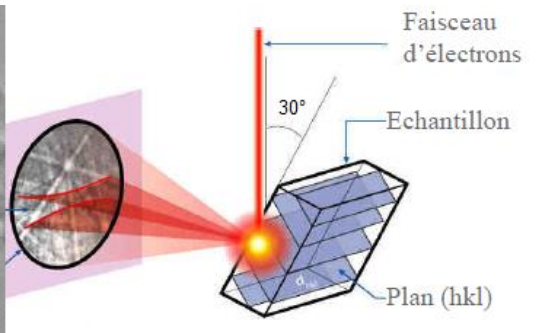
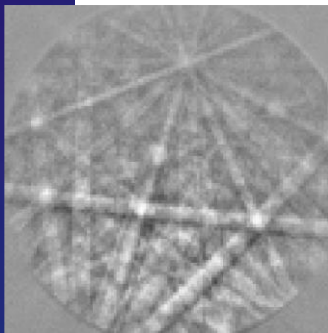


e-twinning and r, f-gliding systems in calcite

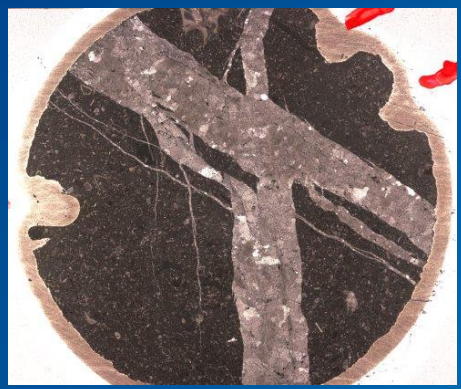


(Turner and Weiss, 1976;
De Bresser et al., 1997)

C, e_j	= 26,5°
e_j, e_j	= 44,5°
e_j, r_j	= 71,5°
e_j, r_j	= 37,5°
r_j, r_j	= 75°
C, r_j	= 44,5°

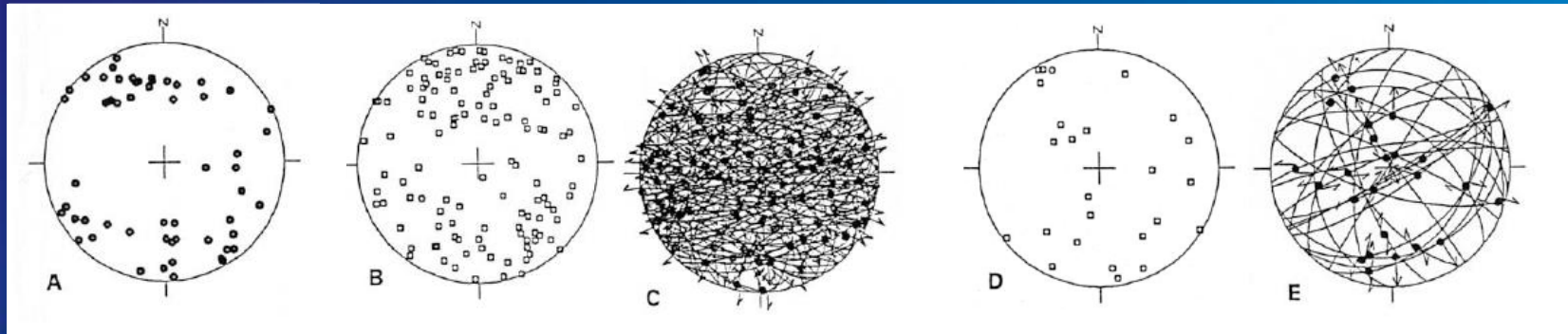


Measurement technique : U-stage /EBSD

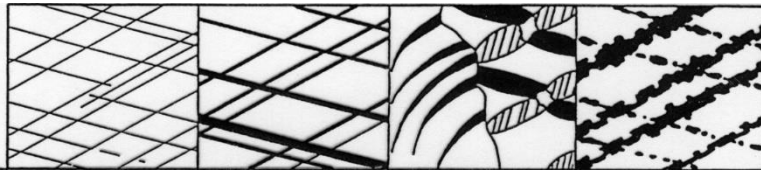


Data : C-axis and twinned/untwinned planes in grains

Material : Host rock matrix / veins
Field samples or cores

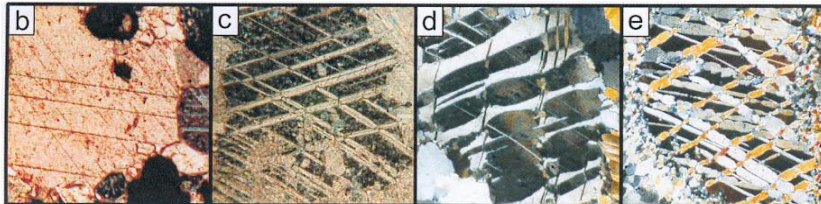


Calcite twins as low T thermometer

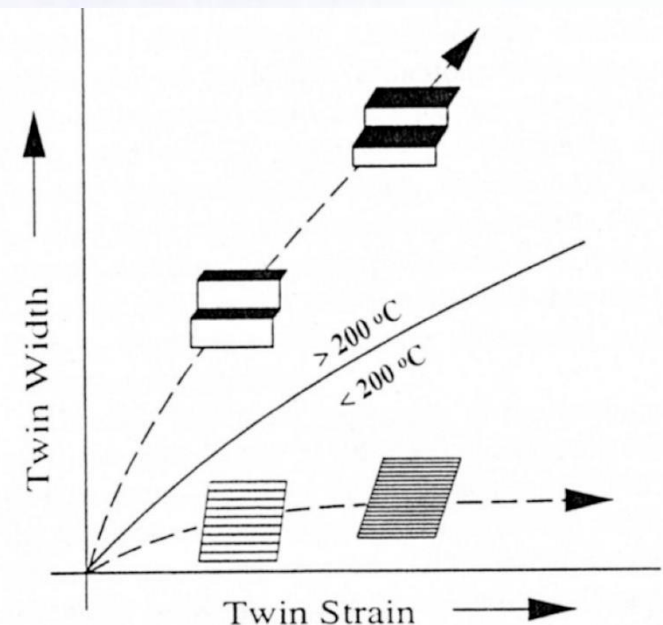
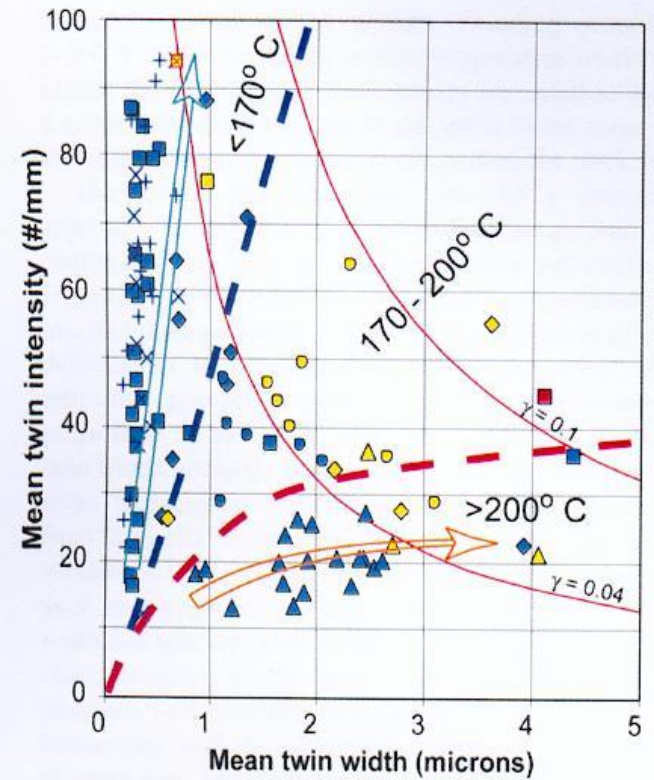


	type I	type II	type III	type IV
Geometry	-thin	-thick ($>> 1\mu\text{m}$)	-curved twins	-thick, patchy
Description	-straight -rational	-straight -slightly lens-shaped -rational	-twins in twins -irrational -completely twinned	-sutured boundaries -trails of tiny grains -irrational
Interpretations	-little deformation -little cover -low temperature -(post-metamorphic) -(late tectonic)	-considerable def. -completely twinned grains are possible -syn- or post-metamorphic	-large deformation, -intracrystalline def. mechanisms e.g. (r- & f-glide) -syn-metamorphic deformation.	-large deformation -recrystallization (grain boundary migration) -pre- or syn-metamorphic
Temperature	$< 200^\circ\text{C}$	$150-300^\circ\text{C}$	$> 200^\circ\text{C}$	$> 250^\circ\text{C}$

Increasing temperature



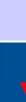
(Burkhard, 1993; Ferrill, 1998;
Ferrill et al., 2004)



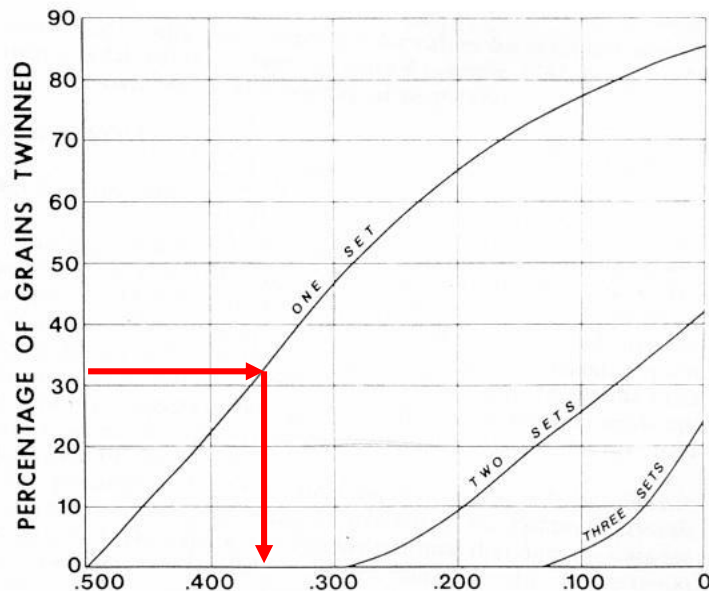
**Stress analysis of calcite twinning :
The 'historical' techniques**

Jamison and Spang (1976) :
determination of differential stress magnitudes

$$\tau_s = \Delta\sigma \cdot S$$



if τ_a is known, $\Delta\sigma$

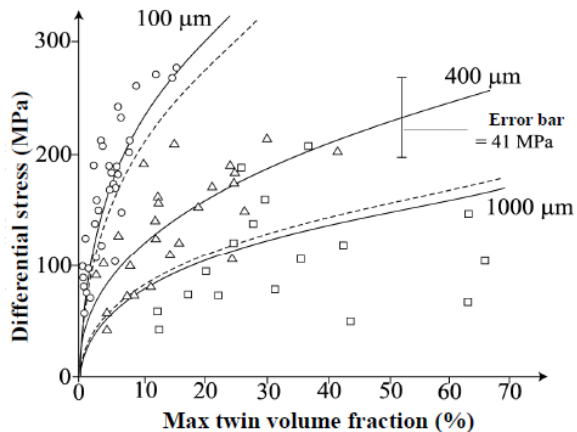


In a sample with no preferred crystallographic orientation, the percentages of grains twinned on 0, 1, 2 or 3 twin planes are functions of the applied differential stress ($\sigma_1 - \sigma_3$) value. Experimentally calibrated

Limitations :

- uniaxial stress
- critical resolved shear stress for twinning = constant $\tau_a = 10$ MPa
- takes into account neither grain size nor mutual compatibility of twin systems

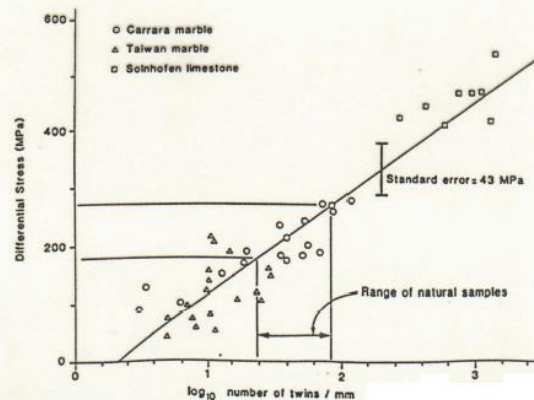
Rowe and Rutter (1990) : determination of differential stress magnitudes



Twin volume fraction, V
 ○ Grain size 100 μm
 △ Grain size 400 μm
 □ Grain size 1000 μm
 % volume of twinned portion

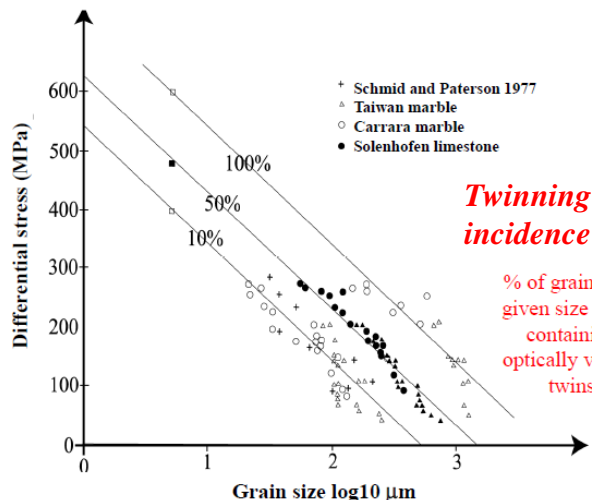
$$\log \sigma = 2,72 + 0,40 \cdot (\log V - \log d)$$

Twin density, D



$$\sigma = -52,0 + 171,1 \cdot \log D$$

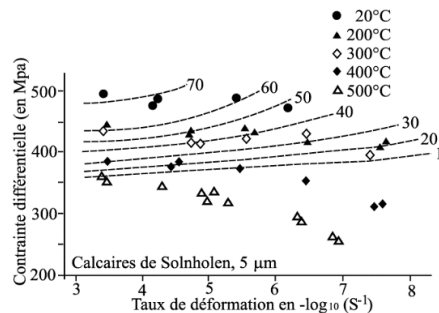
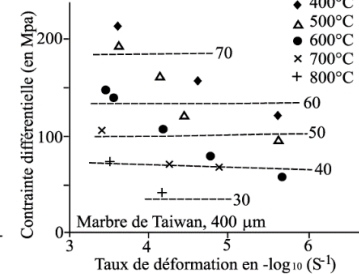
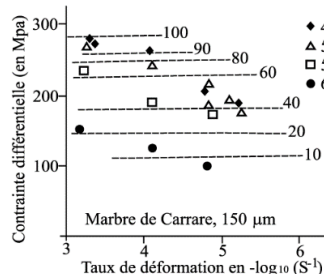
Independent on grain size



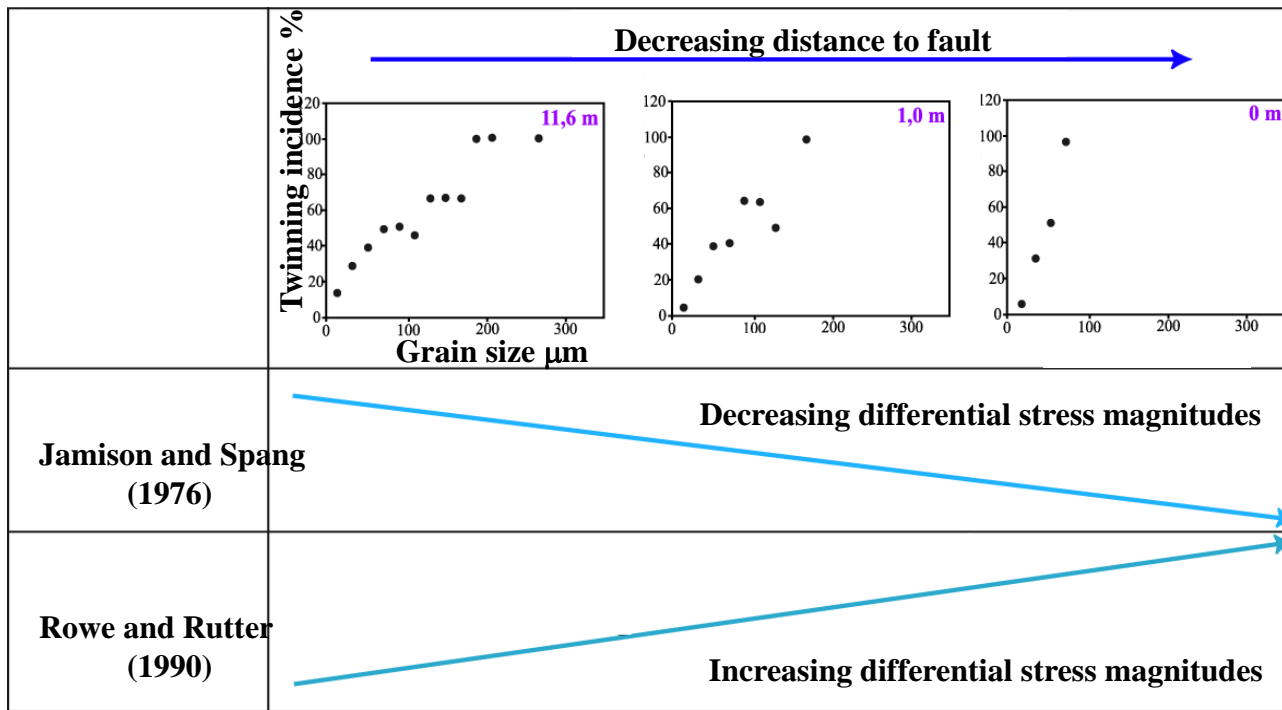
Twinning incidence

% of grains in a given size range containing optically visible twins

$$\sigma = 523 + 2,13 It - 204 \cdot \log d$$



Good paleopiezometer !

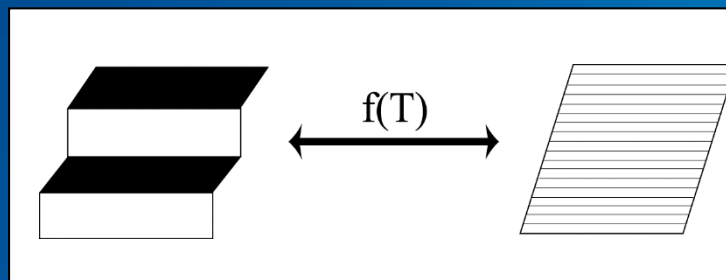


Influence of grain size distribution on estimates of differential stress magnitudes (Newman, 1994)

Région étudiée	Référence	Technique	Contraintes différentielles moyennes	Température de déformation
Nord de la chaîne subalpine	Ferrill (1998)	Jamison et Spang (1976)	44 MPa	75 - 250 °C
		densité de macle de Rowe et Rutter (1990)	235 MPa	
Sud des Pyrénées	Holl & Anastasio (1995)	Jamison et Spang (1976)	65 MPa	190 - 235 °C
		densité de macle de Rowe et Rutter (1990)	249 MPa	

Influence of temperature on estimates of differential stress magnitudes (Ferrill, 1998)

Rowe and Rutter technique : well calibrated for $T > 400^{\circ}\text{C}$, BUT cannot be used at low T



To sum up :

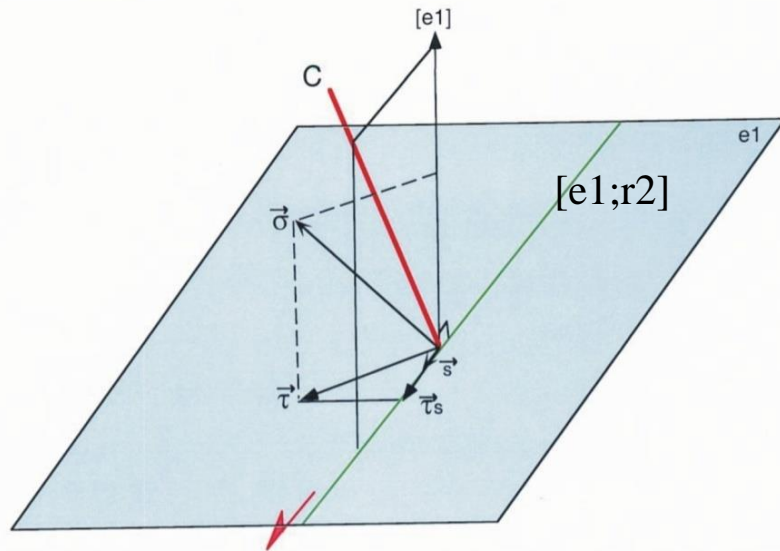
None of these techniques allows to relate differential stresses to principal stress orientations and stress regimes.

→ significance of 'bulk' maximum differential stresses in case of polyphase tectonics ?

Moreover,
techniques are commonly used separately
without care of their specific limitations

The Calcite Stress Inversion Technique, CSIT /CSIT-2
(Etchecopar, 1984; Parlangeau, 2018)

Determination of the reduced stress tensor



$$-(\sigma_1 - \sigma_3)/2 \leq \tau_s = (\vec{\sigma} \cdot \vec{s}) \leq (\sigma_1 - \sigma_3)/2$$

τ_a : seuil de maclage

plan maclé si $\tau_s \geq \tau_a$
plan non maclé si $\tau_s < \tau_a$

The inversion process is very similar to that used for fault-slip data :
twin gliding along the twinning direction within the twin plane is geometrically comparable to slip along a slickenside lineation within a fault plane.

But the inversion process takes into account both twinned planes (resolved shear stress > CRSS)

AND

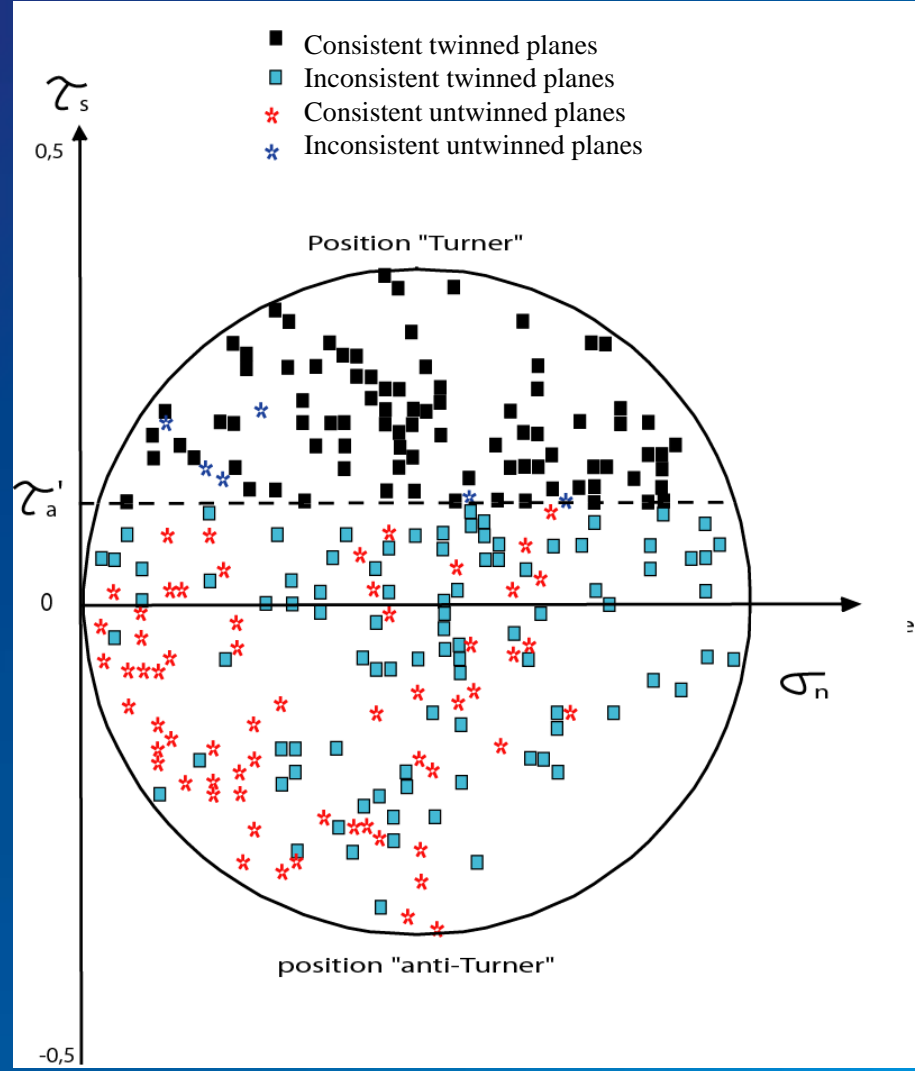
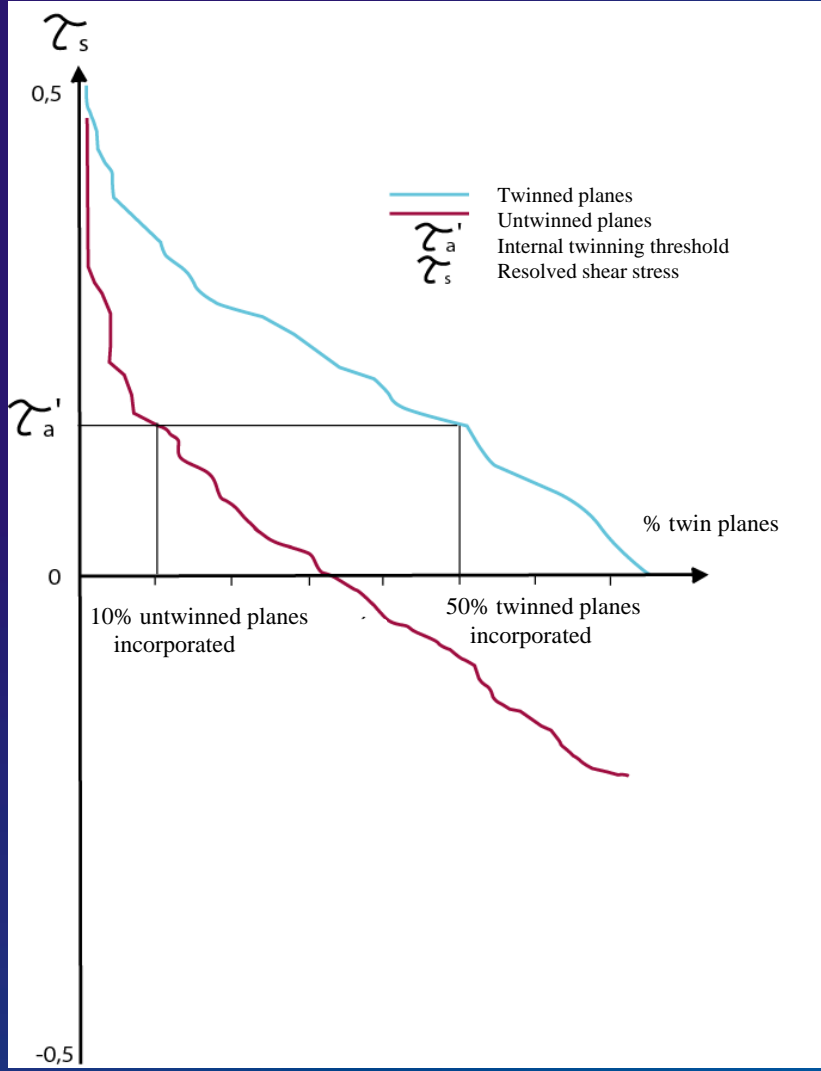
untwinned planes (resolved shear stress < CRSS),
a major difference with inversion of fault-slip data

Inversion of calcite twin data \rightarrow **Reduced stress tensor (4 parameters)**

Orientation of principal stresses and stress ratio

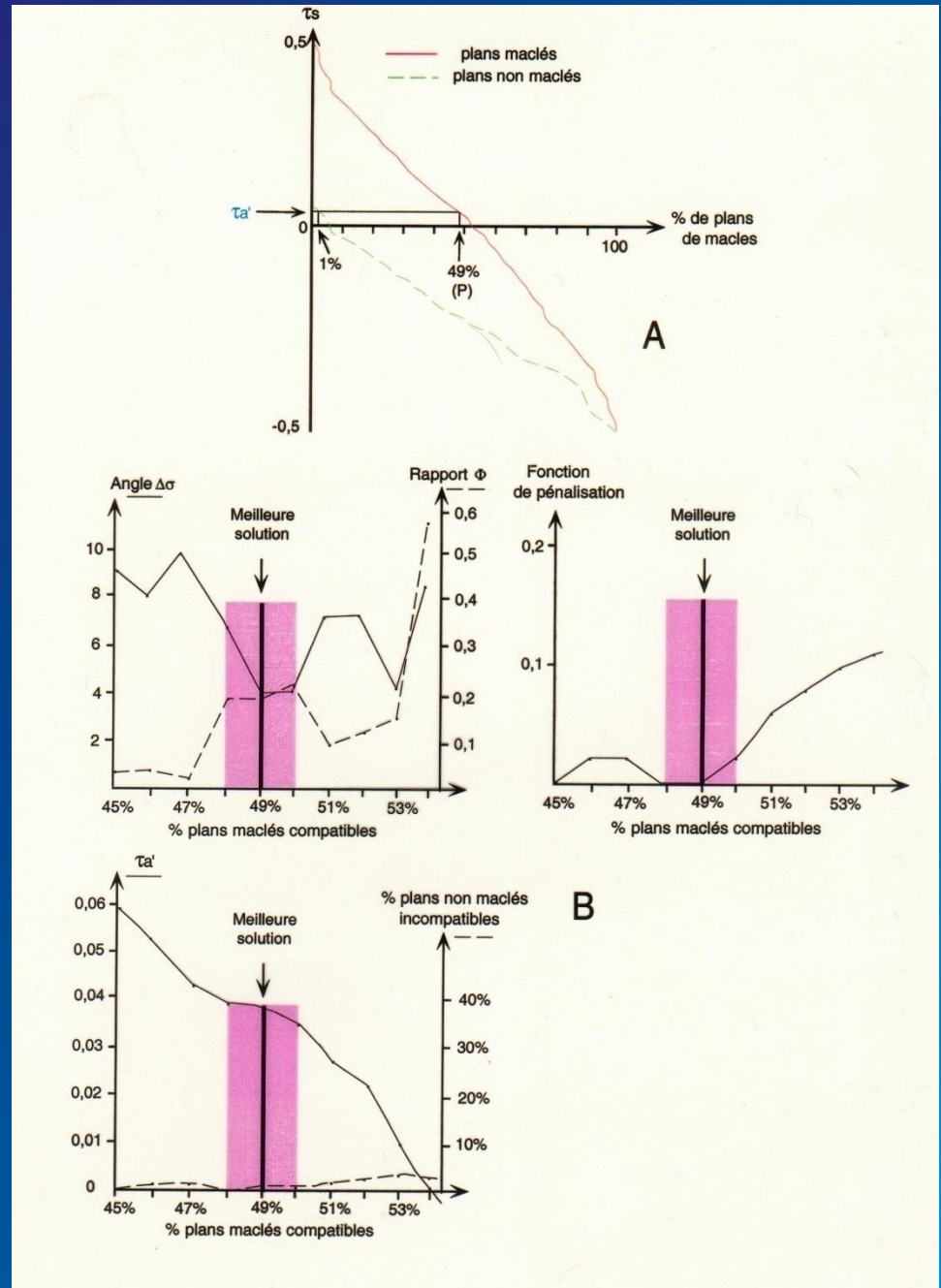
$$\Phi = \frac{(\sigma_2 - \sigma_3)}{(\sigma_1 - \sigma_3)}$$

+ dimensionless differential stress magnitudes



Definition of optimal stress tensor solution

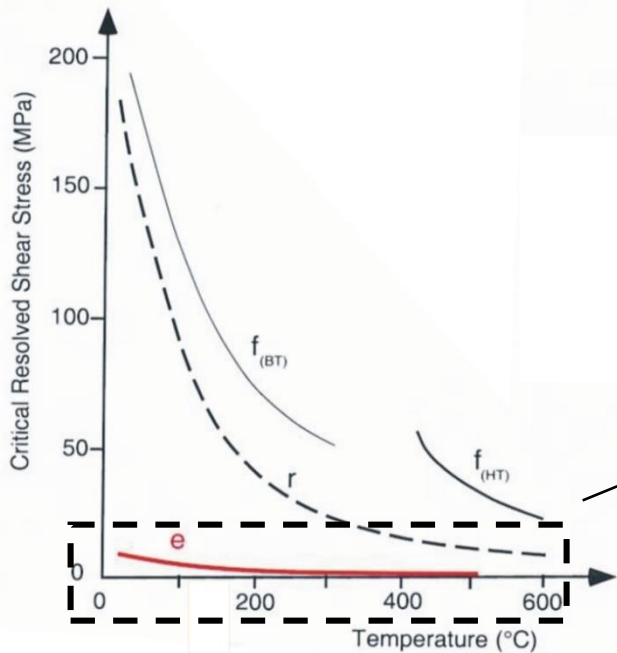
(Laurent et al., 2000;
Lacombe, 2000)



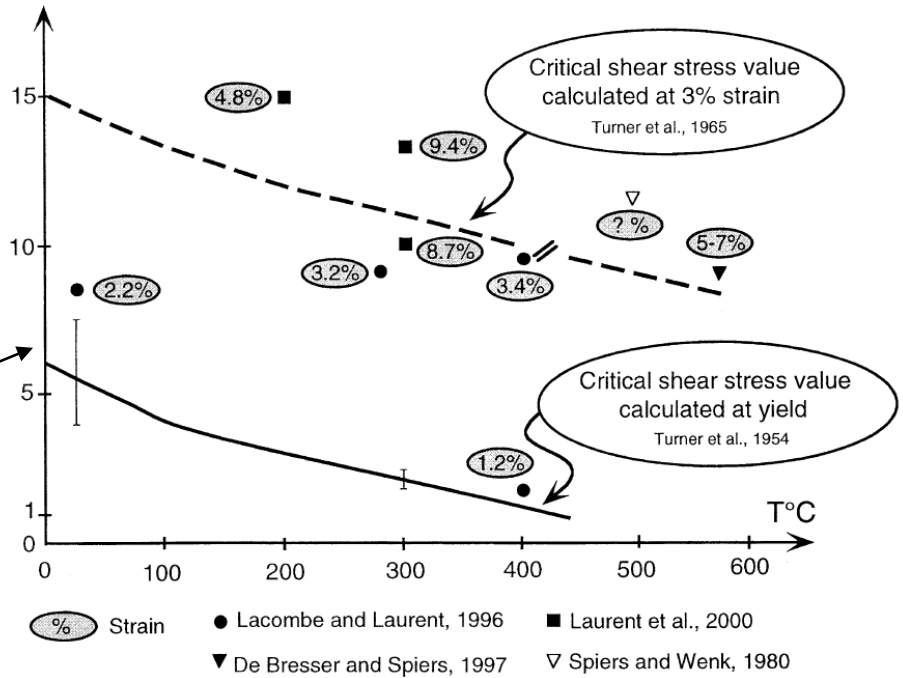
The strength of a sliding system (twinning or sliding ss) is conventionally expressed by a Critical Resolved Shear Stress (CRSS). It corresponds to the resolved shear stress along the sliding plane along the sliding direction that must be reached to induce a significant plastic (permanent) deformation, i.e., to induce motion of a number of dislocations, so that sliding becomes macroscopically observable independently of the orientation of the deformed grain. Such a behavior is commonly associated with a critical point on the stress-strain curve for a monocrystal.

The value of the CRSS is given by : $\tau_C = s \times S$. s corresponds to the applied stress at the critical point; S is the Schmid's factor, such as $S = \cos \alpha \times \cos \beta$, with α the angle between compression and the normal to the twin plane and β the angle between compression and the twin vector. The RSS along the twin vector is maximum when α et β are equal to 45° , S varying between 0 and 0,5 depending on crystal orientation.

The sources of stress concentrations like grain-scale heterogeneities being very numerous in natural crystals (dislocations, fractures, indenters, preexisting twins), the twinning threshold (= CRSS) likely reflects the stress required to propagate rather than to nucleate twins.

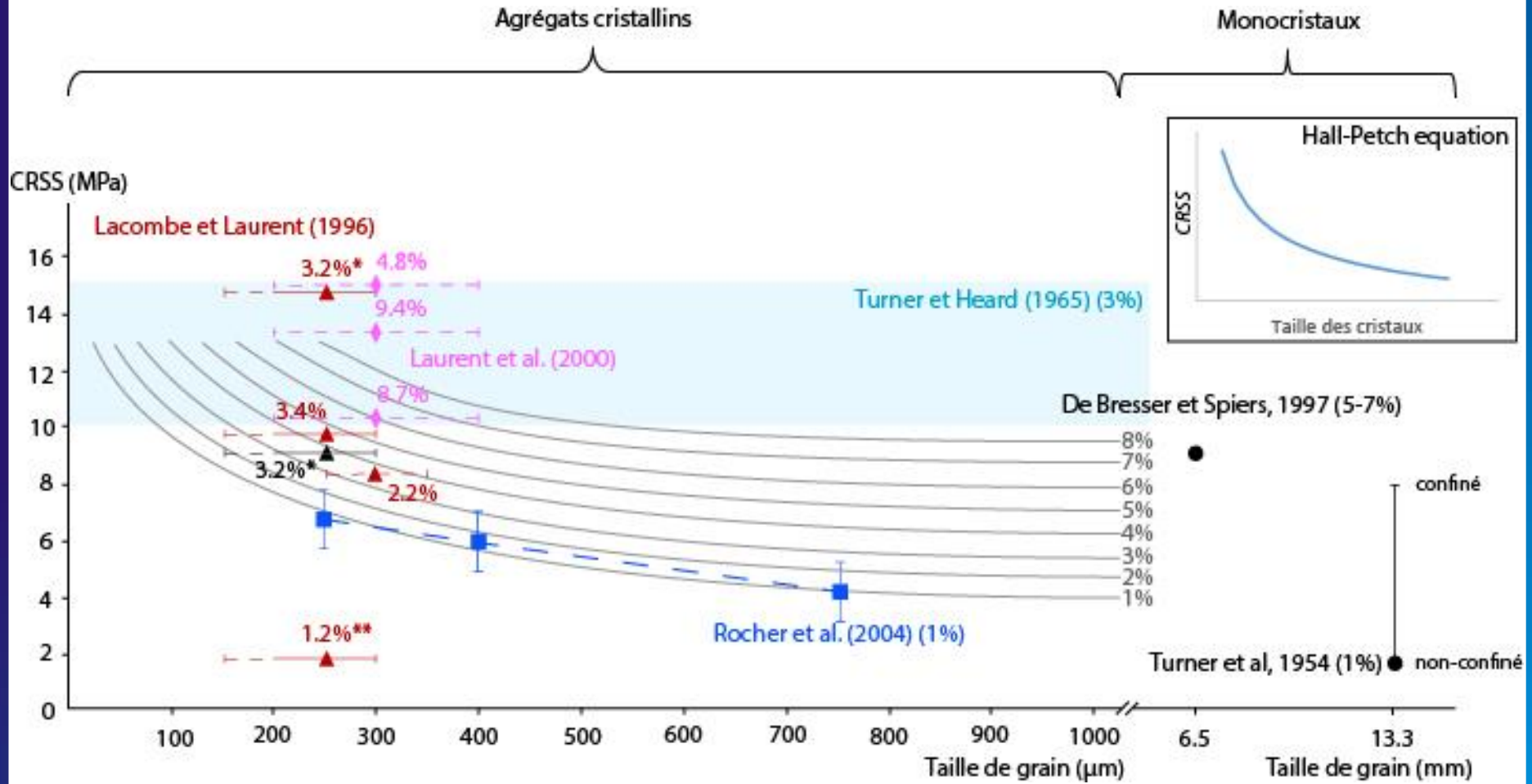


Critical shear stress value for twinning (MPa)

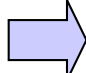


(Lacombe, 2001, 2010)

The CRSS is ~ independent on T°C but depends on grain size and internal strain (hardening)



(Parlangeau, 2017)

Inversion of calcite twin data  **Reduced stress tensor
(4 parameters)**

Orientation of principal stresses and stress ratio

$$\Phi = \frac{(\sigma_2 - \sigma_3)}{(\sigma_1 - \sigma_3)}$$

+ dimensionless differential stress

$$(\sigma_1 - \sigma_3) / \tau a$$



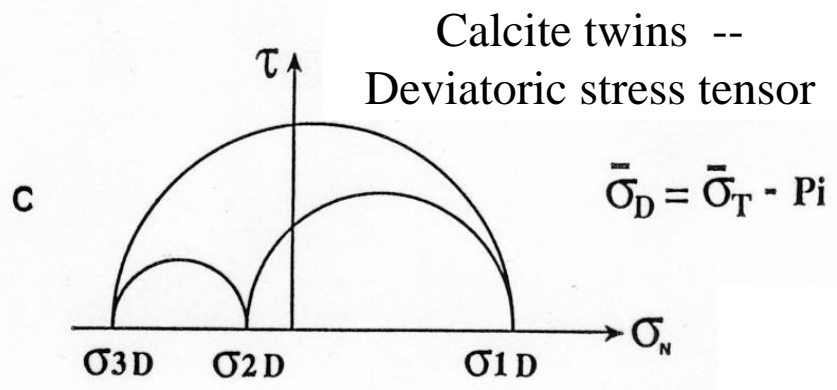
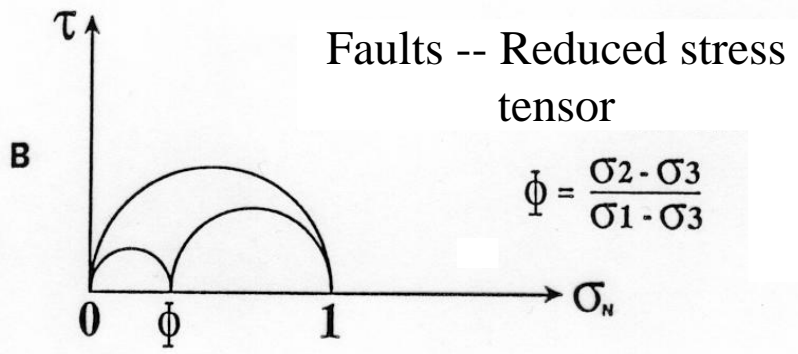
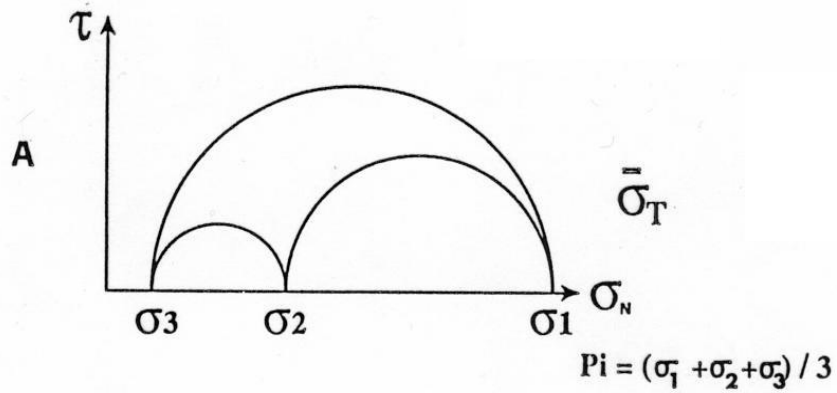
'constant' CRSS τa
for a set of calcite grains
of homogeneous size

Deviatoric stress tensor (5 parameters)

$$T_D = T - \left(\frac{\sigma_1 + \sigma_2 + \sigma_3}{3} \right) \cdot I$$

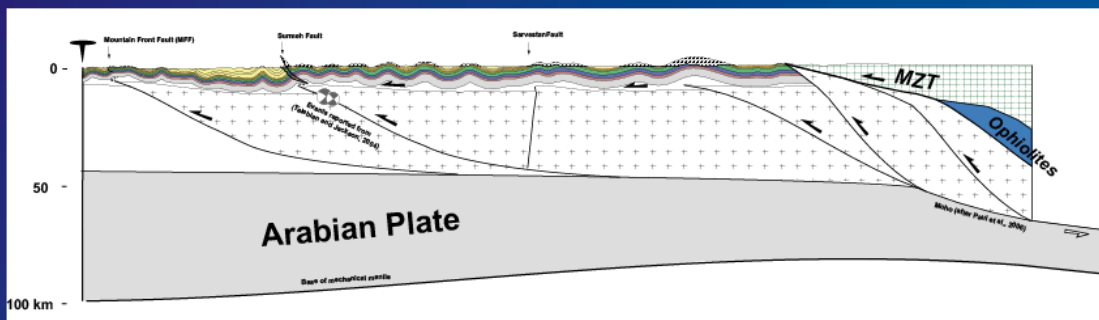
Orientation of principal stresses and differential stress magnitudes

$$(\sigma_1 - \sigma_3) \quad (\sigma_2 - \sigma_3)$$

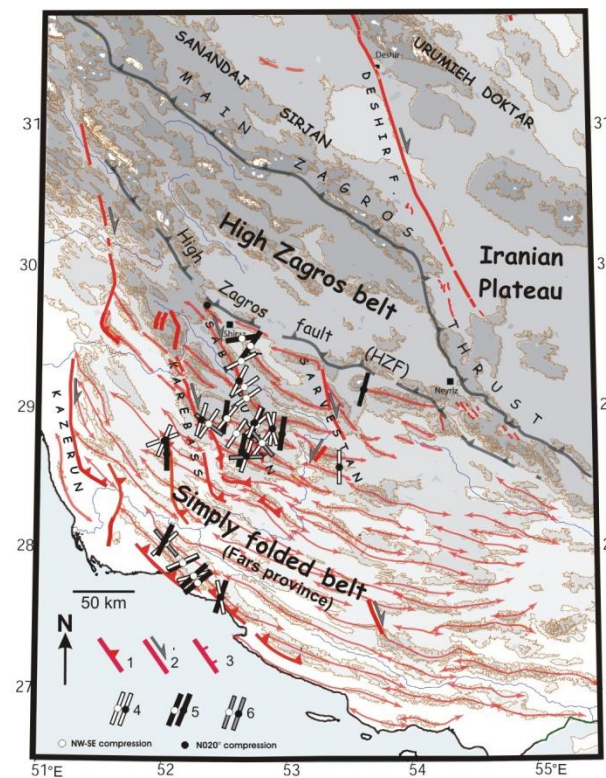


**Differential stress magnitudes
in fold-and-thrust belts and orogenic forelands
Some examples**

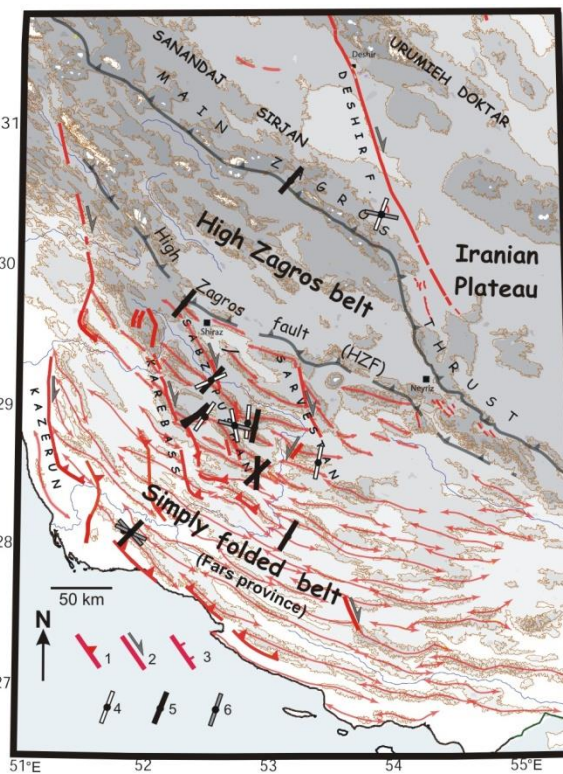
Zagros : Neogene/ongoing collision between Arabia and Central Iran



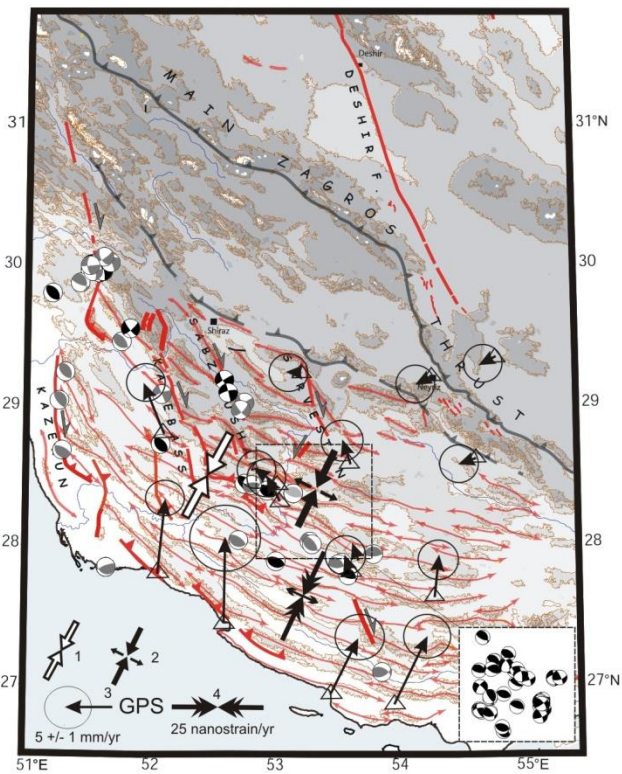
Collisional stresses consistently recorded at all scales



Neogene compressional trends from fault slip data (Lacombe et al., 2006)

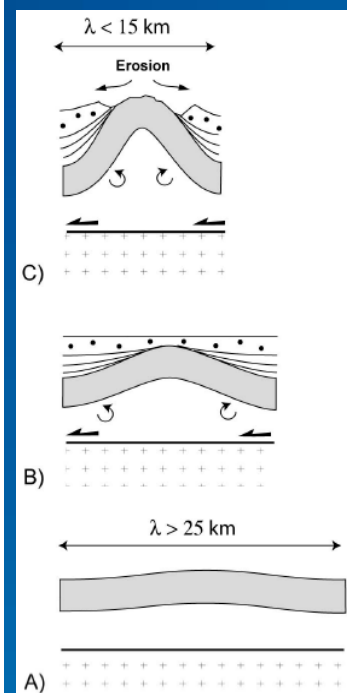
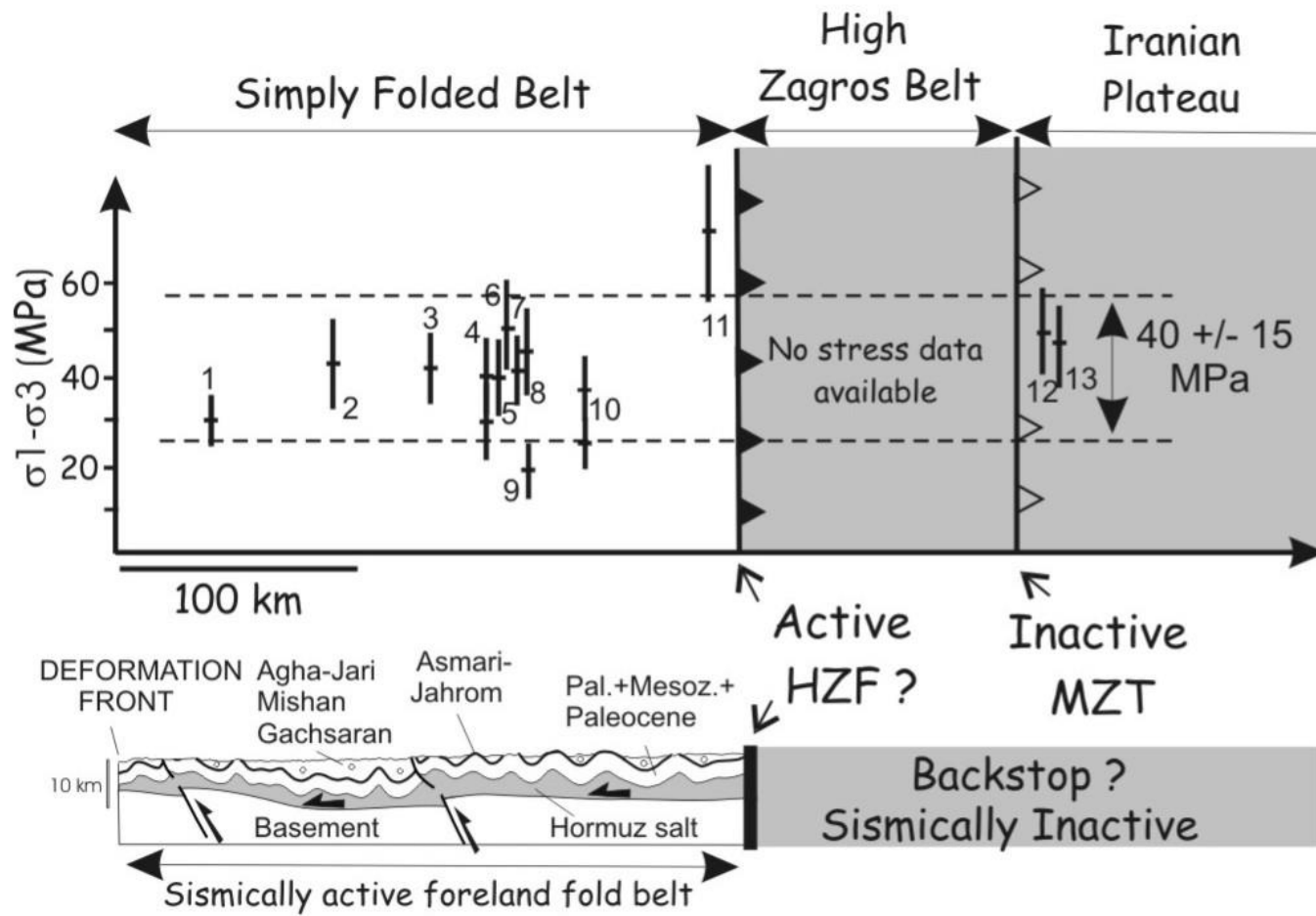


Neogene compressional trends from calcite twin data (Lacombe et al., 2007)



Current compressional trends from earthquake focal mechanisms (Lacombe et al., 2006) and GPS shortening rates (Walpersdorf et al., 2006)

(Lacombe et al.,
Geology,
2007)

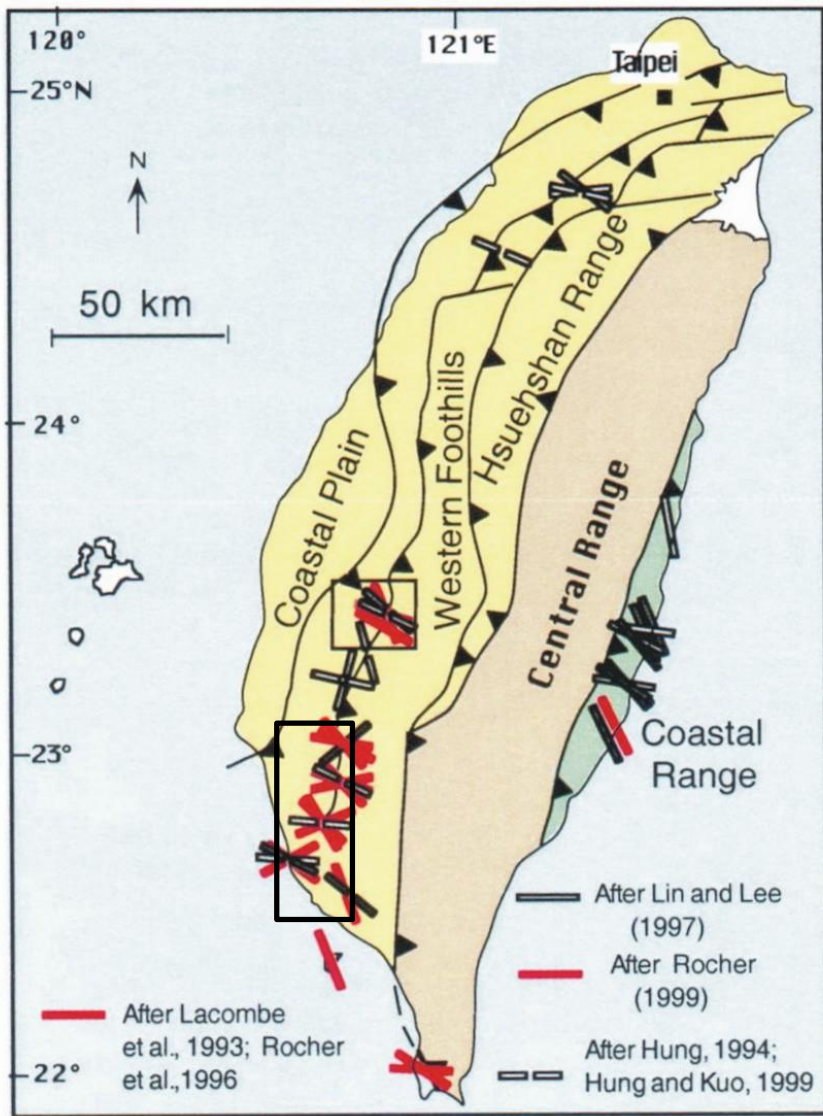


The relative homogeneity of differential stresses agrees with the homogeneously distributed shortening across the SFB, where no deformation gradient toward the backstop is observed in contrast to classical fold-thrust wedges

Both pre- and post-folding differential stresses are low --> folding likely occurred at low stresses; this favours pure-shear deformation and buckling of sedimentary rocks rather than brittle tectonic wedging.

Arabia-Eurasia collisional stresses were consistently recorded by calcite twinning in the detached cover of the Zagros (Fars).

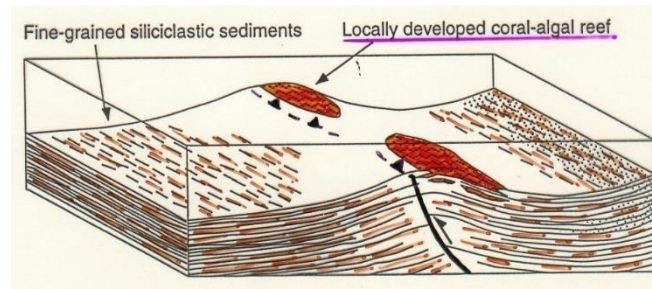
Calcite twinning paleopiezometry reveals an unexpected low level and first-order homogeneity of differential stresses across the SFB, which supports an overall mechanism of buckling of the cover sequence.



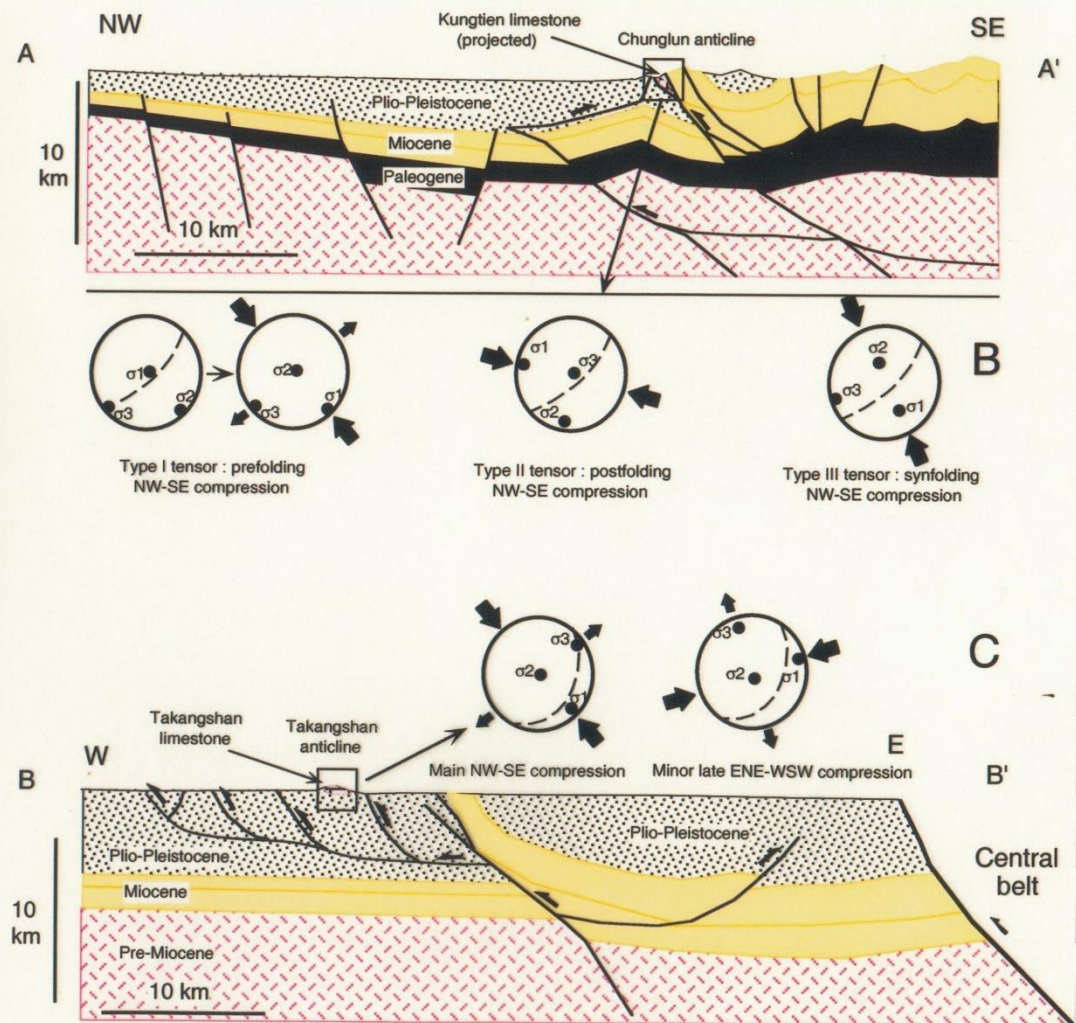
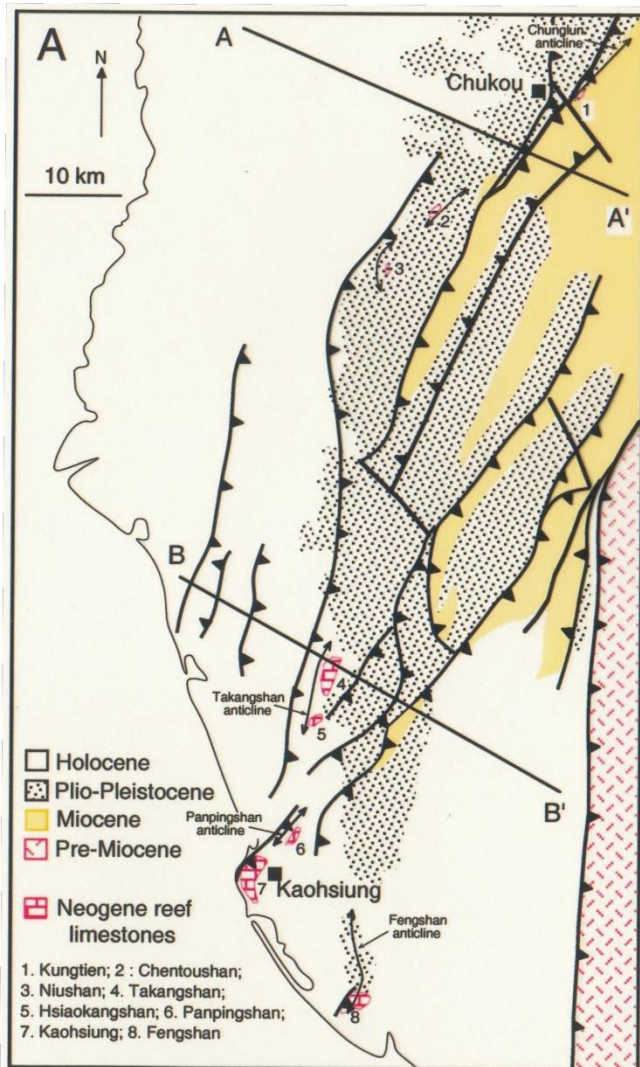
(Lacombe, 2001)

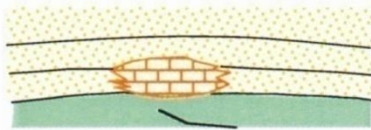
Age	Martini's zones	Chiayi-Hsinying area		Kaohsiung area		
		Units	Units	Units	Units	
Pliocene	Late	NN20	Liushuang	Taiwan	FS	
			Erchungchi	Liushuang	Lingkou Congl.	
	Early	NN19	U.	Kanhshialiao	Erchungchi	Lingkou Congl.
			M.	NS	U. Gutingkeng	
		L.	Liuchungchi	HKS PPS KH		
Pliocene	Early	NN16-18	Yunshuichi	L. Gutingkeng	Nanshihulun	
		NN15 NN13	KT CTS	F		
	Late	NN12	Niaotsui		Kaitzeliao	
		NN11	Chunglun	Mucha	Wushan	

Stratigraphy of the reef limestones of the southwestern Taiwan.

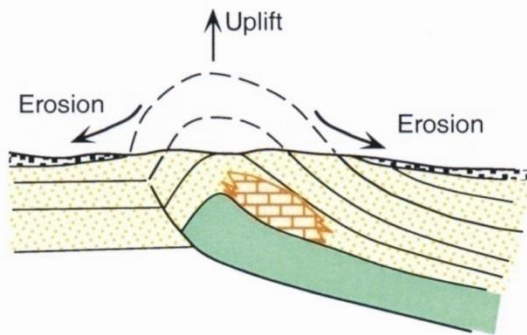


(Gong et al., 1995)

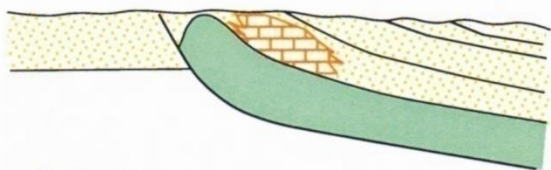




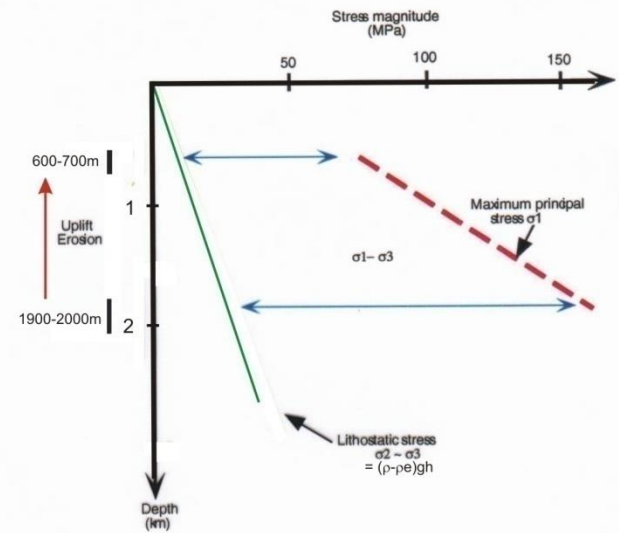
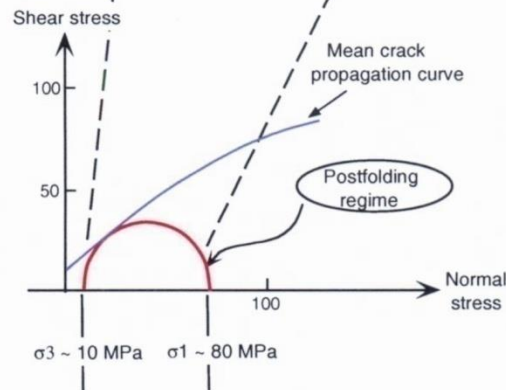
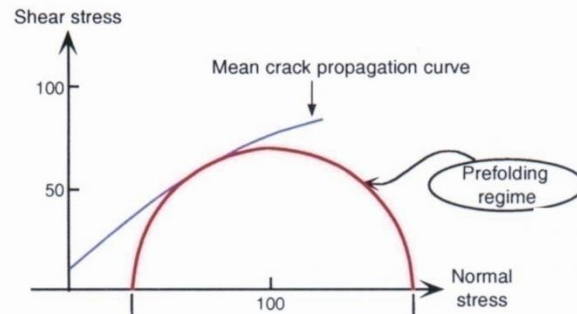
A Prefolding compression (LPS)
Main twinning event

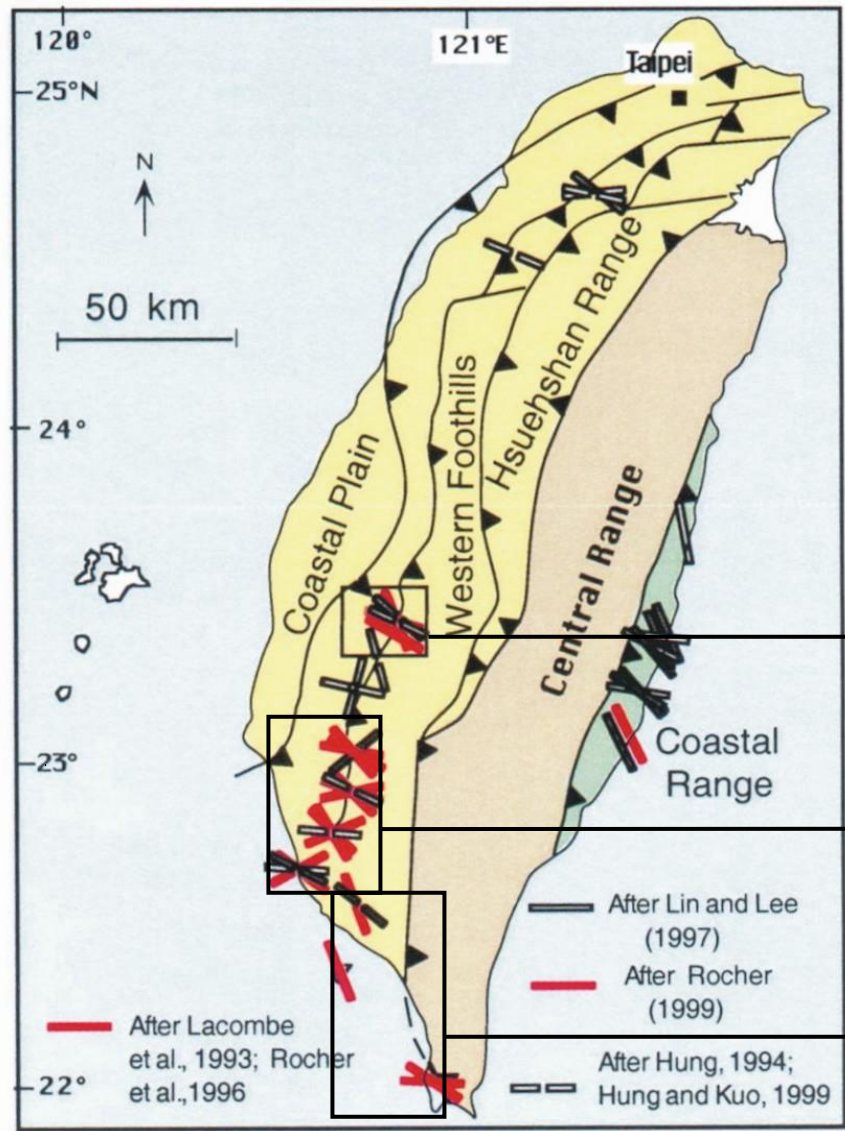


B Synfolding compression and erosion



C Postfolding compression
Main twinning event





After removing the effect of lateral variations of burial...

~ 140 MPa
~ 70 MPa

~ 60 MPa

~ 25-35 MPa

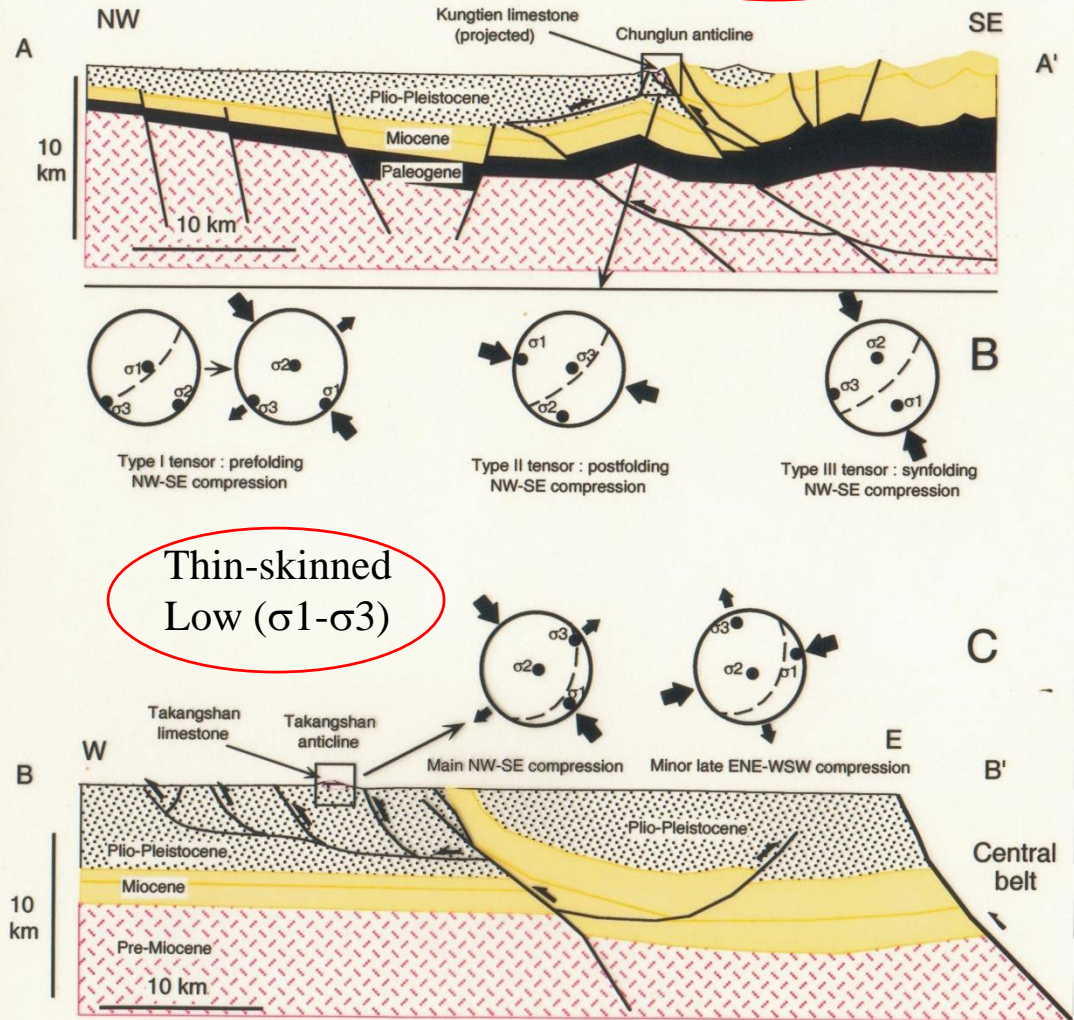
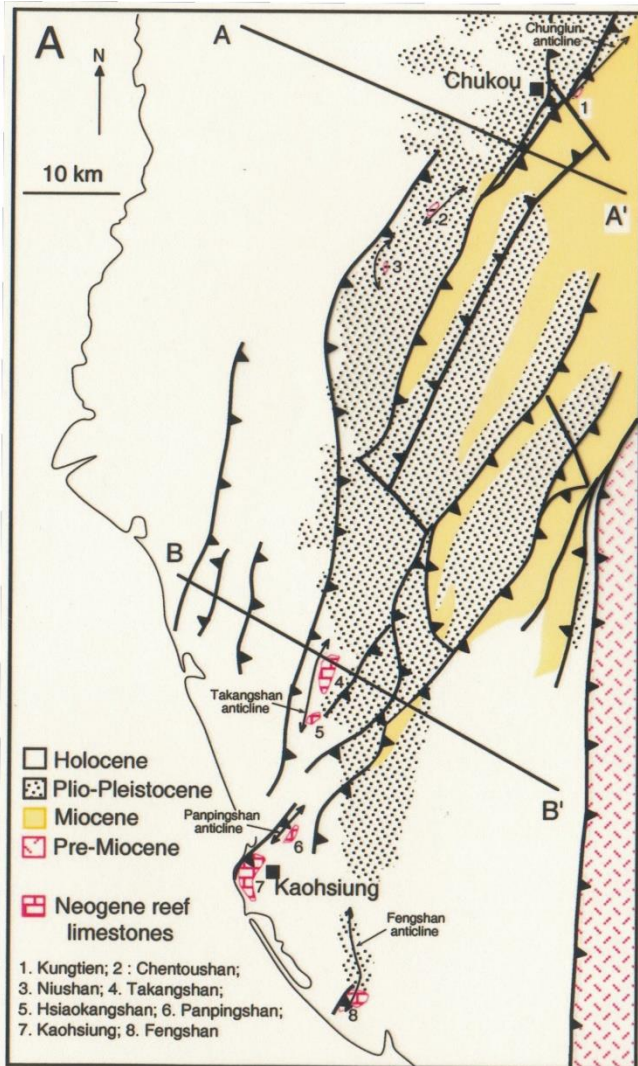
Differential stress decrease

« Collision » stage
Thick-skinned tectonics

« Accretionary wedge » stage
Thin-skinned tectonics

After removing the effect of lateral variations of burial...

Thick-skinned High (σ_1 - σ_3)



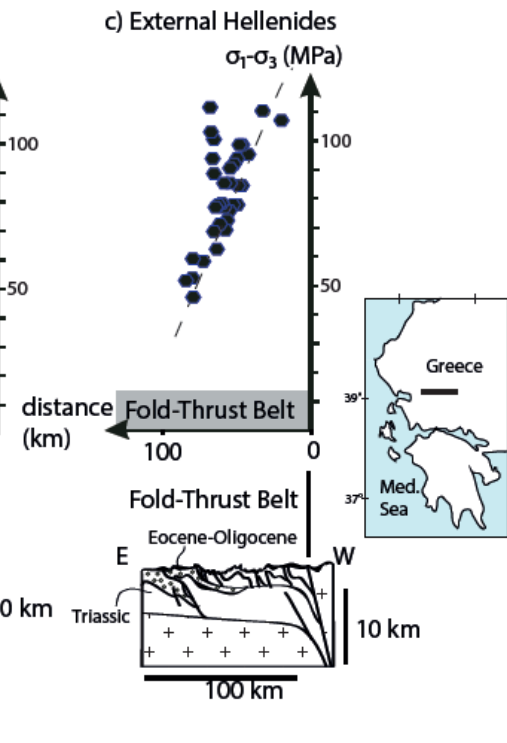
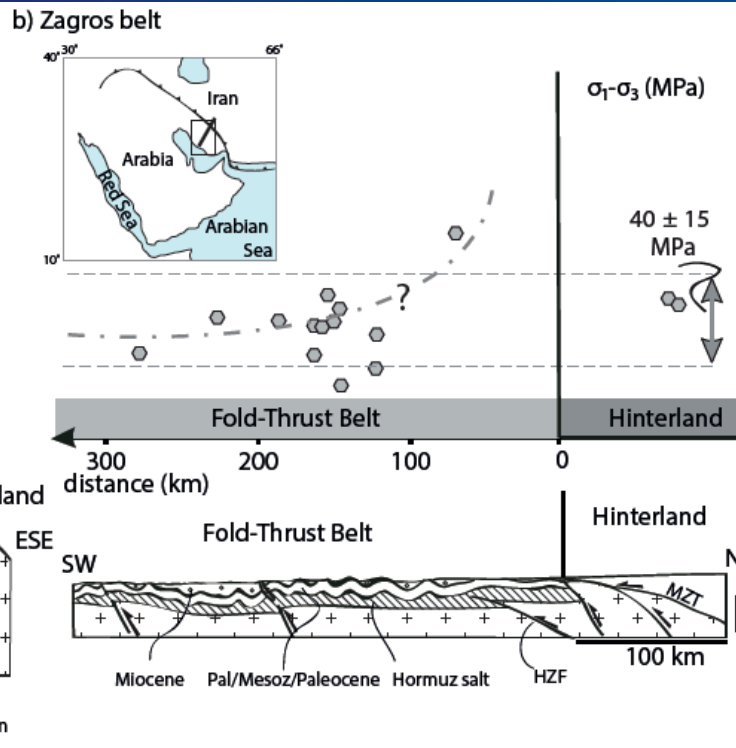
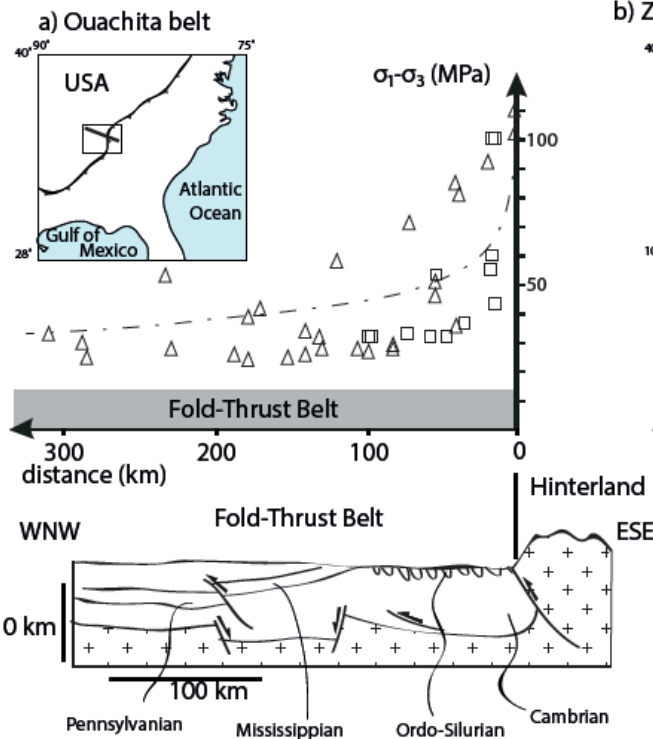
Calcite twinning analyses in Taiwan Foothills document possible along-strike changes in differential stress magnitudes recorded by cover rocks depending on the tectonic style.

Calcite twinning analyses in orogenic foreland possibly document a decrease of differential stress magnitudes with increasing distance to the belt

(Hnat et al., 2013;
Van der Pluijm et al., 1997)

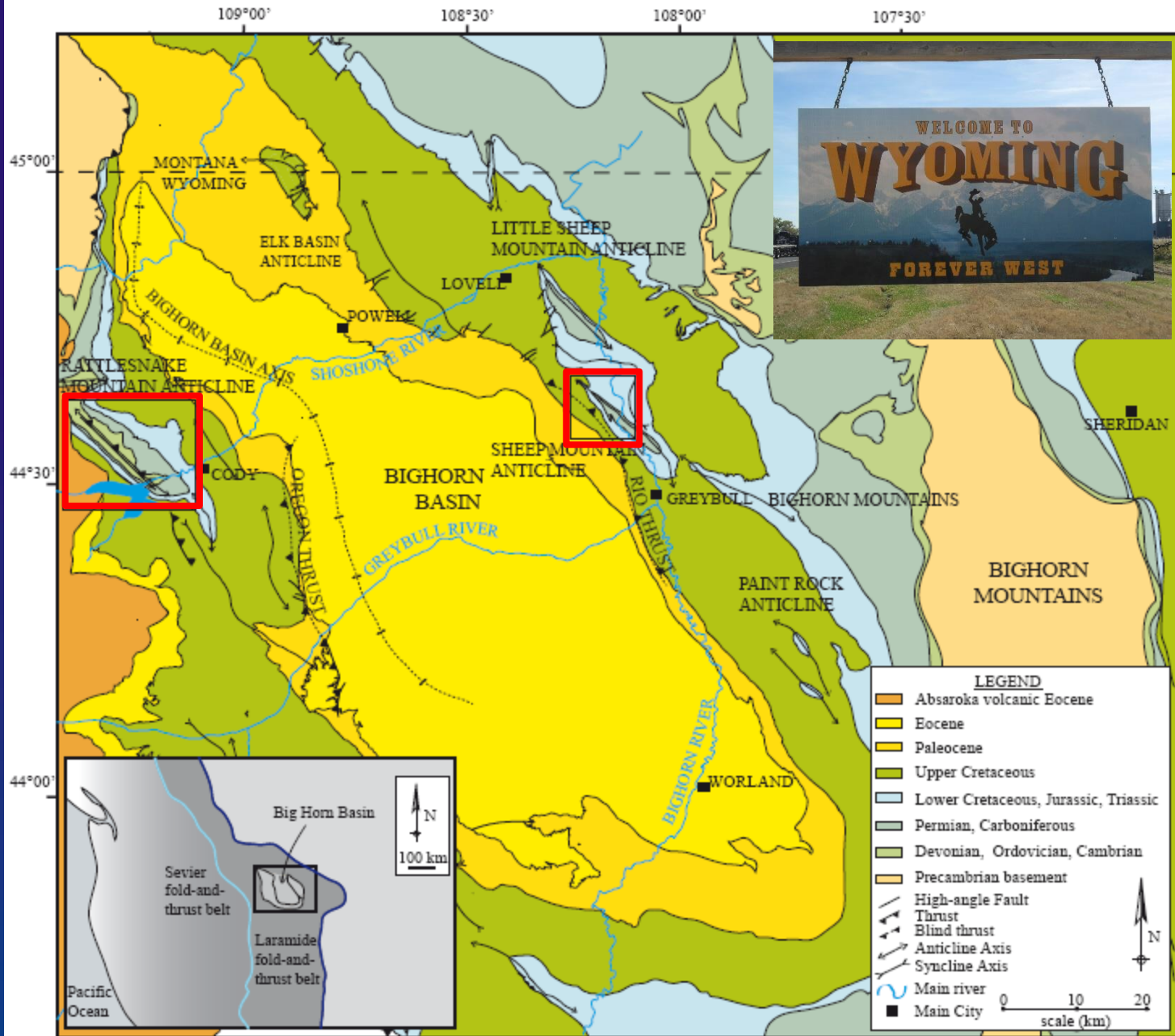
(Lacombe et al., 2007)

(Xypolias & Koukouvelas,
2005)



(Beaudoin and Lacombe, 2018)

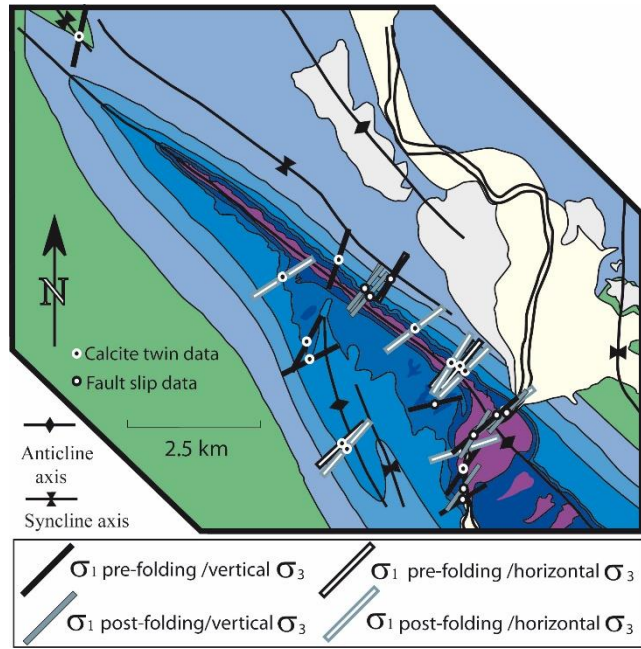
... and also in the north Pyrenean foreland
(Lacombe et al., 1996; Rocher et al., 2000)...



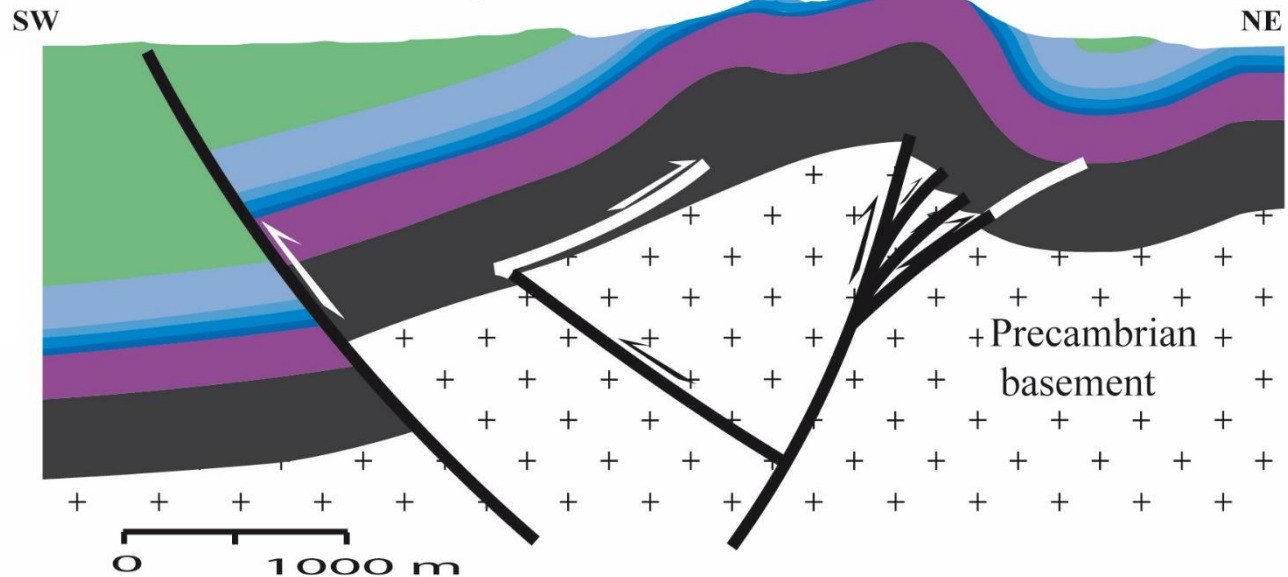
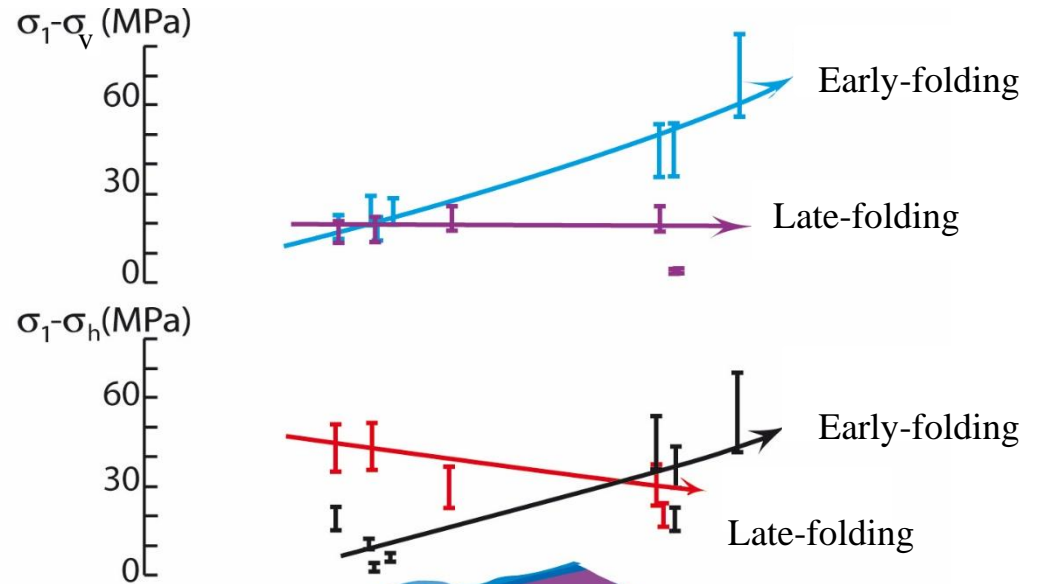
Sheep Mountain anticline



Early-folding and late-folding paleo-differential stress magnitudes from calcite twinning paleopiezometry

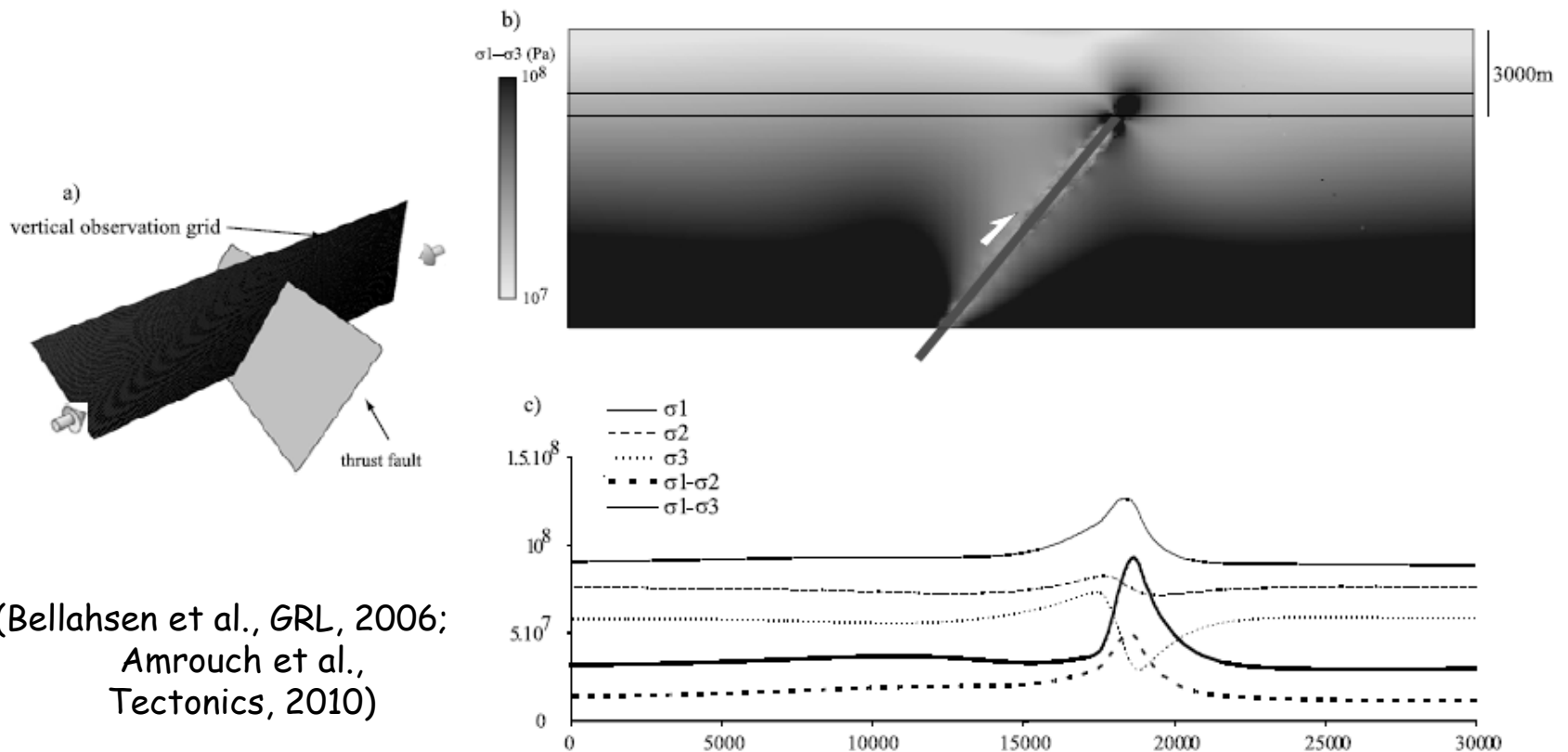
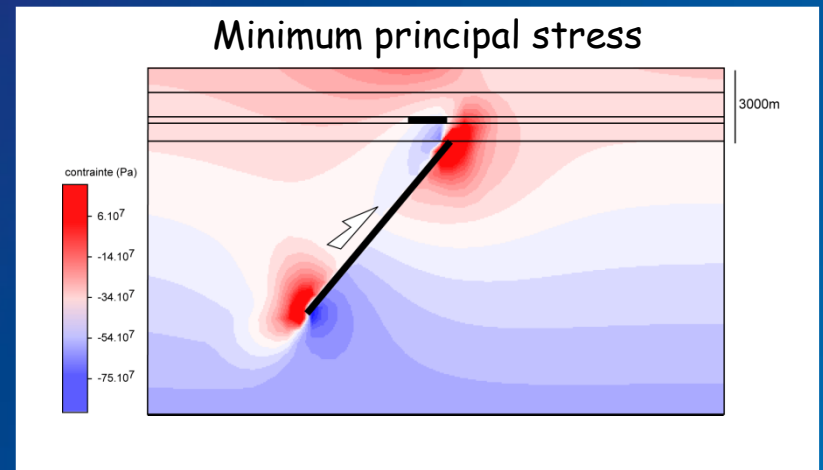


Sheep Mountain anticline



(Amrouch et al.,
Tectonics, 2010)

Stress perturbations in the sedimentary cover at the tip of the underlying basement fault starting to move during Laramide stress build-up

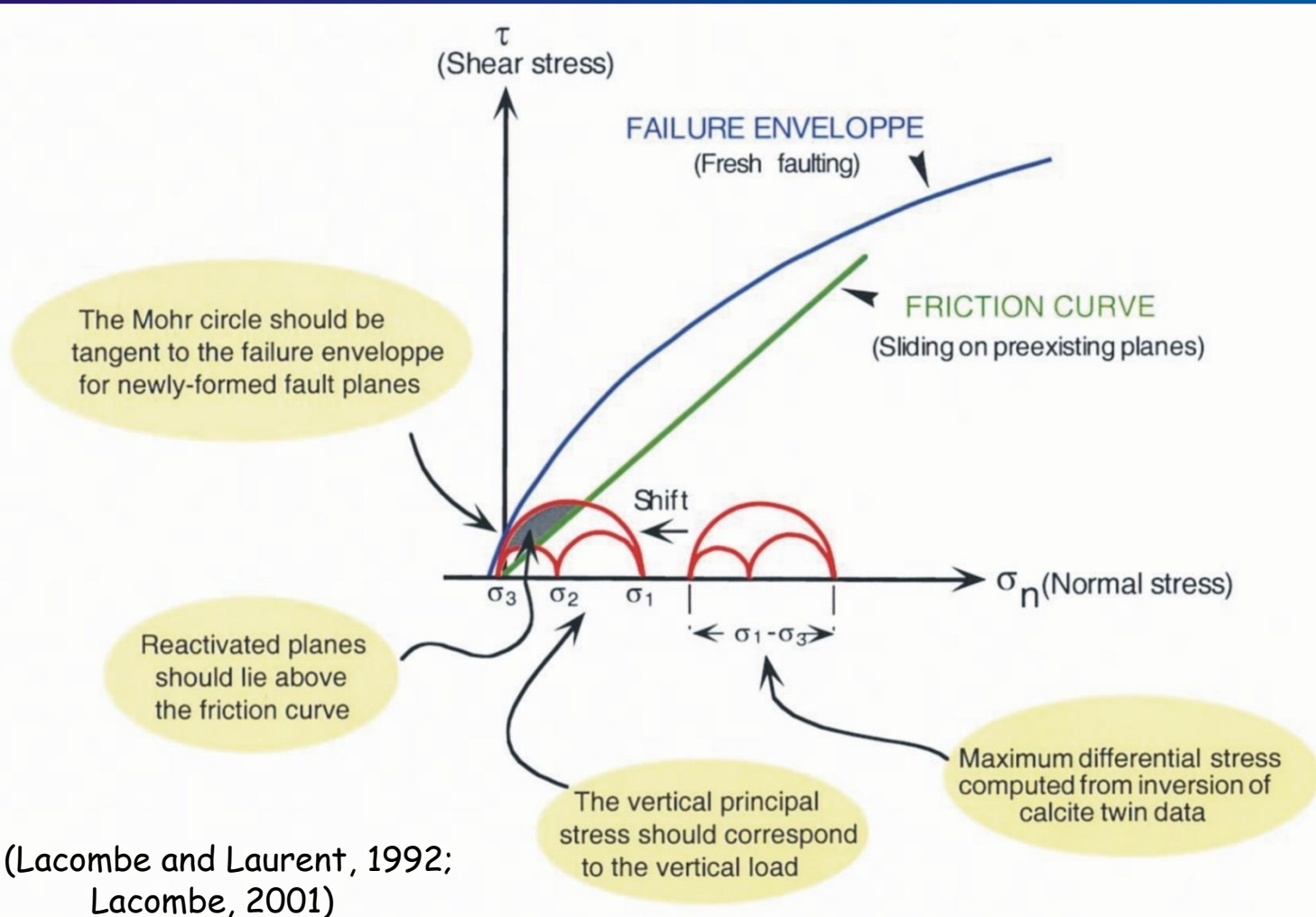


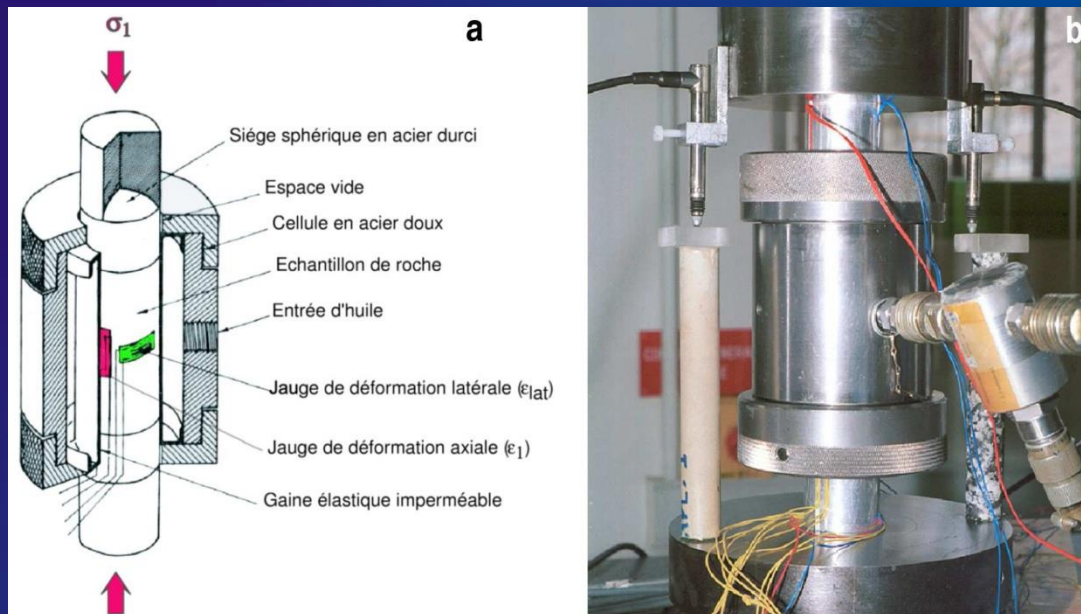
(Bellahsen et al., *GRL*, 2006;
Amrouch et al.,
Tectonics, 2010)

**Determination of principal stress magnitudes,
(i.e., the complete stress tensor)**

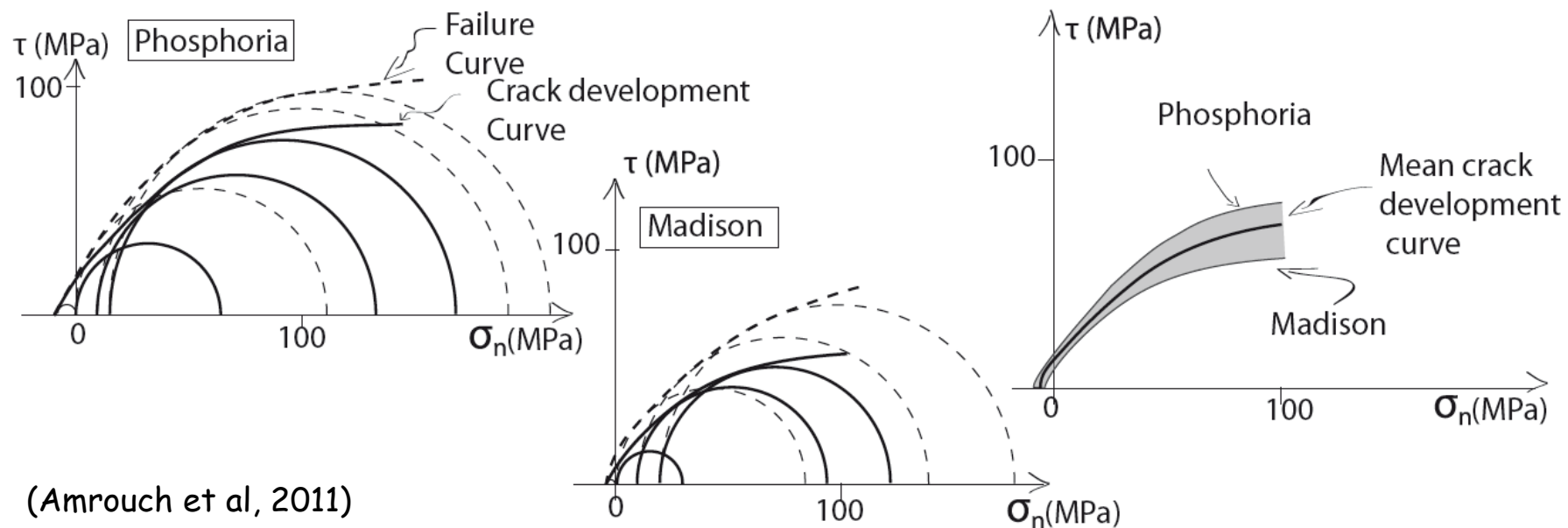
Quantifying principal stress magnitudes

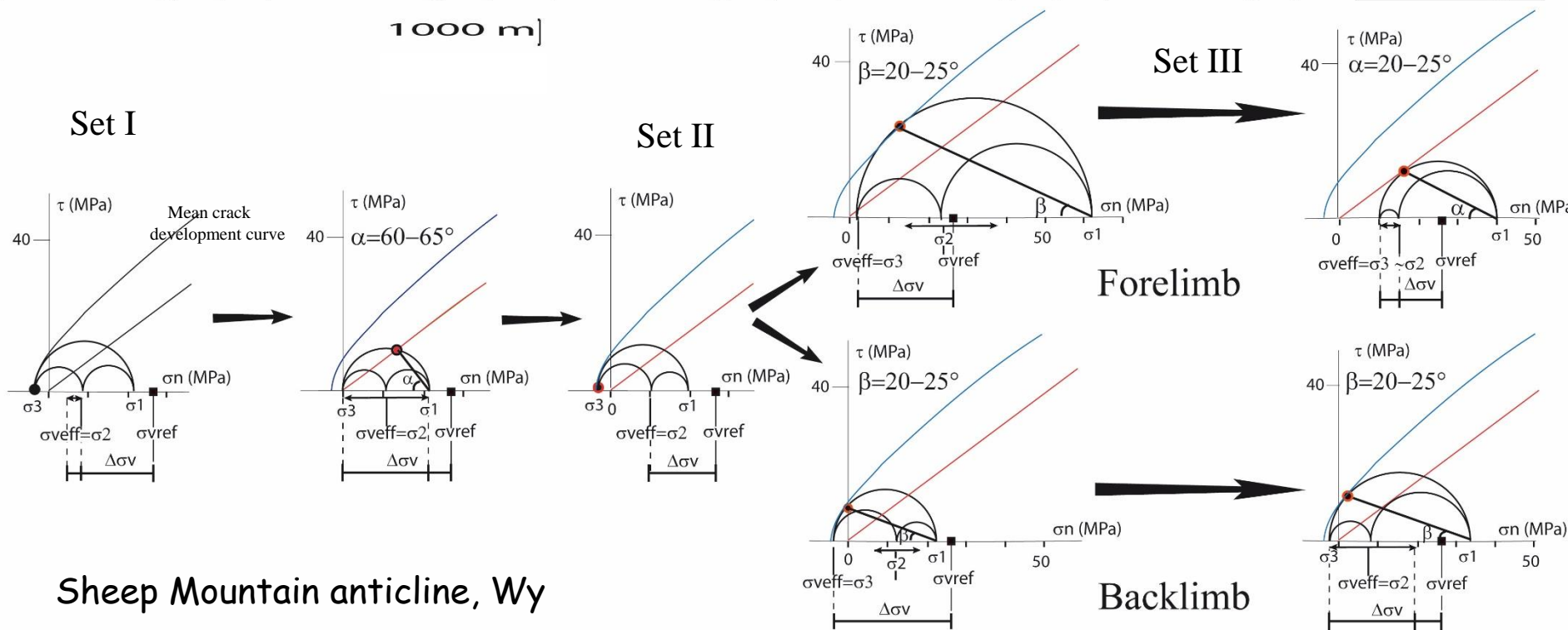
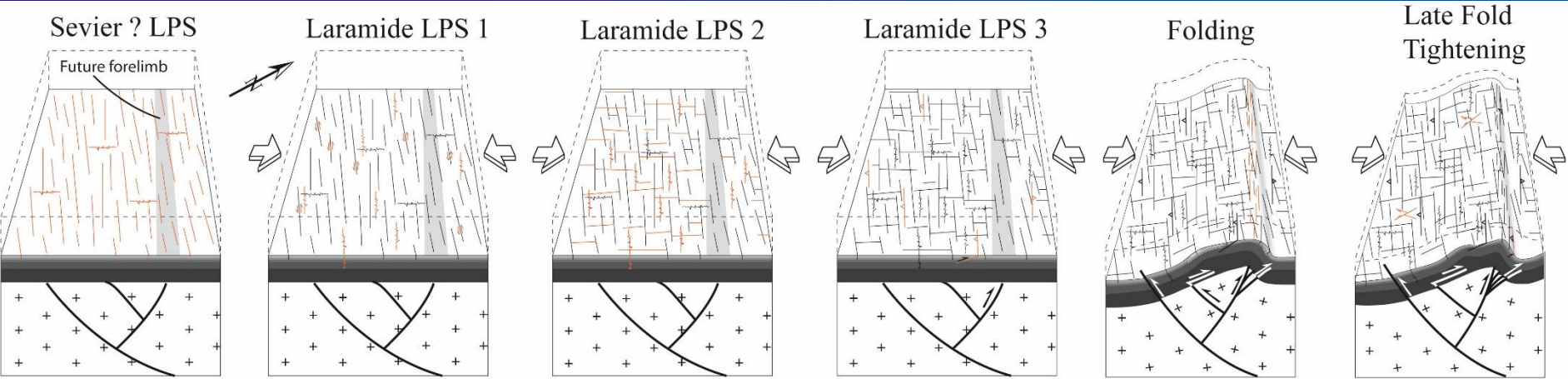
Finding for each deformation step, using a simple Mohr construction, the values of σ_1 , σ_2 and σ_3 required for consistency between differential stresses estimated from calcite twinning, frictional sliding along preexisting planes (i.e., Byerlee's law) and newly formed faulting/fracturing.





Experimental determination of the intrinsic failure envelopes of the Phosphoria and Madison formations





Determination of principal stress magnitudes and $\Delta\sigma_v$ (Amrouch et al, 2011)

Styrolite roughness paleopiezometry

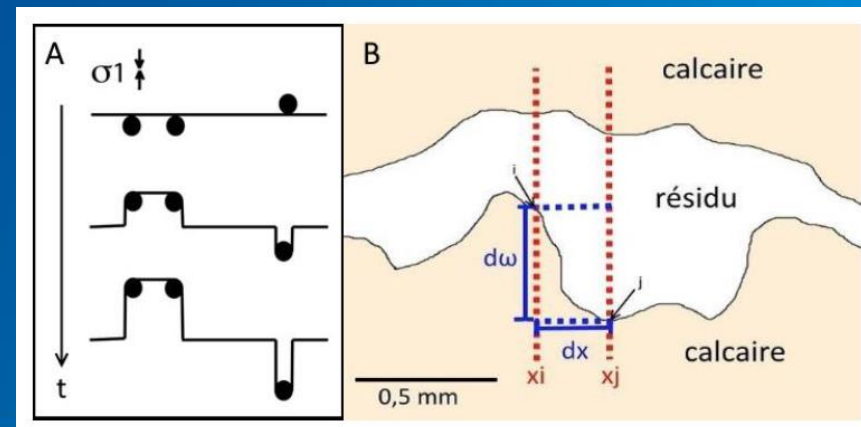
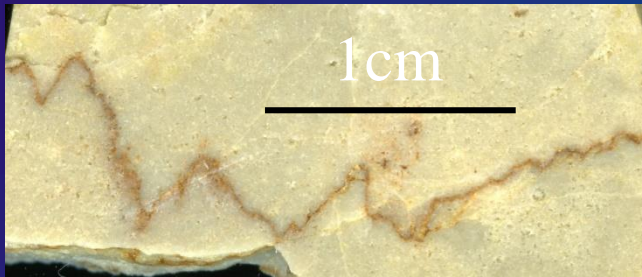
**Principle of inversion of stylolite roughness
for stress (SRIT)**

Thermodynamics and kinetics of the growth of a stylolite :

Once dissolution starts, there is a competition between:

- two stabilizing (smoothing) forces, long-range elastic forces and local surface tension, that tend to reduce the Helmholtz free energy of the solid \rightarrow they flatten the surface by preferentially dissolving areas of local roughness ;

- a destabilizing (roughening) force due to pinning particles on the stylolitic surface, that resists dissolution in specific locations, locally increasing the free energy and producing peaks and teeth.

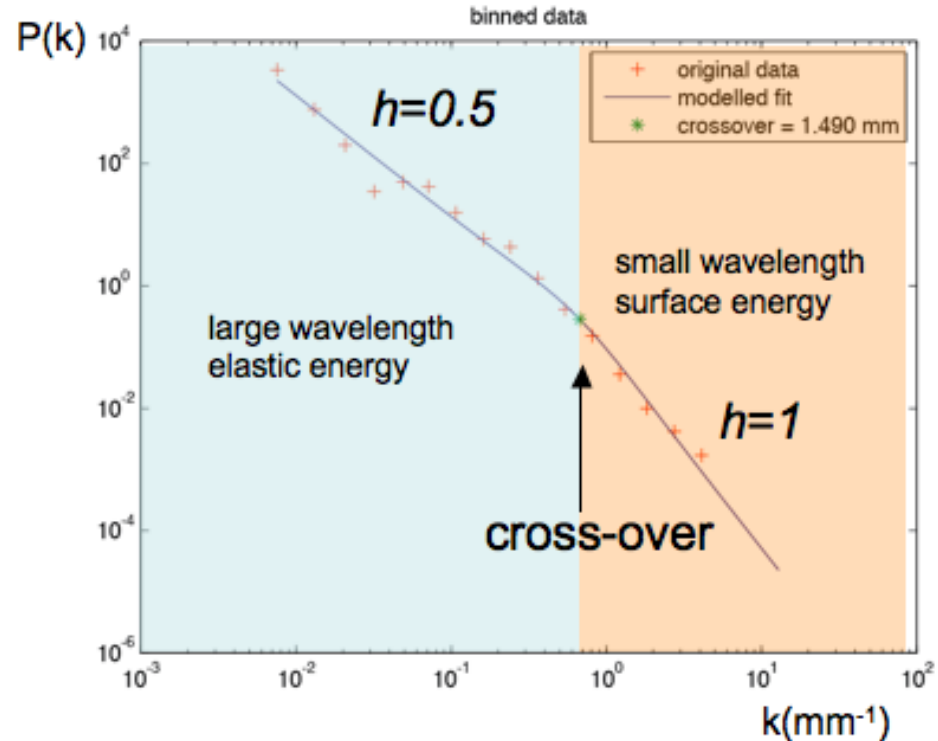
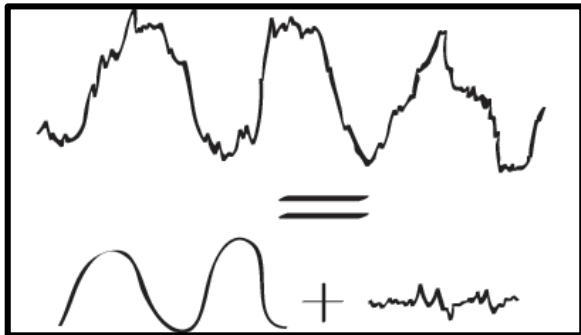


scaling of the roughness

Fourier Power Spectrum

$$P(k) = k^{D-2h}$$

if the signal is self-affine



→ two growth regimes (elastic / surface energy dominated regimes), each of those being characterized by a roughness exponent (Hurst exponent) and separated by a crossover length (L_c) that describes the scale at which the switch between regimes of control occurs.

(Schmittbuhl et al., 2004)

$$L_c = \frac{\gamma E}{\beta \sigma_m \sigma_d}$$

γ : surface energy at the solid-fluid interface, E : Young modulus,
 $\beta = \nu(12\nu)/\pi$: dimensionless number with ν : Poisson ratio,
 σ_m : mean stress, σ_d : differential stress.

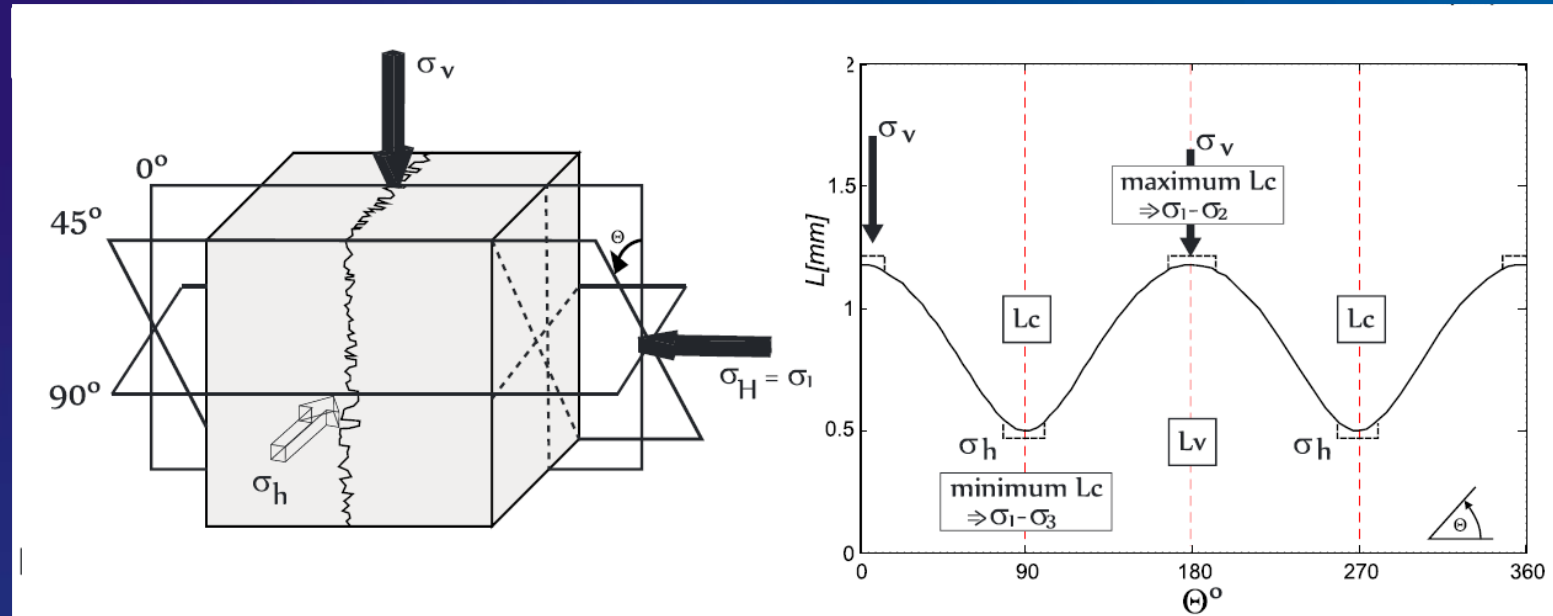
Considering an isotropic stress in the stylolite plane
(sedimentary/bedding-parallel stylolites - BPS) :

$$\left| \begin{array}{l} \sigma_v > \sigma_H = \sigma_h \\ \sigma_H = \sigma_h = \left(\frac{\nu}{1-\nu}\right) \sigma_v \end{array} \right. \rightarrow \left| \begin{array}{l} L_c = \frac{\gamma E}{\beta \alpha \sigma_v^2} \\ \alpha = \frac{1}{3} \begin{pmatrix} 1+\nu & (1-2\nu) \\ 1-\nu & 1-\nu \end{pmatrix} \end{array} \right. \rightarrow \left| \begin{array}{l} \sigma_v = \sqrt{\frac{\gamma E}{L_c \beta \alpha}} \\ \sigma_H = \sigma_h = \left(\frac{\nu}{1-\nu}\right) \sigma_v \end{array} \right.$$

This allows to predict the magnitudes of the normal-to-the-plane stress
and of the two in-plane stresses

In contrast, a tectonic stylolite records a stress anisotropy within the stylolite plane (σ_2 different from σ_3): depending on the orientation of the stylolite the crossover length L_c reflects the differential stress $\sigma_1 - \sigma_2$, $\sigma_1 - \sigma_3$ or a value in between.

If L_c is determined from a 2-D signal, then it depends on the orientation of the cut through the stylolite with respect to σ_2 and σ_3 (σ_1 horizontal and normal to stylolite).

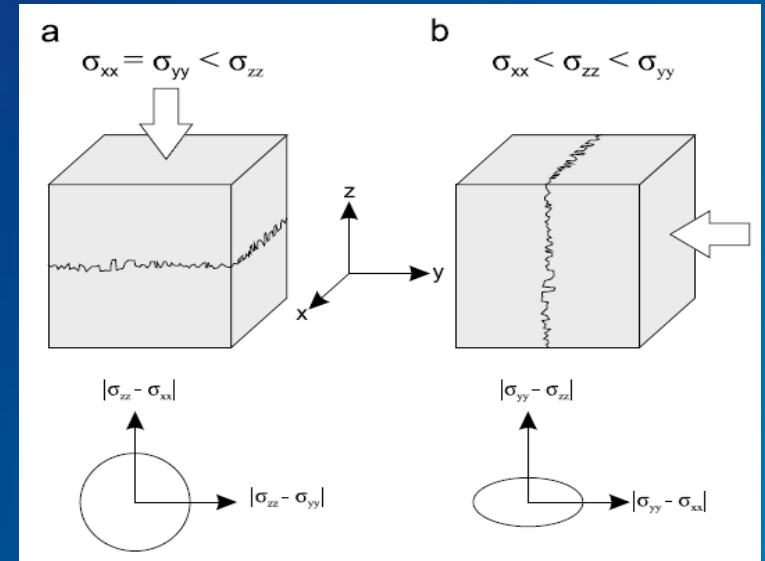


The relationship between L_c and the angle θ is a periodic function, with minimum and maximum L_c separated by $90^\circ \rightarrow$ roughness inversion on 2-D scans of three surfaces normal to the stylolite yields 3 L_c and the 3 corresponding angles θ between the cuts and the vertical direction.

The minimum and the maximum L_c correspond to $(\sigma_1 - \sigma_3)$ and $(\sigma_1 - \sigma_2)$. If θ associated with L_{cmin} is close to the vertical plane ($\theta = 0^\circ$), then σ_2 is horizontal (R regime); otherwise, if θ associated with L_{cmax} is close to 0° , then σ_3 is horizontal (SS regime).

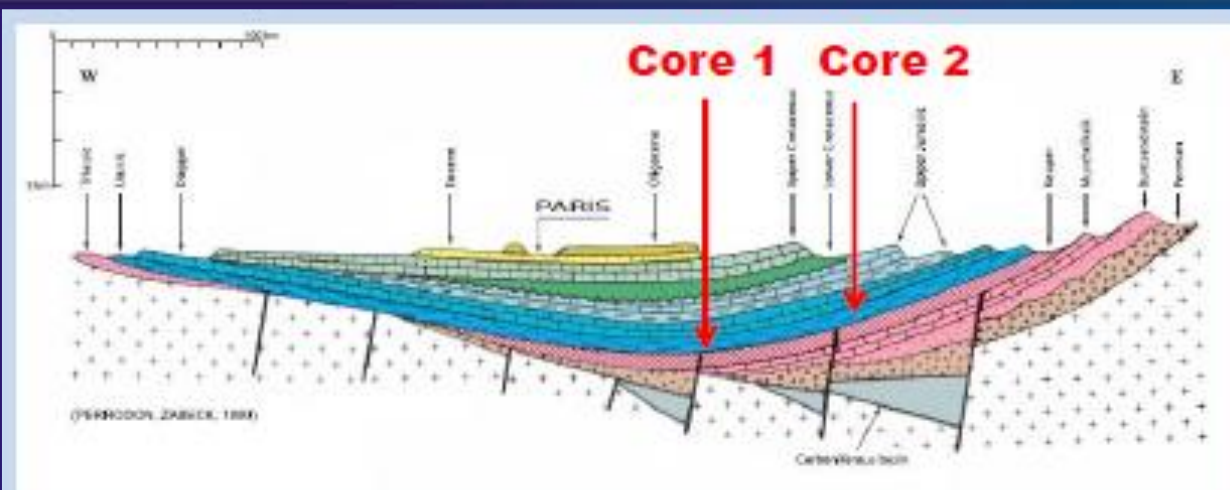
To summarize, Stylolite Roughness Inversion Technique (SRIT) works for :

- Stress direction
- Depth of sedimentary stylolites (from shallow to 4000m)
- Tectonic stylolites (needs 3D and assumption of depth)

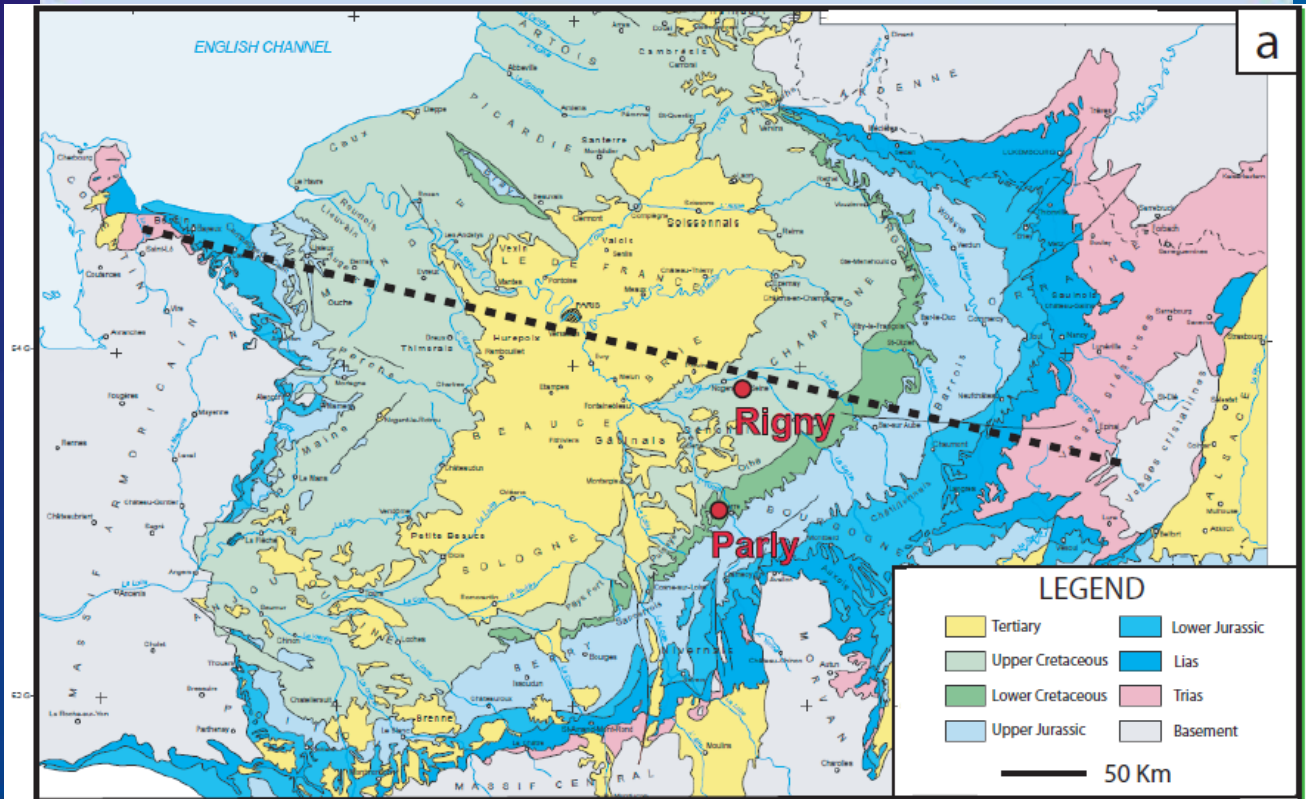


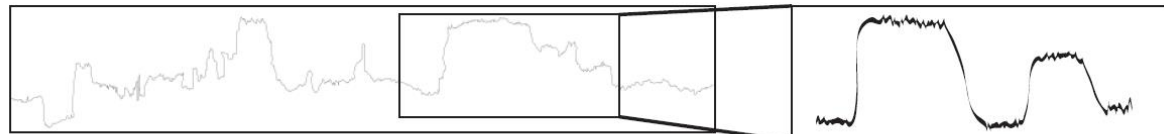
Sedimentary stylolites	Tectonic stylolites
$\sigma_z^2 = \frac{\gamma E}{\alpha \beta L_c}$	$\sigma_y = f\left(\frac{L_v}{L_h}; \sigma_z\right) \pm \sqrt{\Delta\left(\frac{L_v}{L_h}, \sigma_z, \frac{a}{L_h}\right)}$
$\sigma_x = \sigma_y = \frac{\nu}{1-\nu} \sigma_z$	$\sigma_x = \sigma_y - \frac{L_v}{L_h} \sigma_y - \frac{L_v}{L_h} \sigma_z$

**Application of SRIT to paleodepth reconstructions
in poorly tectonized sedimentary basins**

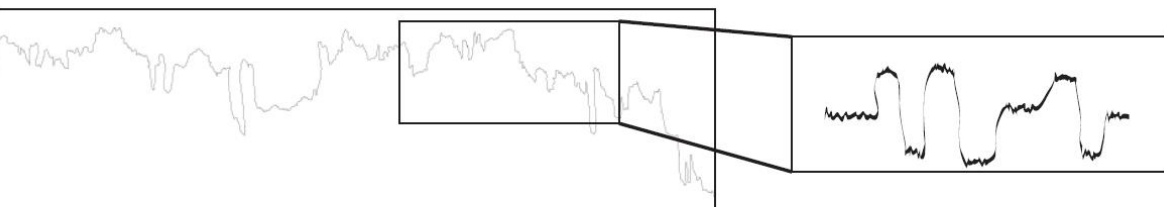


2 Jurassic cores (margin versus depocenter) were chosen.

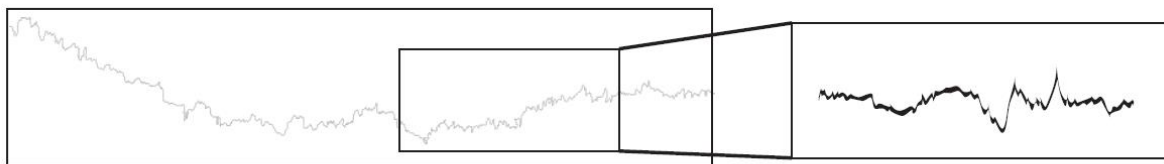
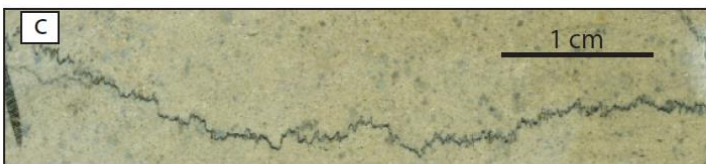




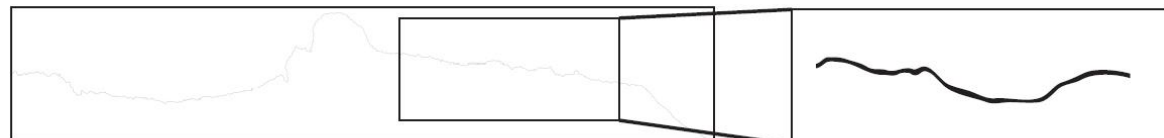
73-S03 - Parly - Class 1: Rectangular columns - Texture 4 (Packstone to Grainstone)



70-S14 - Parly - Class 2: Seismogram with narrow columns - Texture 3 (Floatstone to Packstone)



18-S01 - Parly - Class 3: Suture and sharp peak - Texture 2 (Wackstone to Floatstone)

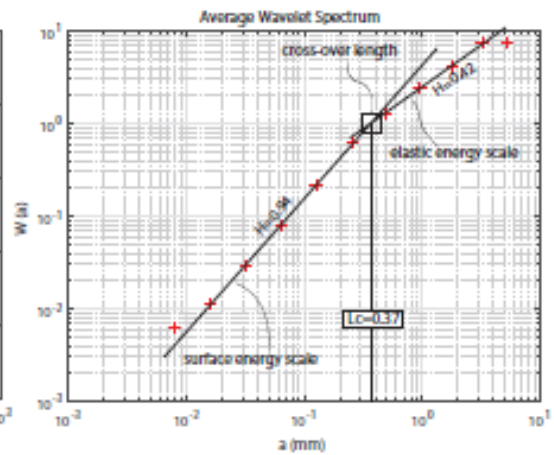
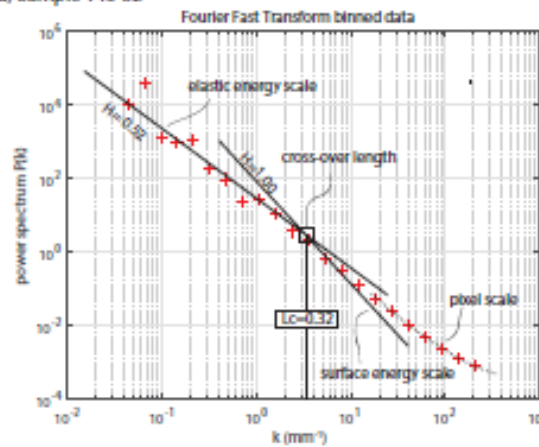


205-S03 - Rigny - Class 4: Simple wave like type - Texture 1 (Mudstone to Wackstone)

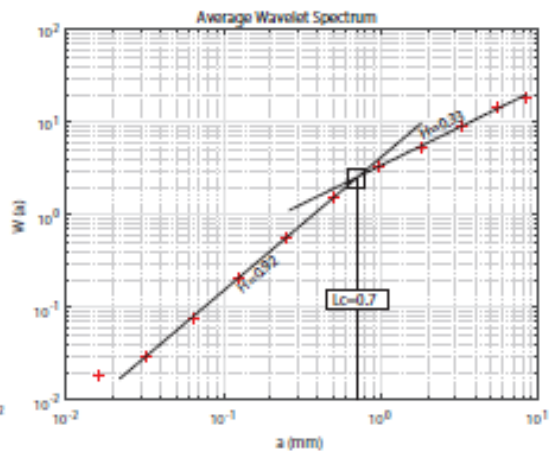
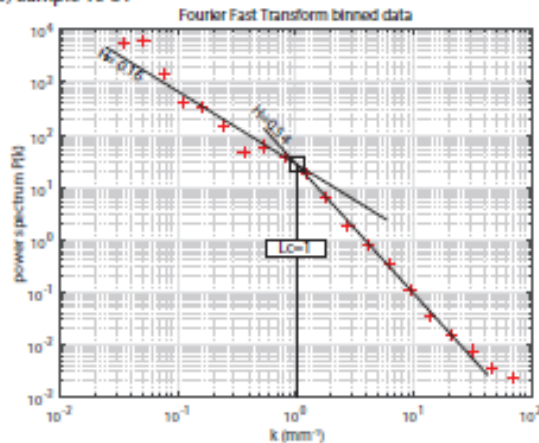
(Beaudoin et al.,
Geological Society of America Bulletin, 2019)

(Beaudoin et al.,
Geological Society of
America Bulletin, 2019)

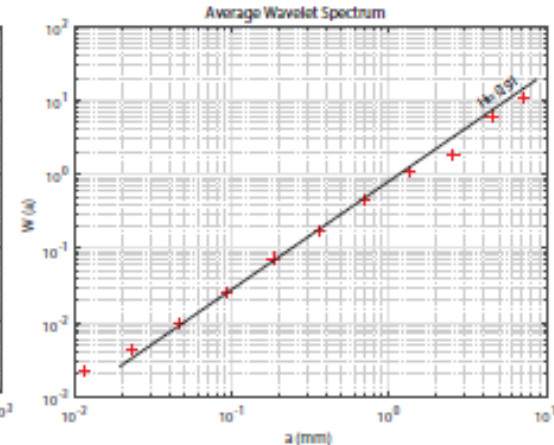
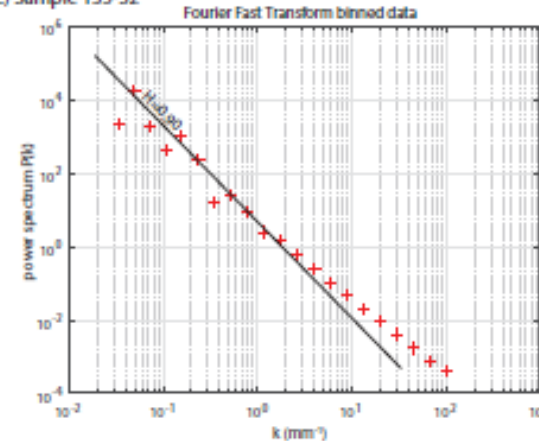
a) Sample 146-S2

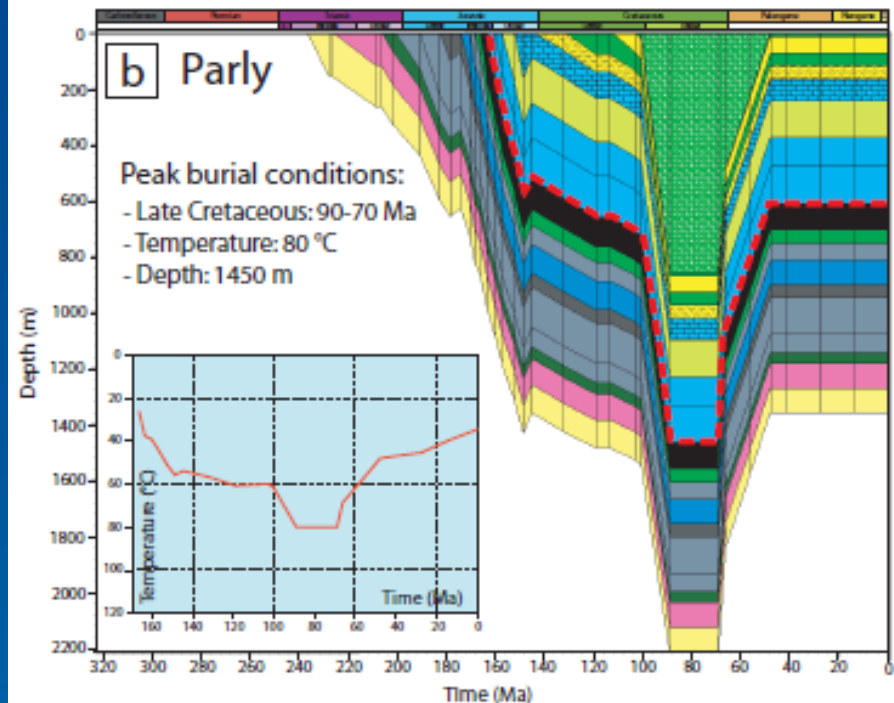
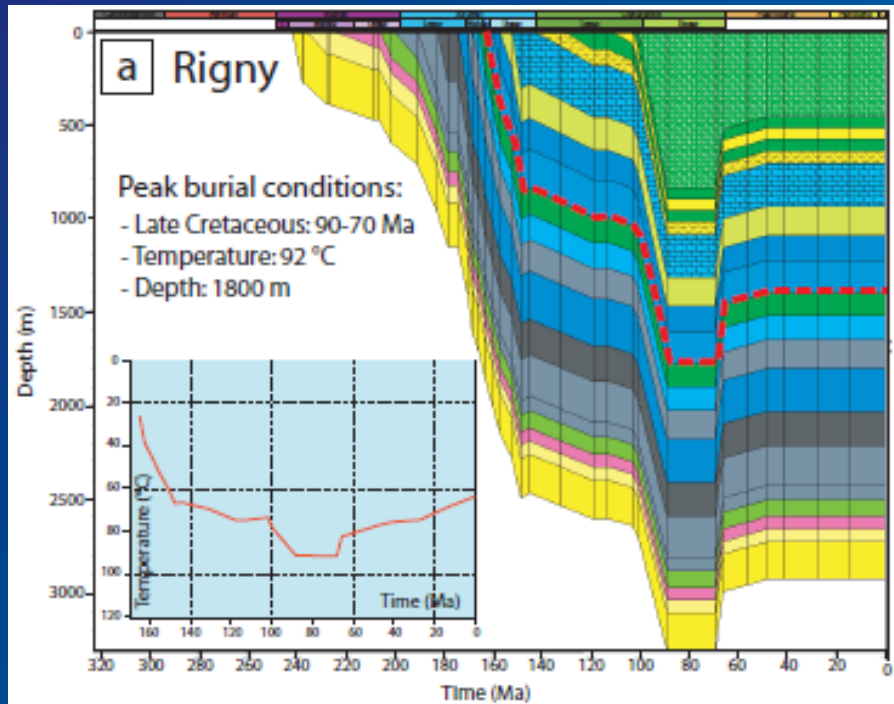
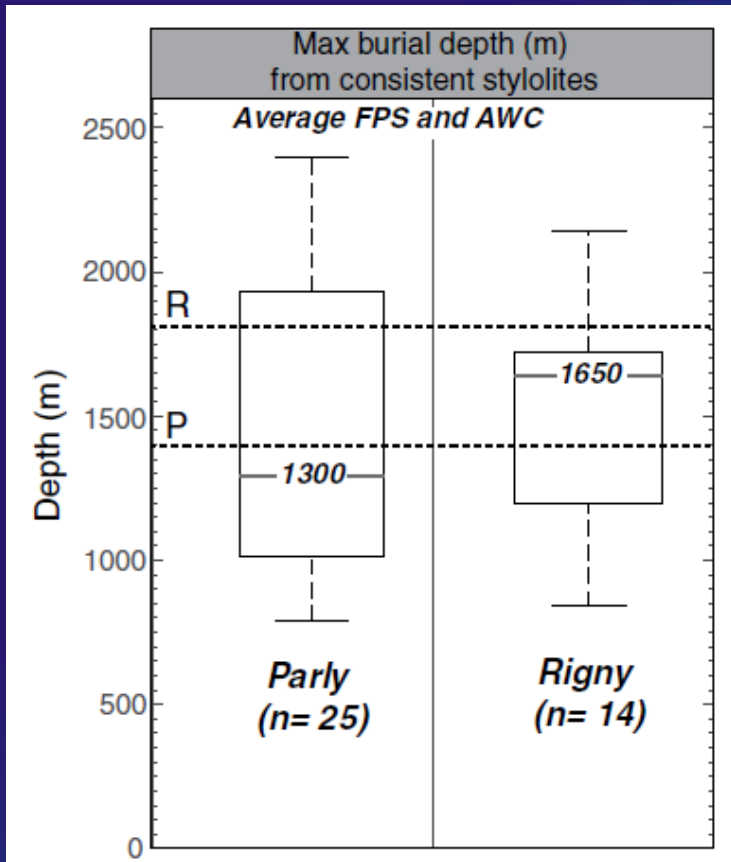


b) Sample 10-S1



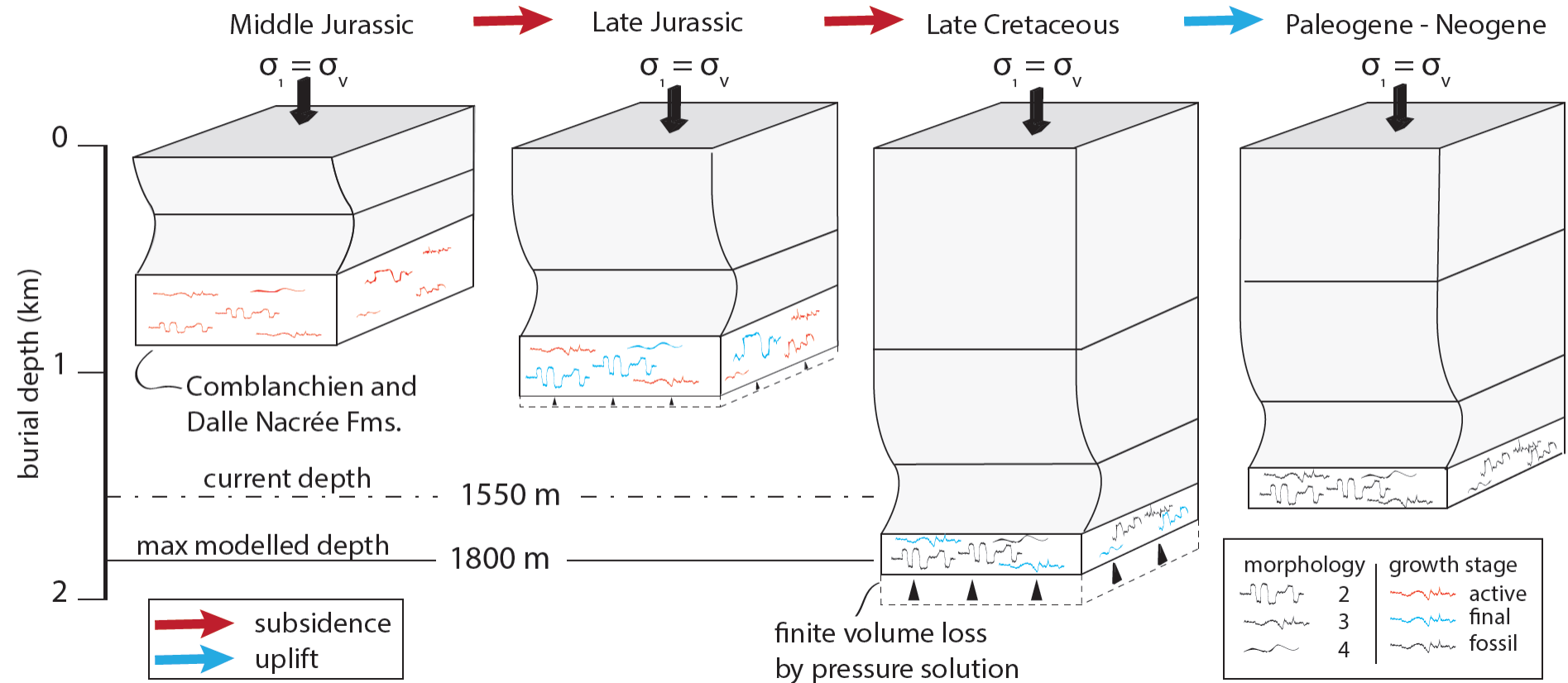
c) Sample 135-S2





Consistency between maximum burial depth from stylolites and results of basin modelling in the Paris basin

(Beaudoin et al.,
Geological Society of America Bulletin, 2019)

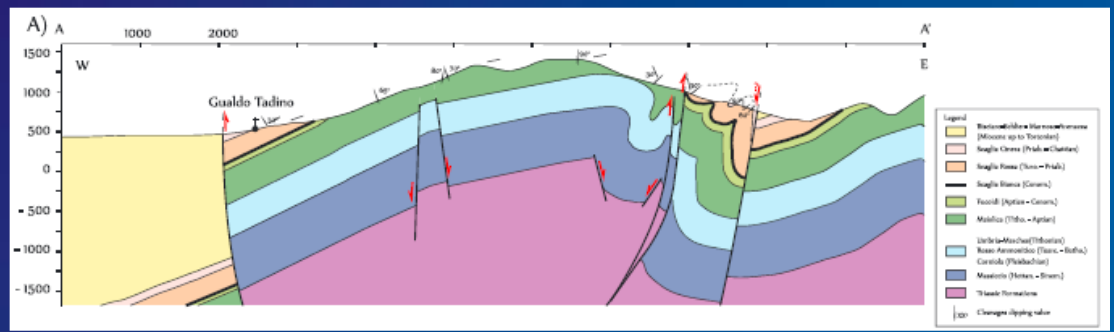
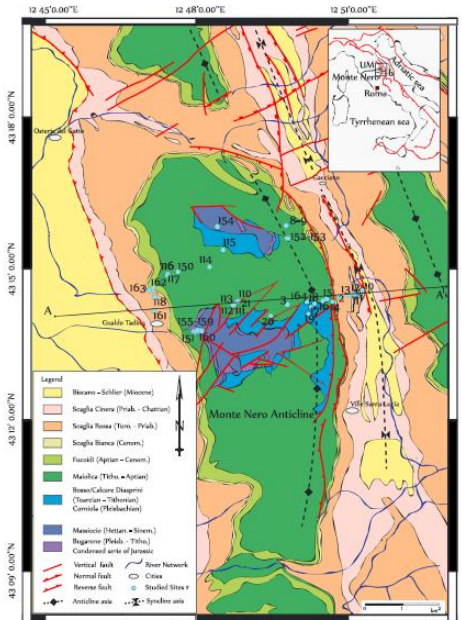


(Beaudoin et al.,
Geological Society of America Bulletin, 2019)

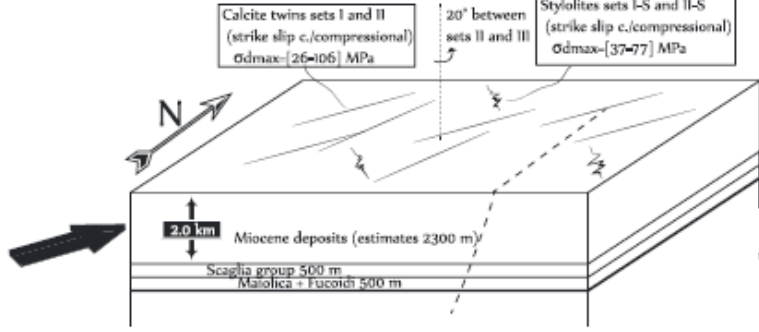
A powerful toolbox : combining
calcite twinning
and stylolite roughness
paleopiezometry

Combining stylolite roughness and calcite twinning paleopiezometry reveals the complexity of progressive stress patterns during folding (Monte Nero anticline, Apennines, Italy)

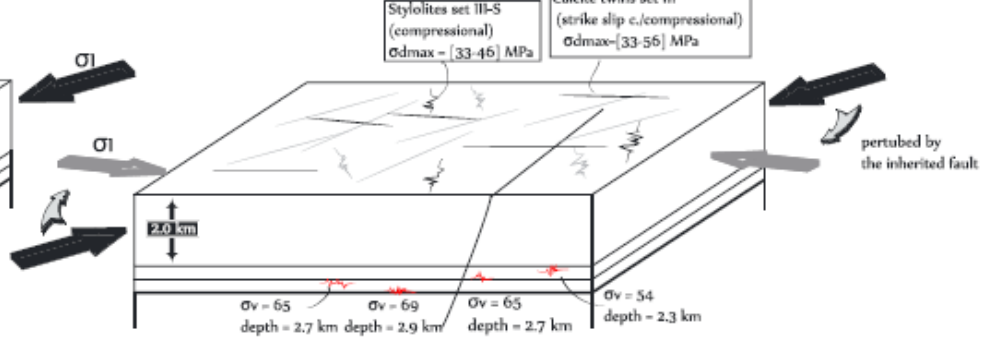
Beaudoin et al.,
Tectonics,
2016



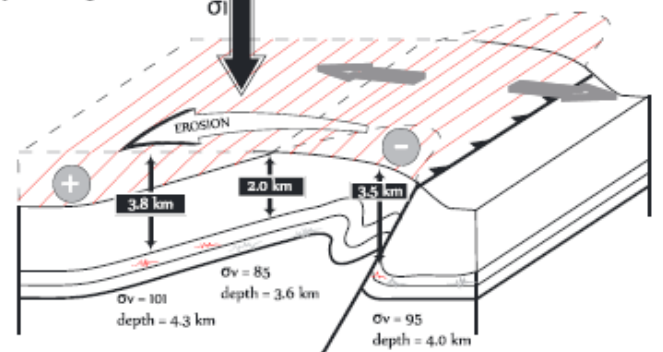
LPS: Pre-folding stage



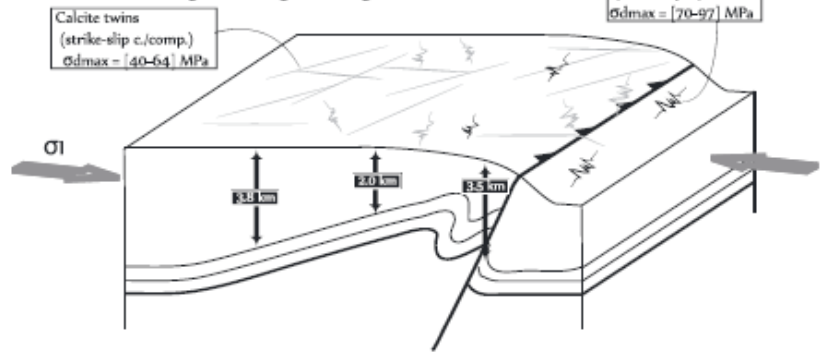
LPS: Early-folding stage



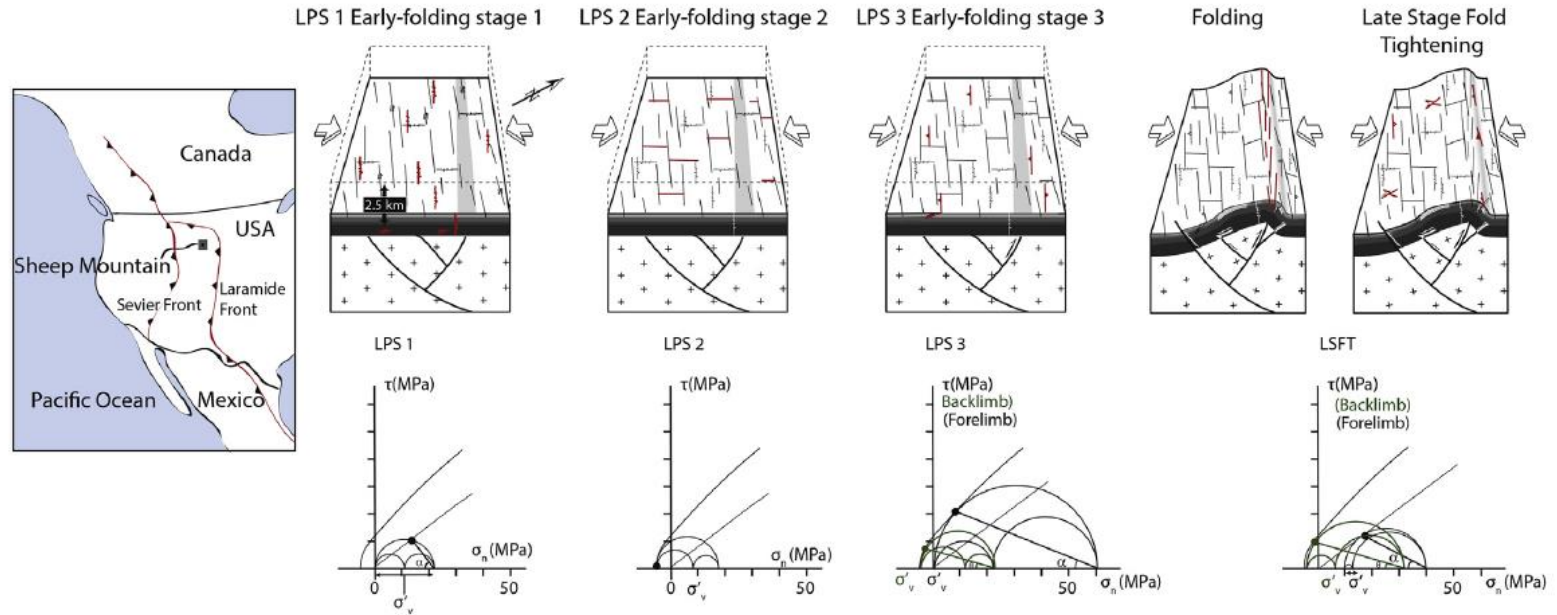
Syn-folding



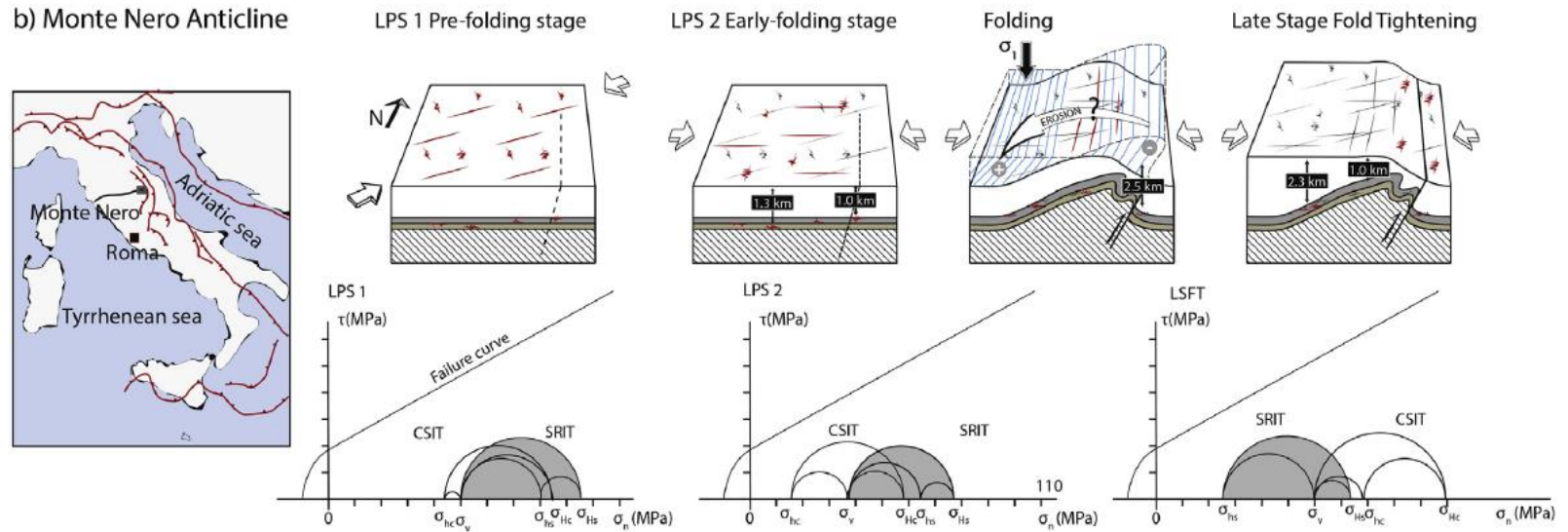
Late Stage Fold Tightening



a) Sheep Mountain Anticline



b) Monte Nero Anticline



Paleo-differential stress vs paleodepth

On the difficulty of establishing a paleostress/ paleodepth relationship

In drill holes, contemporary stresses are determined directly at a given depth / in a narrow depth interval.

In contrast, paleopiezometers are generally sampled and analysed after they have reached the surface, i.e., after exhumation from an unknown depth z , and establishing a $\Delta\sigma$ vs z relationship for paleostresses requires independent determination of $\Delta\sigma$ and z .

In FTBs, paleo- z estimates are usually derived from stratigraphic/ sedimentological studies or from thermometry coupled with assumption on paleothermal gradient

In addition, in case of polyphase tectonism, deciphering the $\Delta\sigma$ vs z evolution requires to unambiguously relate $\Delta\sigma$ to both z and to a specific tectonic event.

For a favourably oriented pre-existing cohesionless fault plane, the condition of reactivation can be written as follows :

$$(\sigma_1 - P_f) / (\sigma_3 - P_f) = [(\mu^2 + 1)^{0.5} + \mu]^2$$

$$\sigma_1 - \sigma_3 = 2\rho g z (\lambda - 1) (1 - [(\mu^2 + 1)^{0.5} + \mu]^2) / (1 + [(\mu^2 + 1)^{0.5} + \mu]^2)$$

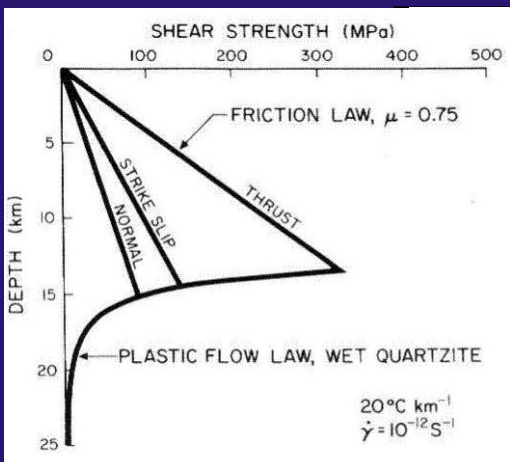
Strike-slip stress regime

and

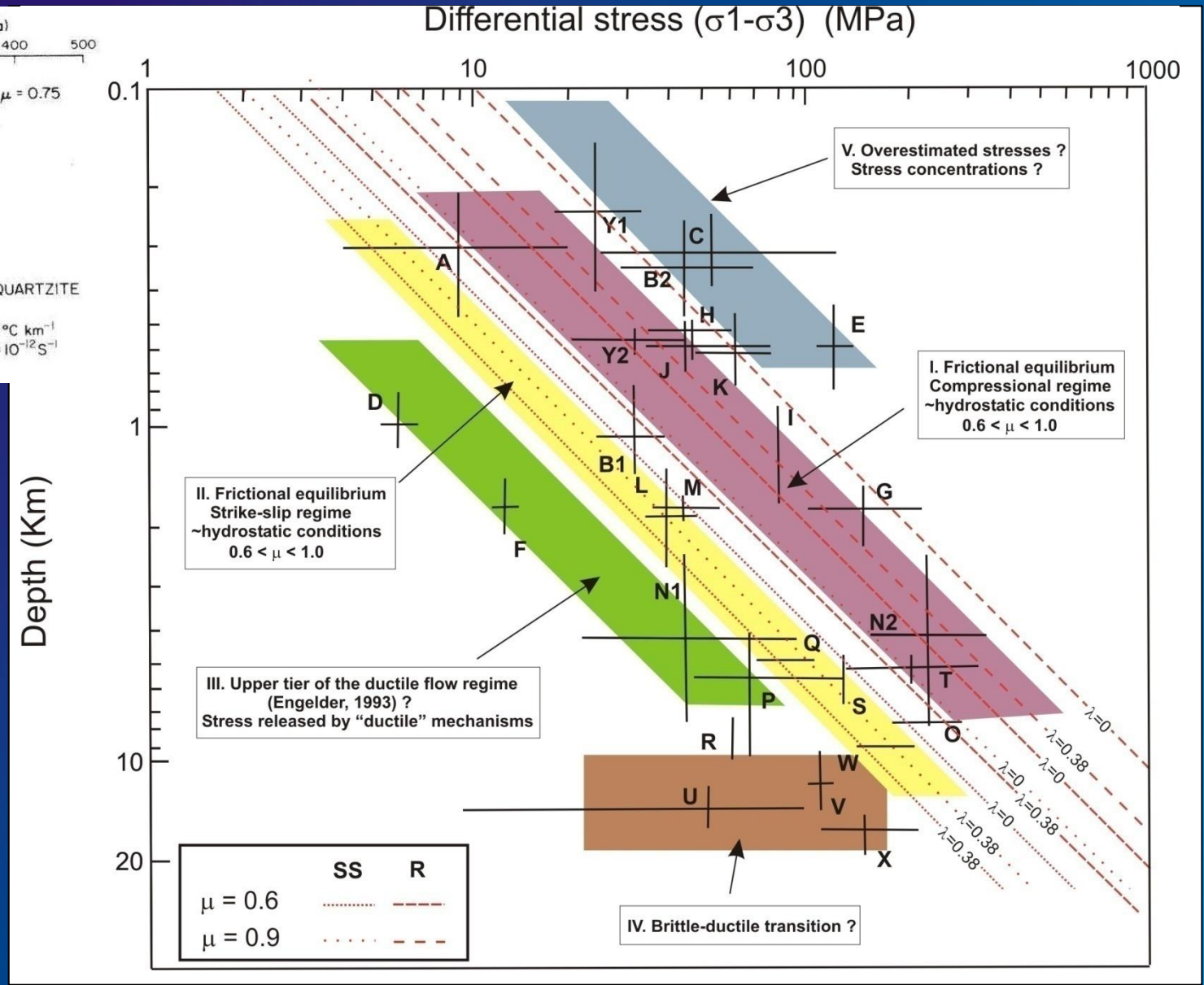
Reverse stress regime

$$\sigma_1 - \sigma_3 = \rho g z (\lambda - 1) (1 - [(\mu^2 + 1)^{0.5} + \mu]^2)$$

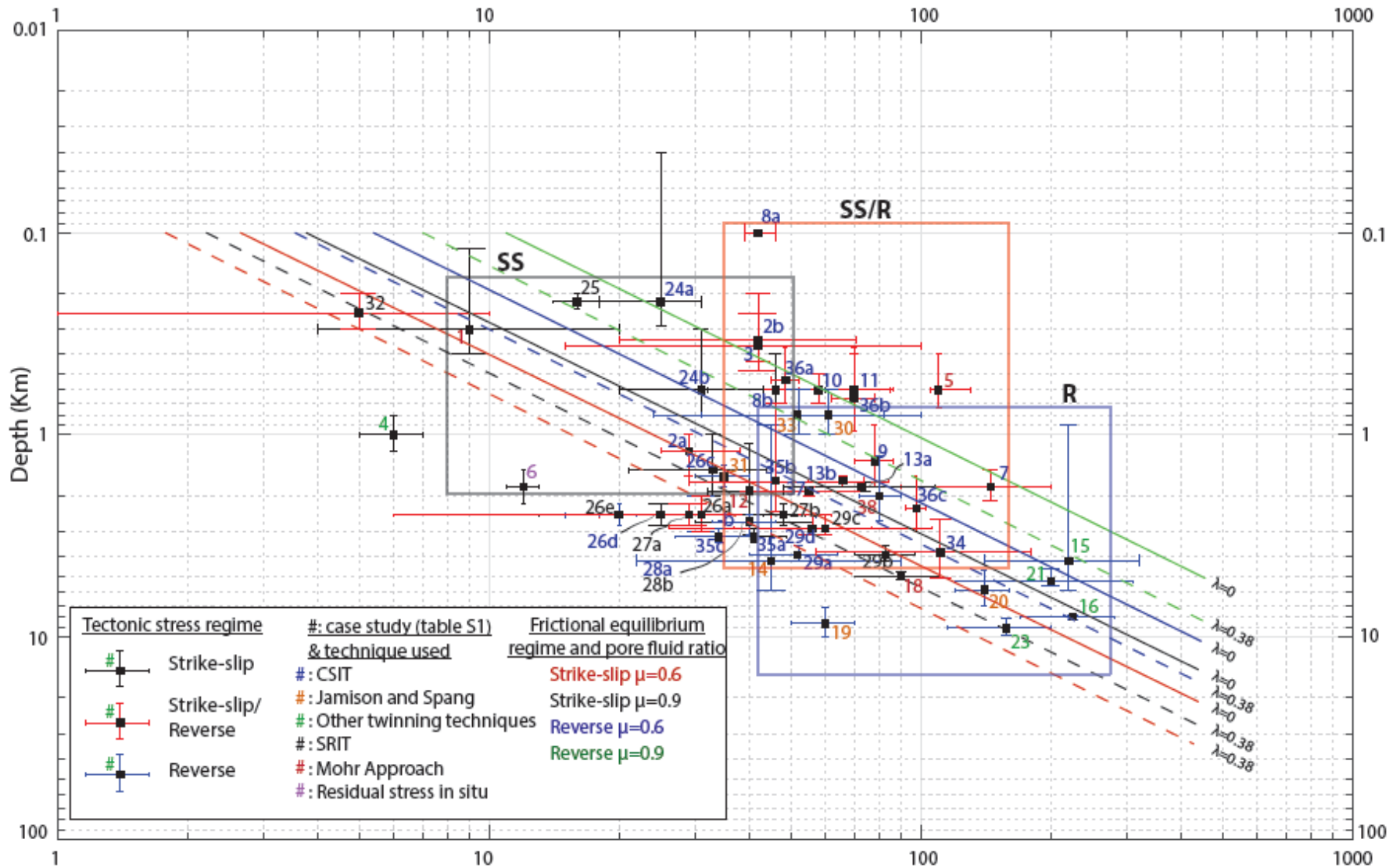
$$\text{with } \lambda = P_f / \rho g z$$



(Lacombe, 2007)



Differential stress magnitudes (MPa)



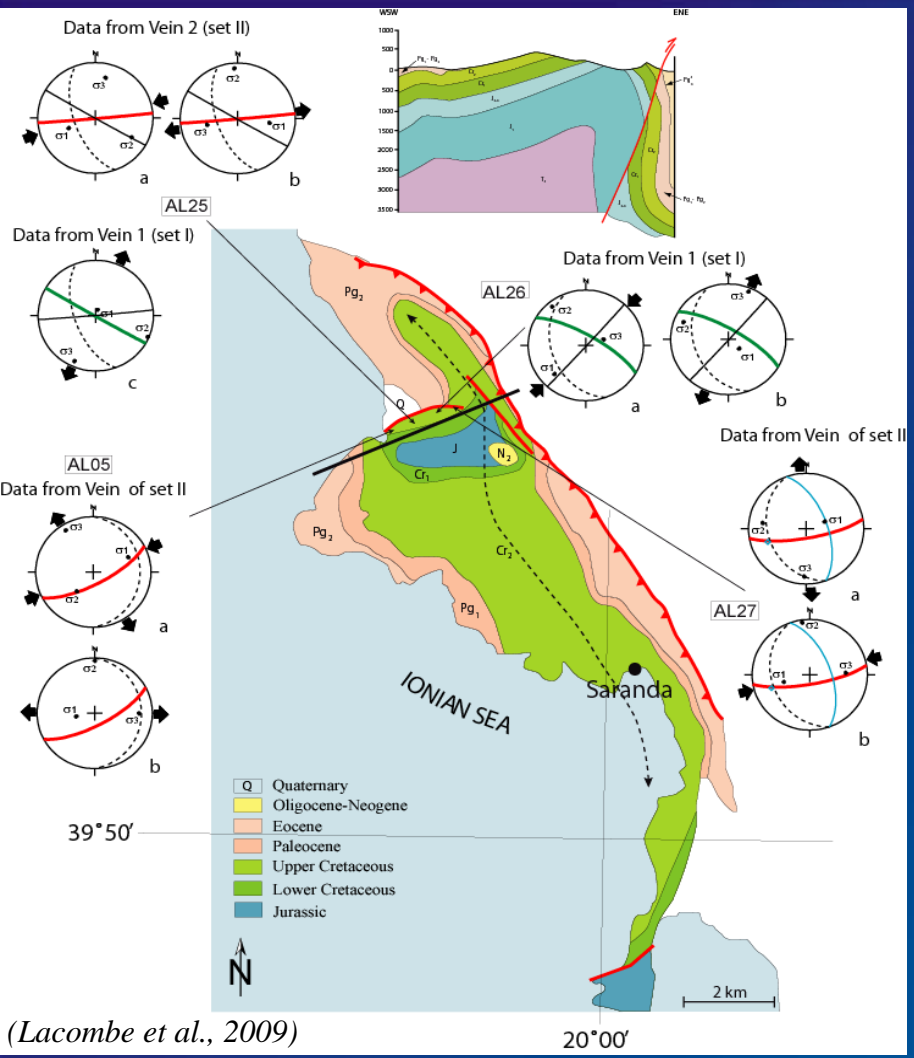
(Beaudoin and Lacombe, 2018)

At the present-day state of our knowledge and with the available dataset, most paleostress data support a first-order long-term frictional behaviour of the upper continental crust.

The crustal strength down to the brittle-ductile transition is generally controlled by frictional sliding on well-oriented pre-existing faults with frictional coefficients of 0.6-0.9 under hydrostatic fluid pressure (frictional stress equilibrium).

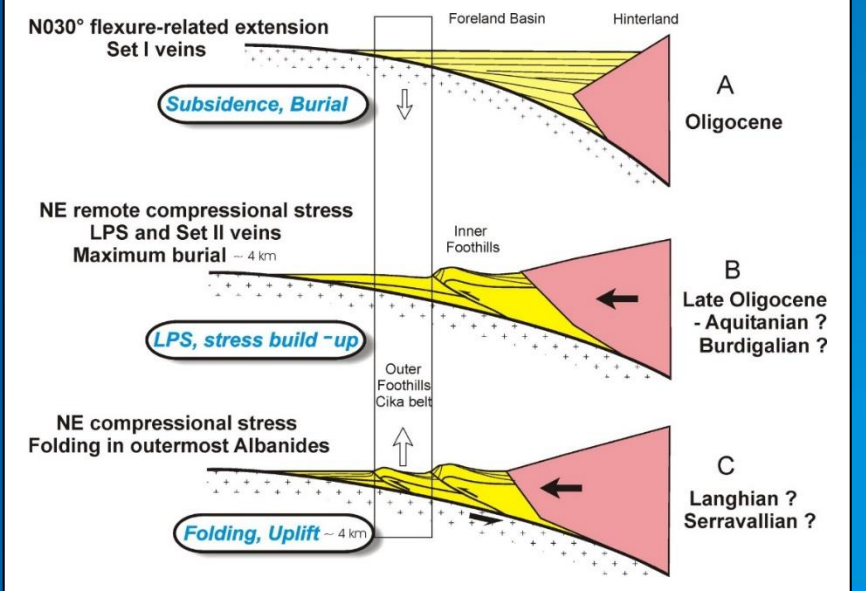
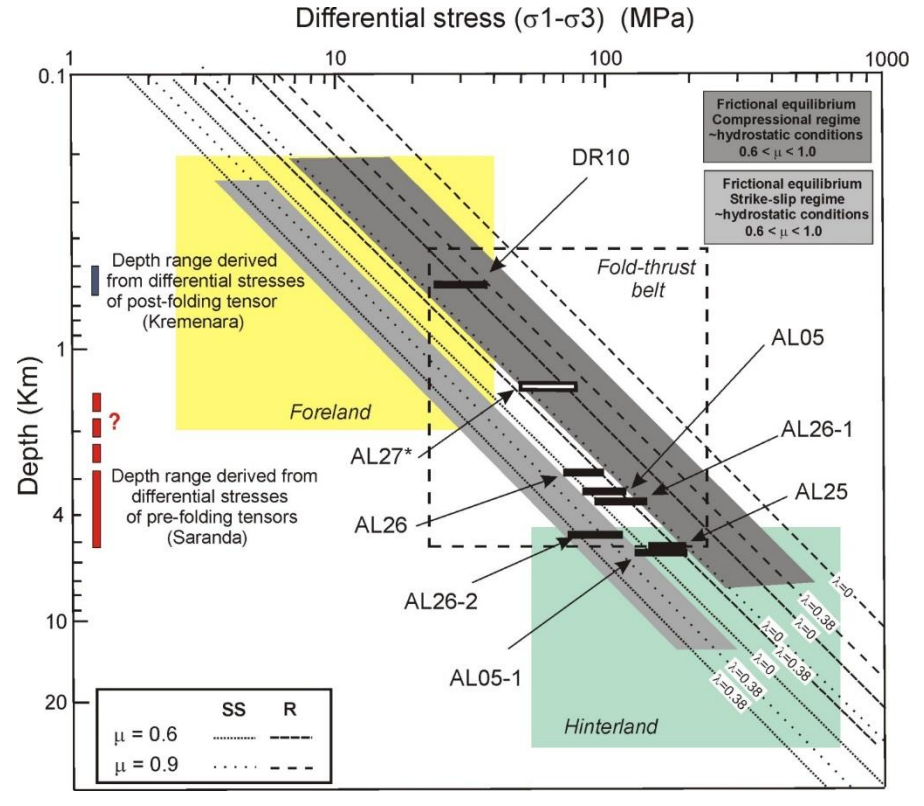
Some ductile mechanisms may, however, relieve stress and keep stress level beyond the frictional yield, as for instance in the detached cover of forelands.

Application to paleodepth reconstruction

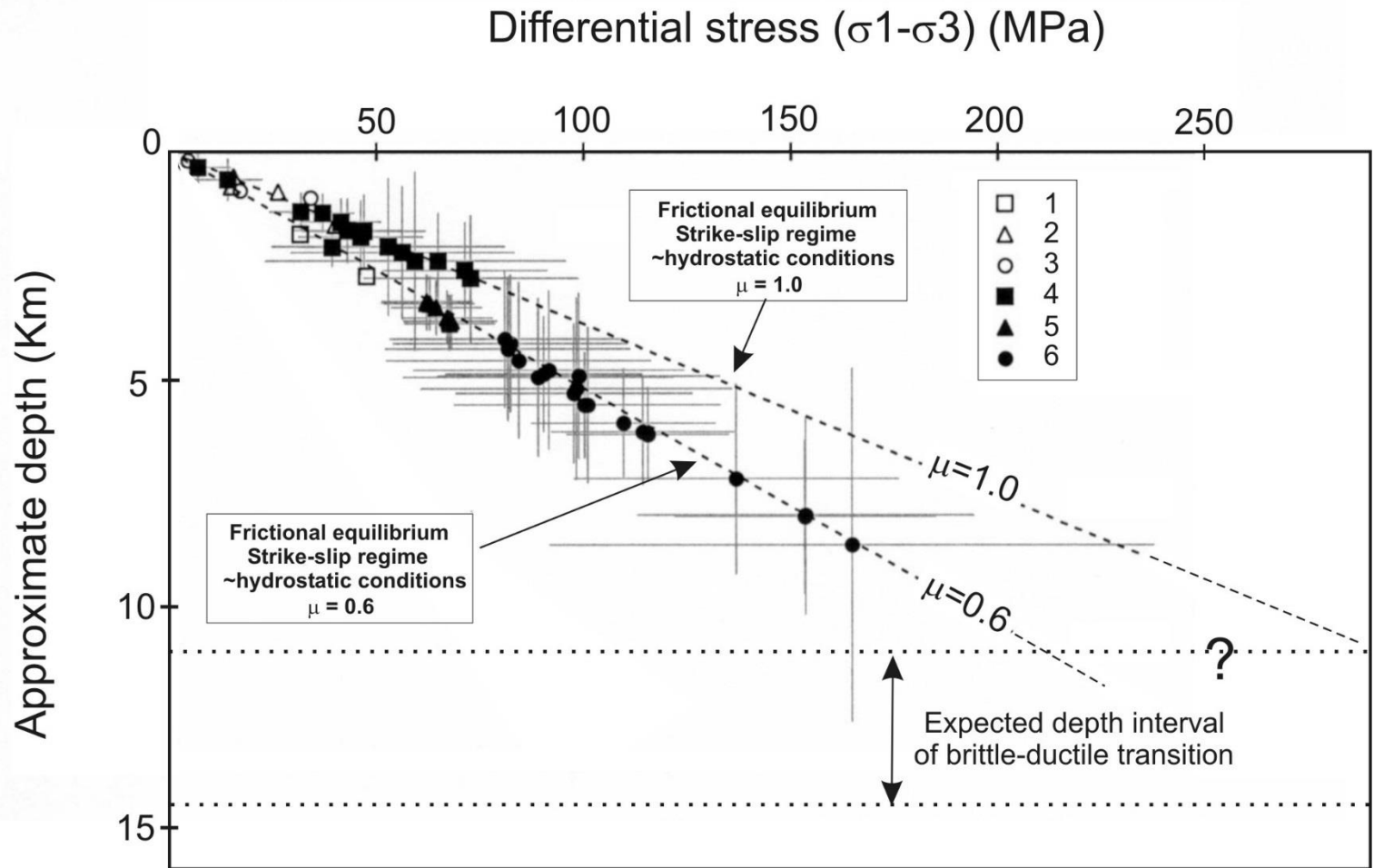


(Lacombe et al., 2009)

Calcite twins provide estimates of pre-folding paleoburial consistent with independent estimates from micro-thermometry of fluid inclusions, maturity of organic matter and results of 1D thermal modeling.



Comparison of paleo differential stress magnitudes with contemporary stress magnitudes and frictional sliding criteria in the continental crust: Mechanical implications



(Townend and Zoback, 2000)

Application of Coulomb faulting theory with laboratory-derived coefficients of friction (e.g., Byerlee, 1978) allows prediction of critical stress levels in reverse, strike-slip, and normal faulting environments as a function of depth and pore pressure.

The *in situ* stress data compiled by Townend and Zoback (2000) and plotted with the theoretical curves for a critically stressed crust under hydrostatic conditions show consistency with Coulomb frictional-failure theory incorporating laboratory-derived frictional coefficients, μ , of 0.6-1.0 and hydrostatic fluid pressure for a strike-slip stress regime.

The crust's brittle strength is quite high (hundreds of MPa) under conditions of hydrostatic pore pressure.

The stress/depth gradient depends explicitly on the stress configuration, i.e., normal, strike-slip or reverse stress regime.

The critically stressed upper continental crust is therefore able to sustain differential stresses as large as 150-200 MPa, so its strength makes it able to transmit a significant part of orogenic stresses from the plate boundary across the far foreland

Concepts and techniques underlying determinations of contemporary stresses and paleostresses are inherently different, and both types of stress data do not have strictly the same geological meaning.

Contemporary stresses measured *in situ* reflect local, instantaneous ambient crustal stresses, while reconstructed paleostresses reflect ancient crustal stresses at the particular time of tectonic deformation, averaged over the duration of a tectonic event and over a given rock volume.

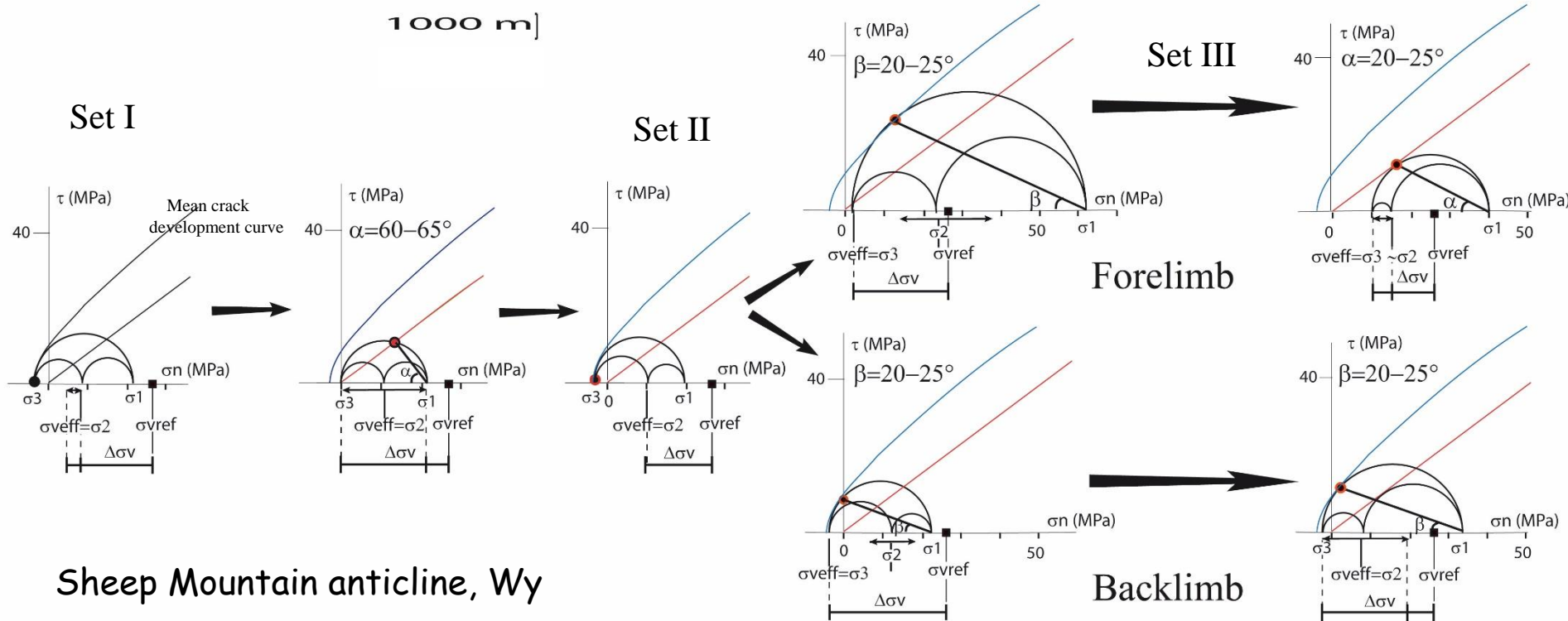
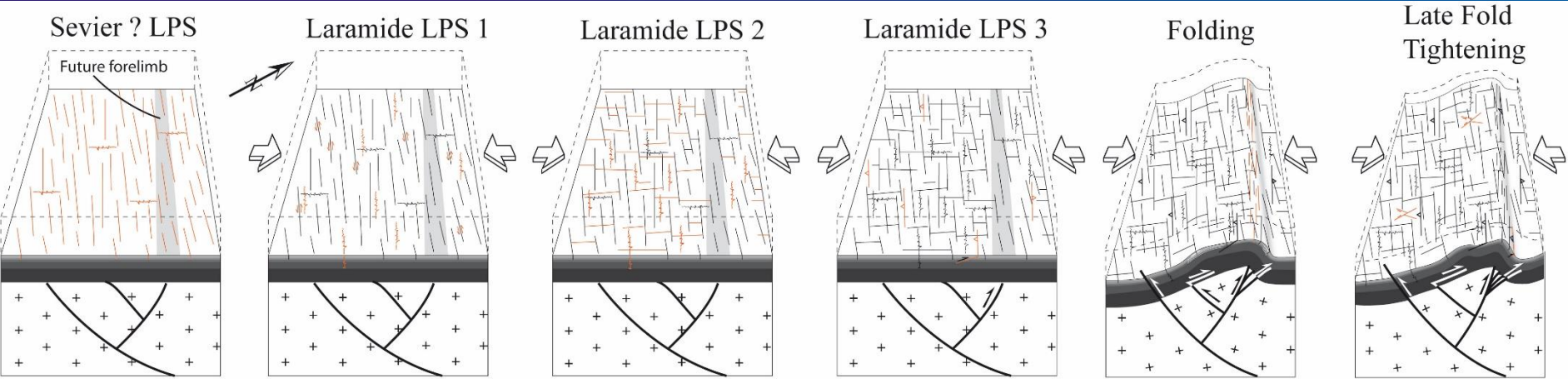
Although to this respect contemporary stresses and paleostresses are not directly comparable, their analyses however rely on the same mechanics, and they constitute complementary stress data sets.

Combination of paleostress and stress data provides new constraints on the differential stress gradients with depth, which are to date still poorly known.

Combining contemporary and paleostress data allows us to extend our stress/depth database in various settings, i.e., away horizontally from drill holes, and vertically by obtaining information on stress magnitudes at depth more or less continuously down to the brittle-ductile transition.

Finally, such a combination of stress data therefore brings useful information on the strength and mechanical behaviour of the upper continental crust over times scales of several tens of Ma, and should be taken into account in future modelling.

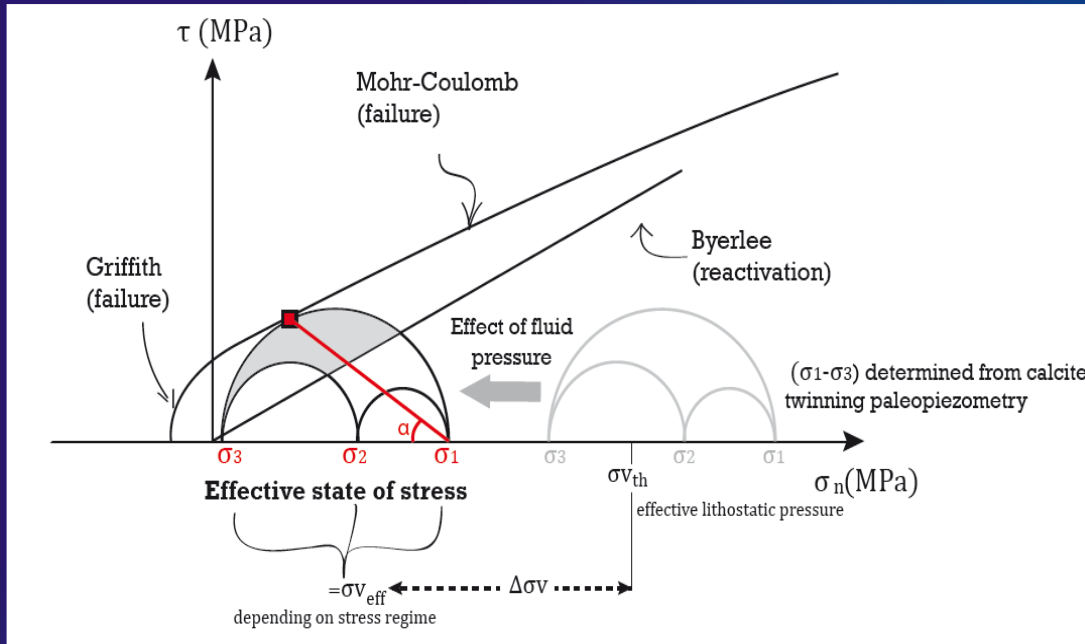
Quantification of principal stress magnitudes
and fluid (over)pressures
at Sheep Mountain
and Rattlesnake Mountain anticlines



Sheep Mountain anticline, Wy

Determination of principal stress magnitudes and $\Delta\sigma_v$ (Amrouch et al, 2011)

Quantifying paleo fluid (over)pressure



Assumption of a vertical principal stress equal to the effective weight of overburden

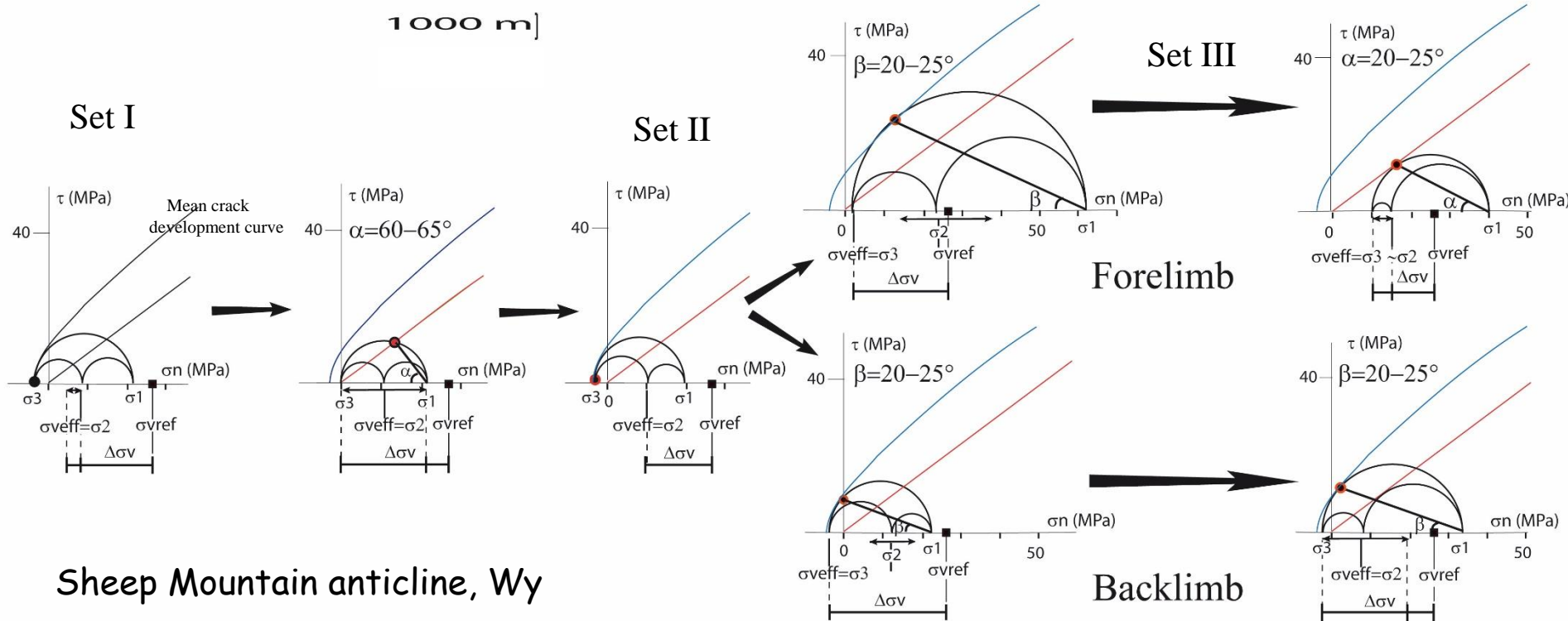
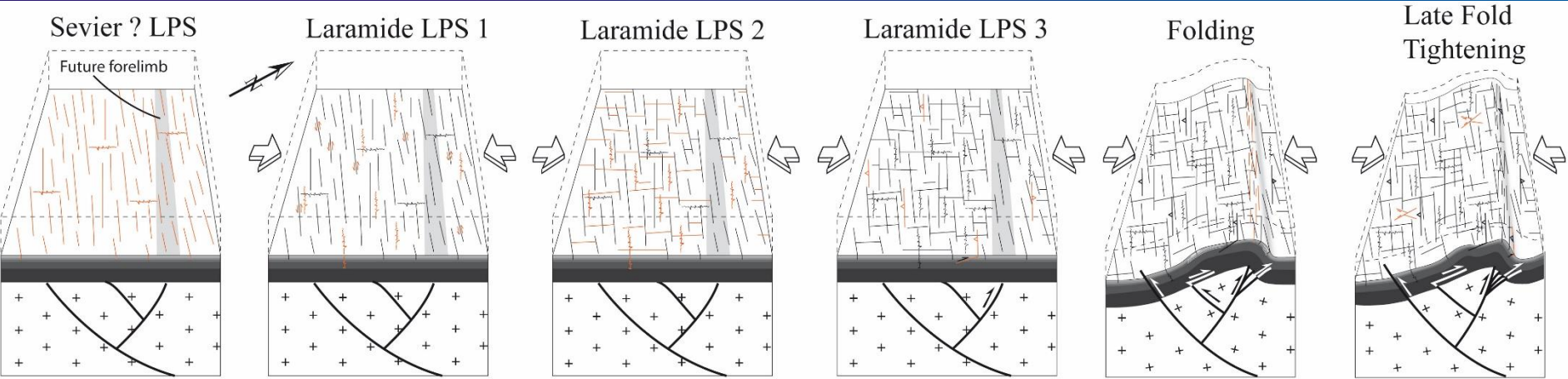
Theoretical effective vertical principal stress calculated considering lithostatic pressure corrected from hydrostatic fluid pressure:

$$\sigma_{vref} = (\rho - \rho_w) \cdot g \cdot h$$

Comparison between σ_{vref} and the reconstructed effective vertical principal stress σ_{veff} :

$$\Delta\sigma_v = \sigma_{vref} - \sigma_{veff}$$

A non-zero $\Delta\sigma_v$ reflects either fluid over- or under-pressure or burial changes (sedimentation or erosion): when $\Delta\sigma_v$ is positive, either the burial depth was less than the value considered for the calculation of σ_{vref} , or the system was overpressured.

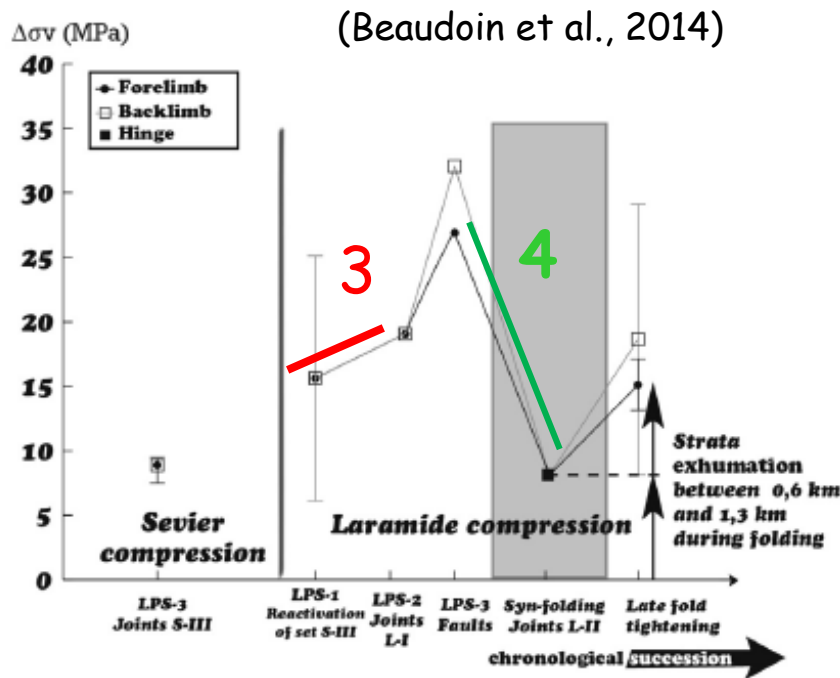


Sheep Mountain anticline, Wy

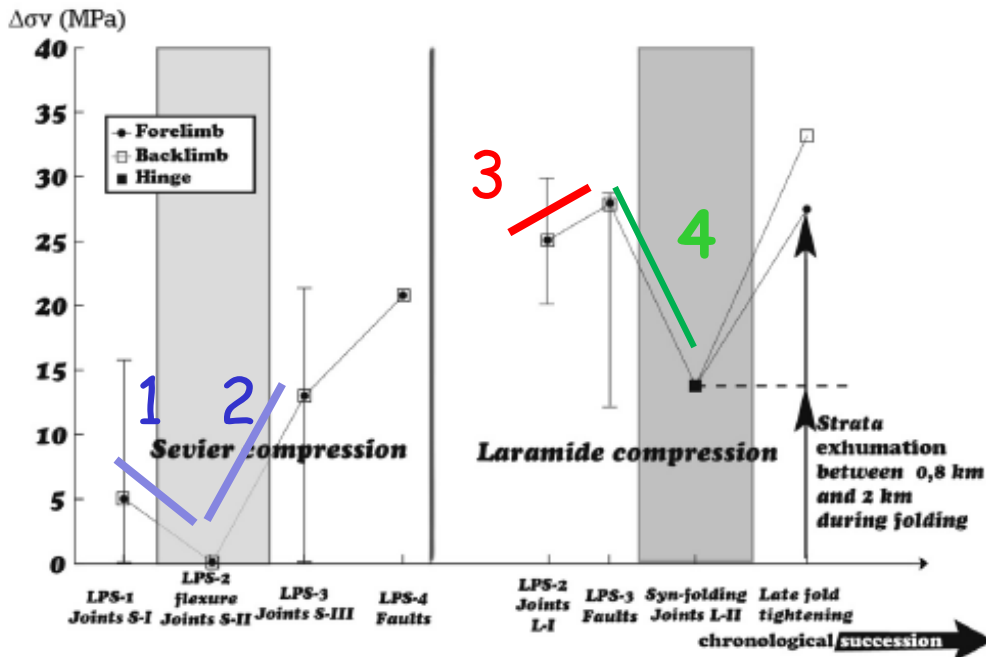
Determination of principal stress magnitudes and $\Delta\sigma_v$ (Amrouch et al, 2011)

Comparison of $\Delta\sigma_v$ evolution

SMA



RMA



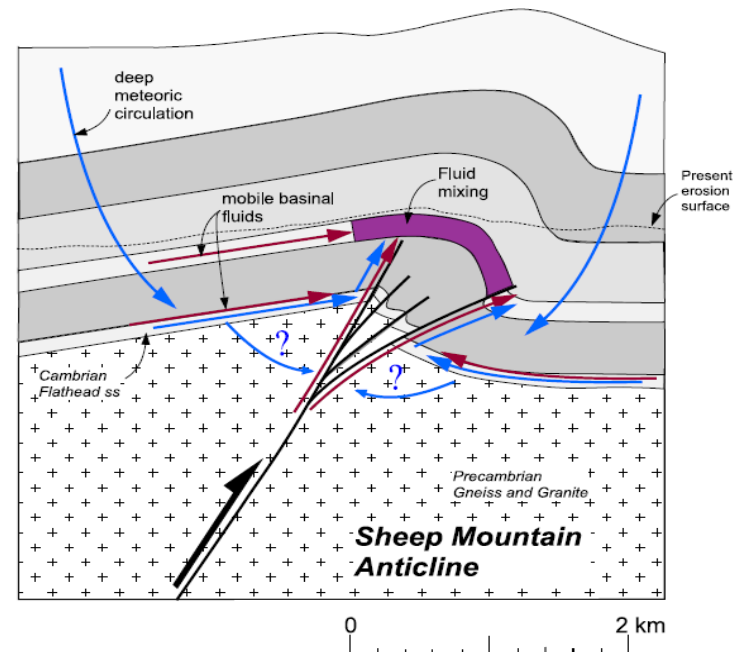
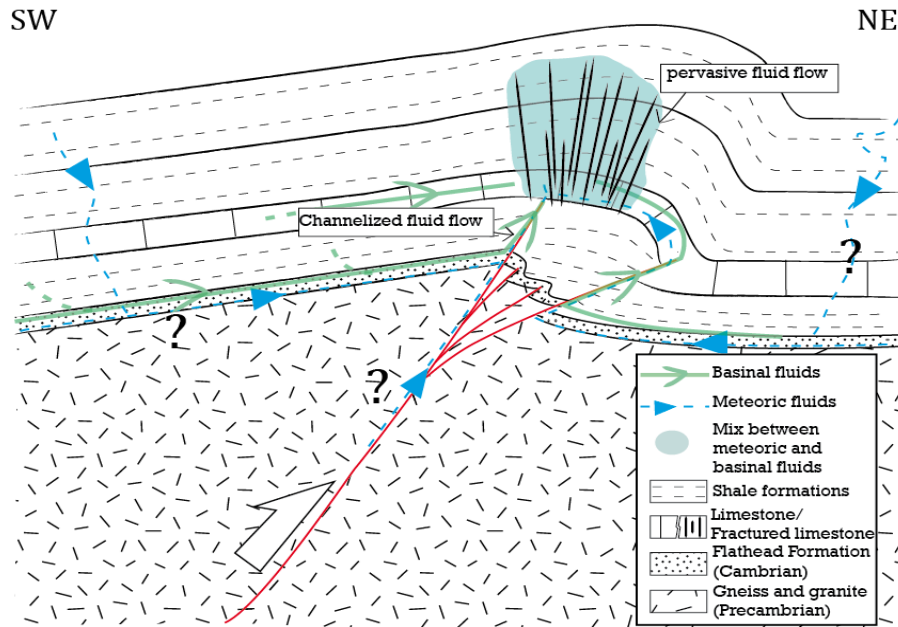
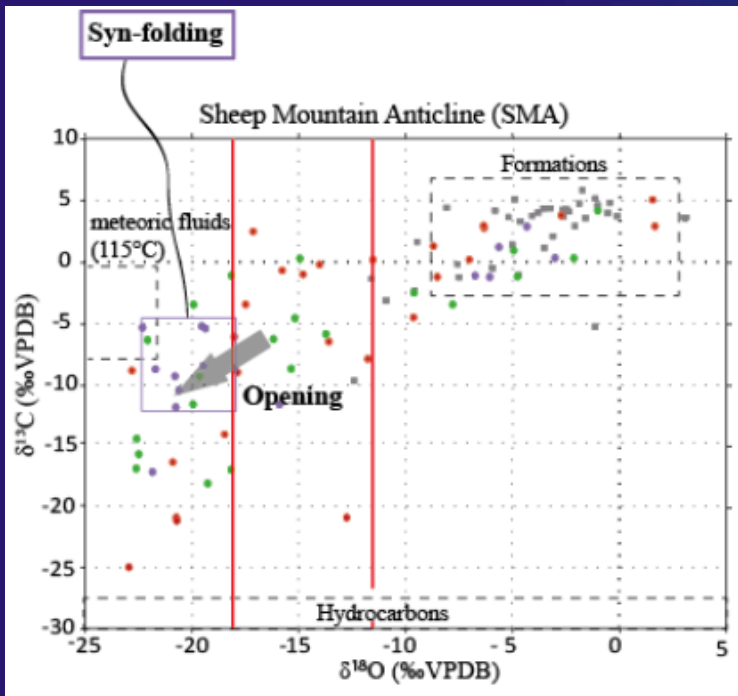
1. Decrease in fluid overpressure from early Sevier LPS to foreland flexure due to enhanced permeability by flexure-related extensional fractures.
2. Increase during late Sevier-LPS by input of exotic fluids as supported by geochemistry of vein cements.
3. Increase during Laramide LPS due to porosity reduction by pressure-solution/poor hydraulic permeability of fracture sets due to low vertical persistence or to their fast healing/strong increase in horizontal stress magnitude / input of exotic fluids into the reservoir in response to a large-scale fluid migration.
4. Drop due to development of curvature-related fractures that enhanced the hydraulic permeability of the reservoir. Break of fluid compartmentalization within the Madison-Phosphoria core consistent with geochemistry of syn-folding vein cements that suggests a vertical migration of deeper radiogenic hot fluids within the sedimentary cover.

Basement-derived hydrothermal fluid pulse at SMA

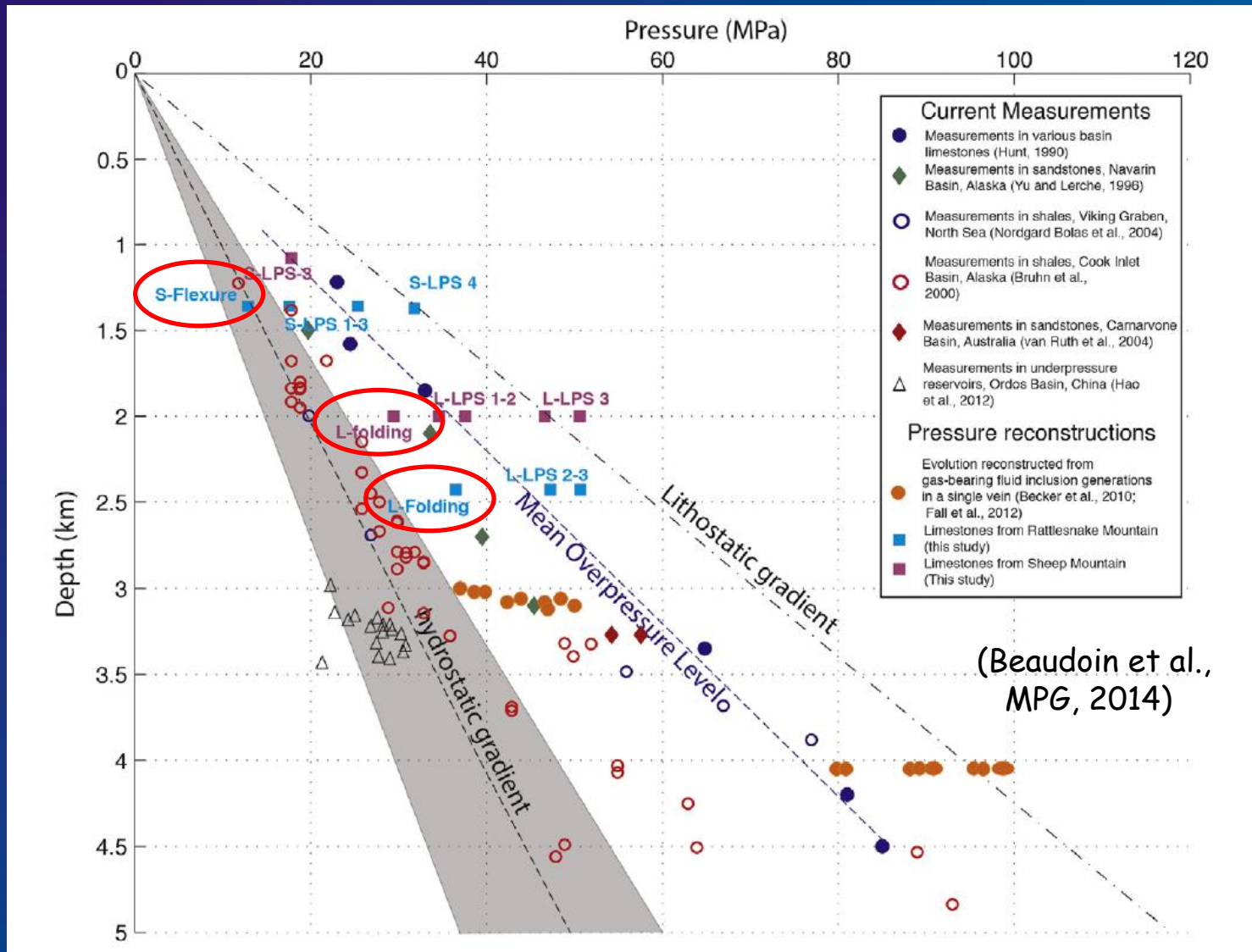
Vertical migration of deeper radiogenic hot fluids within the sedimentary cover explained by the development of curvature-related fractures that enhance the hydraulic permeability of the reservoir and break fluid compartmentalization by stratigraphy.

Link with structural style

(Beaudoin et al, 2011; Evans and Fischer, 2012)



Comparison with values of fluid overpressures in sedimentary basins derived from paleo-pressure reconstructions based on gas composition in hydrocarbon fluid inclusions or from direct measurements in limestone or shale/sandstone reservoirs.

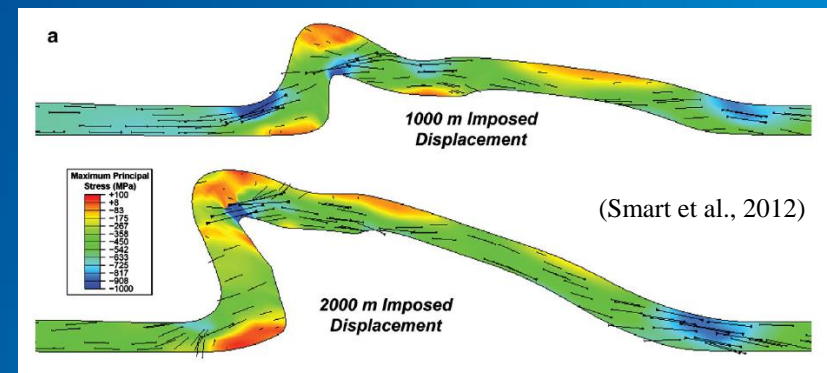
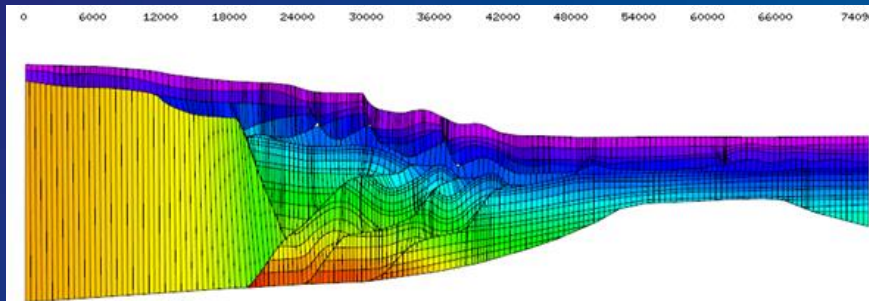


Take home message

Combining paleopiezometers (e.g., calcite twins / stylolites) : a powerful toolbox that helps constrain ...

- stress orientations, regional tectonic history
- values of tectonic (paleo)stress magnitudes
- pore fluid (over) pressure through time in reservoir analogues
- transmission of orogenic stresses to the foreland
 - upper crust rheology
- put mechanics into basin/thrust belt kinematic modelling

among others...



(Smart et al., 2012)



Thank you for your attention...

Suggested readings :

- *Amrouch K., Beaudoin N., Lacombe O., Bellahsen N. & Daniel J.M., 2011, Paleostress magnitudes in folded sedimentary rocks. Geophys. Res. Lett., 38, L17301
- *Beaudoin, N., Koehn. D., Lacombe O., Lecouty A, Billi A., Aharonov., E. & Parlangeau C., 2016. Fingerprinting stress: stylolite and calcite twinning paleopiezometry revealing the complexity of stress distribution during folding – the case of the Monte Nero anticline in the Apennines, Italy. Tectonics, 35, 1687-1712
- *Beaudoin N., Bellahsen N., Lacombe O., Emmanuel L. & Pironon J., 2014. Crustal-scale fluid flow during the tectonic evolution of the Bighorn Basin (Wyoming, USA). Basin Research, 26, 403–435
- *Beaudoin N., Lacombe O., Bellahsen N., Amrouch K. & Daniel J.M., 2014. Evolution of fluid pressure during folding and basin contraction in overpressured reservoirs: insights from the Madison-Phosphoria carbonate formations in the Bighorn basin (Wyoming, USA). Marine and Petroleum Geology, 55, 214-229,
- *Beaudoin N. & Lacombe O., 2018. Recent and future trends in paleopiezometry in the diagenetic domain: insights into the tectonic paleostress and burial depth history of fold-and-thrust belts and sedimentary basins. J. Struct. Geol., 114, 357-365
- *Beaudoin N., Gasparrini M., David M.E., Lacombe O. & Koehn D., 2019. Bedding-parallel stylolites as a tool to unravel maximum burial depth in sedimentary basins: application to Middle Jurassic carbonate reservoirs in the Paris basin. Geological Society of America Bulletin, 131, 7/8, 1239–1254
- *Lacombe O., 2001. Paleostress magnitudes associated with development of mountain belts : insights from tectonic analyses of calcite twins in the Taiwan Foothills. Tectonics, 20, 6, 834-849
- *Lacombe O., 2007, Comparison of paleostress magnitudes from calcite twins with contemporary stress magnitudes and frictional sliding criteria in the continental crust : Mechanical implications. J. Struct. Geol., 29, 86-99
- *Lacombe O., 2010, Calcite twins, a tool for tectonic studies in thrust belts and stable orogenic forelands. Oil and Gas Science and Technology, 65, 6, 809-838